Studies of the gene for NADPH-dependent oxidoreductase involved in the biosynthesis of plant secondary metabolites

2016.3

Tokyo University of Agriculture and Technology
Graduate School of Bio-Applications and Systems Engineering

Nuoendagula

ACKNOWLEDGEMENTS

My deepest gratitude goes first and foremost to Professor Shinya Kajita, my supervisor. Without his consistent and illuminating supervision, consistent encouragement, and confidence in my capability, this thesis could not have reached its present form.

I wish to thank Professor Shinya Kawai, Professor Ryoichi Sato, Professor Taishi Umezawa and Professor Koki Toyoda for careful reading my manuscript and for giving useful comments.

I would like to express my heartfelt gratitude to Dr. Naofumi Kamimura, Dr. Tetsuya Mori, Dr. Ryo Nakabayashi and Dr. Yukiko Tsuji, Mr. Hiroshi Mizuno for providing technical assistance to complete the work, also thanks for providing useful discussions and experimental materials for this study.

I wish to thank Professor Eiji Masai for providing experimental materials and excellent technical support for this study.

I wish to thank Dr. Shojiro Hishiyama for providing experimental materials.

I sincerely thank all the colleagues in Professor Kajita' s lab for their enthusiastic supports and provided me with a helpful and congenial environment.

Table of contents

ACKNOWLEDGEMENTS II

List of figures VI

List of tables IX

Abstract 1

Chapter 1 Background of the study

1.1 Plants secondary metabolites 3

1.2 Lignans and their biosynthetic enzymes 5

1.3 Lignans biosynthesis enzymes in *Arabidopsis thaliana* 14

1.4 Figures 16

Chapter 2 Sequence and expression analysis of *AtPCBER1*

2.1 Introduction 21

2.2 Materials and Methods 22

2.2.1 Sequence analysis 22

2.2.2 Isolation of genomic DNA and total RNA 22

2.2.3 Construction of the promoter-GUS fused construct for generation of transgenic plants 23

2.2.4 Plant materials and growth conditions 24

2.2.5 Expression analysis of AtPCBER1 using sqRT-PCR 24

2.2.6 Histochemical staining for GUS activity 25

2.2.7 Abiotic stress treatment 25

2.3 Results 25

2.3.1 Sequence characterization of *AtPCBER1* gene 25

2.3.2 Expression analysis using semi-quantitative RT-PCR 27

2.3.3 Histochemical analysis of *AtPCBER1* gene using promoter GUS fusion system 27

2.2.4 *AtPCBER1* was induced by abiotic stresses 28

2.4 Discussion 28

2.5 Tables and Figures 32

Chapter 3 Catalytic analysis of recombinant AtPCBER1

3.1 Introduction 45

3.2 Materials and Methods 46

3.2.1 Cloning of cDNA of *AtPCBER1* 46

3.2.2 Heterologous expression in *E. coli* and purification of the recombinant protein 47

3.2.3 Enzymatic assay 48

3.2.4 Kinetic analysis of His-AtPCBER1 48

3.3 Results 49

3.3.1 Amplification of cDNA of *AtPCBER1* and purification of the recombinant enzyme prepared with the cDNA 49

3.3.2 Catalytic analysis of the recombinant AtPCBER1 49

3.4 Discussion 50

3.5 Tables and Figures 52

Chapter 4 Analysis of transgenic plants with up- or down-regulated *AtPCBER1* gene

4.1 Introduction 62

4.2 Materials and Methods 64

4.2.1 Plant materials and transgenic selection 64

4.2.2 Metabolomic analysis of wild-type and transgenic plants 65

4.2.3 Quantification of lignin in stem 65

4.3 Results 66

4.3.1 Metabolomic analysis of wild-type plants and transgenic plants 66

4.3.2 Measurement of lignin contents toward wild-type plants and transgenic plants 68

4.4 Discussion 69

4.5 Tables and Figures 74

Chapter 5 Final conclusions 90

References 95

List of figures

1-1 Common phenolics derived from phenylpropanoid pathways and some adjacent pathways 16

1-2 The predicted biosynthesis pathway of monolignol-derived typical lignans 17

1-3 The predicted biosynthesis pathway of monolignol-derived typical neolignans 18

1-4 The predicted biosynthesis pathway of monolignol-derived typical norlignans 19

1-5 Catalytic properties of NADPH-dependent reductases PCBER, PLR and IFR 20

2-1 **A**lignment of amino acid sequences of AtPCBER1 (accession number: AY150409) and other PCBERs from various species of plants 33

2-2 Phylogenetic relationships of NADPH-dependent reductases PCBERs (black), PLRs (blue), and IFRs (green) derived from various plant species 35

2-3 The cloned sequence of the promoter region of *AtPCBER1* (*At4g39230*) and predicted *cis*-regulatory elements 37

2-4 Representative structure of promoter-GUS fusion cassette 40

2-5 Expression profiles of *AtPCBER1* in 48-day-old *A. thaliana* organs measured by semi-quantitative RT-PCR analysis 41

2-6 Histochemical localization of *uidA* gene expression driven by the promoter of *AtPCBER1* 42

2-7 Histochemical staining of transgenic plants harboring the promoter:*uidA* contruct after mechanical wounding and exposure to ultraviolet (UV) radiation 44

2-8 RT-PCR investigation of *AtPCBER1* gene expression in wild type plants treated with the stresses 44

3-1 Representative structure of expression vector for production of His-AtPCBER1 57

3-2 Sodium dodecyl sulfate-polyacrylamide gel electrophoresis analysis of protein derived from transgenic *E. coli* 58

3-3 Characterization of recombinant His-AtPCBER1 using substrates DDC 59

3-4 Characterization of recombinant His-AtPCBER1 using a substrate, PR 60

3-5 Characterization of recombinant His-AtPCBER1 using a substrate, LR 61

4-1 Expression cassette of expression vector for over expression of *AtPCBER1* gene in plants 78

4-2 Analysis of *AtPCBER1* transcripts in wild-type (WT) and *AtPCBER1* up- and down- regulated plants by RT-PCR 79

4-3 *AtPCBER1* up- (middle) and down- (left) regulated transgenic Arabidopsis and wild type plants (right) 80

4-4 Principal component analysis (PCA) of metabolites detected in untargeted metabolomic analysis of flower from wild-type and *AtPCBER1* up- and down-regulated plants 81

4-5 Biosynthetic pathway of lignans and flavones 85

4-6 Characterization of recombinant His-AtPCBER1 with quercetin as substrate using LC-Q-TOF-MS analysis 86

4-7 MS/MS characterization of reaction product in reaction mixture containing recombinant His-AtPCBER1 and quercetin 87

4-8 Lignin contents in stems of wild-type and transgenic lines 88

4-9 *AtPCBER1* (*AT4G39230*) Gene co-expression networks 89

List of tables

2-1 Composition of Murashige and Skoog medium 32

3-1 Composition of Lysogeny broth (LB) medium 52

3-2 Composition of buffers for histidine-tagged protein purification 53

3-3 Compositions of SDS-PAGE gel and loading buffer 54

3-4 Compositions of 0.2 M sodium phosphate buffer (pH 5.8–8.0) used in this study 55

3-5 Kinetic parameters of recombinant AtPCBER1 measured toward two different substrates 56

4-1 Untargeted metabolomic analysis of the wild-type and transgenic plants in which *AtPCBER1* was up- or down-regulated 74

Abstract

Lignans, including neolignans and norlignans, are phenylpropanoid-derived secondary metabolites found in a wide range of plant species with varied content and composition. It has been presumed that secondary metabolites such as these are involved in defense against biotic and abiotic stresses and physiological integrity of plant cells, but few roles and functions have been clarified. Lignan and neolignan have two C6-C3 units, the former linked by an 8–8′-bond and the latter linked by carbon-carbon bond(s) at other positions. Studies showing advantageous effects of the natural compounds on human health have attracted much attention to lignan biosynthesis processes as a focus of recent research.

Phenylcoumaran benzylic ether reductase (PCBER), a member of the isoflavone reductase family, is thought to be an enzyme crucial in the biosynthesis of 8-5′-linked neolignans. It has been isolated and characterized in several plant species, as the enzyme responsible for conversion of dehydrodiconiferyl alcohol and dihydrodehydrodiconiferyl alcohol to isodihydrodehydrodiconiferyl alcohol and tetrahydrodehydrodiconiferyl alcohol, respectively. PCBER has a close phylogenetic relationship to pinoresinol-lariciresinol reductase (PLR), which catalyzes the two reduction steps of typical lignans PR and LR. Overlap in the substrate specificity of PCBER and PLR should be derived from their close phylogenetic relationship and structural similarity of the substrates with aryl-dihydrobenzofuran and diaryl-furofuran rings.

Although genes that encode polypeptides with sequences similar to identified PCBERs are found in the genome of *Arabidopsis thaliana*, no functional

characterization studies have been reported thus far in this species. In this study, we characterized a putative PCBER (*At4g39230*, designated *AtPCBER1*) in *A. thaliana*. We cloned cDNA and the promoter region of one *AtPCBER1* from *A. thaliana*. At the amino acid level, AtPCBER1 shows high sequence identity (64-71 %) with PCBERs identified from other plant species. Expression analyses of *AtPCBER1* by reverse transcriptase-polymerase chain reaction and histochemical analysis of transgenic plants harboring the promoter region of *AtPCBER1* linked with *gus* coding sequence indicate that expression is induced by wounding and is expressed in most tissues, including flower, stem, leaf, and root. Catalytic analysis of recombinant AtPCBER1 with neolignan and lignans in the presence of NADPH suggests that the protein can reduce not only the 8-5′-linked neolignan, dehydrodiconiferyl alcohol, but also 8-8′ linked lignans, pinoresinol and lariciresinol with lower activities. To investigate further, we performed metabolomic analyses of transgenic plants in which the target gene was up- or down- regulated. Our results indicate no significant effects of *AtPCBER1* gene regulation on plant growth and development. However, levels of some secondary metabolites, including lignans, flavonoids, and glucosinolates, differ between wild-type and transgenic plants. Taken together, our findings indicate that *AtPCBER1* encodes a polypeptide with PCBER activity and has a particular role in the biosynthesis of secondary metabolites in *A. thaliana*.

Chapter 1

Background of the study

1.1 Plants secondary metabolites

It has been previously inferred that, plants produce primary and secondary metabolites. The primary metabolites including carbohydrates, lipids, proteins and nucleic acids are mostly derived from and involved in primary metabolic processes such as photosynthesis and respiration. So that the primary metabolites are present in all plant species and essential to plant reproduction, growth and development. In contrast, the secondary metabolites are assumed to be determined by metabolic pathways of primary metabolites and do not involved primarily in plant reproduction, growth and development as primary metabolites do. The secondary metabolites are contained large number of phenolics, terpenoids and nitrogen-containing alkaloids and considered to be involved in plant defense. But structures and biological rules of these natural compounds are not well understood (Hartmann. 2007).

Phenolics are major group of secondary metabolites and mainly derived from shikimic acid pathway. The shikimic acid pathway is branched from primary carbon metabolites (carbohydrates) of erythrose 4-phosphate and phospho*enol*pyruvate and leads to accumulate the aromatic amino acids; phenylalanine, tryptophan and tyrosine (Herrmann and Weaver. 1999). These aromatic amino acids are further synthesized to various phenolic compounds. Among them, the phenylpropanoid synthetic pathway derived from phenylalanine serve as the important branch of shikimic acid pathway in plants

(Gomes *et al.* 2015; Tohge *et al*. 2013).

In phenylpropanoid synthetic pathway, the aromatic amino acid, phenylalanine, is carried out series of hydroxylation, methylation and dehydration steps after the non-oxidative deamination reaction catalyzed by phenylalanine ammonia-lyase (PAL). This pathway not only per se can create large number of phenolic compounds, the intermediates produced in this pathway are adducted with other compounds derived from distinct metabolic pathways can produce various secondary metabolites, such as lignans, isoflavonoids, flavonoids, lignins, coumarins, numerous esters and amides (**Fig. 1-1**).

In the natural environment, plants suffered various biotic and abiotic stresses including pests and pathogen invasions, UV irradiation and wounding stress. Experimental studies indicate that, the compounds and corresponding biosynthetic enzymes consist in phenylpropanoid synthetic pathway play some crucial roles in plant defense. For instance, lignins provide mechanical support (Whetten and Sederoff. 1995); Hydroxycinnamic acid esters and flavonoids are complementary UV protective compounds (Burchard *et al*. 2000); In bean cell culture, transcription levels of genes for PAL and chalcone synthase (CHS) markedly increased when treated with reduced form of glutathione (Wingate *et al*. 1988), and *PAL* expression level significantly increased when elicitor-treated (Edwards *et al*. 1985). Among others, Dixon and Paiva (1995) and Caldo *et al.* (2004) revealed that phenylpropanoid synthetic pathway produces various antioxidants, antipathogenic compounds, in addition to these, they observed many biosynthetic enzymes in this pathway have induced by UV irradiation, mechanical wounding and pathogenic attack.

1.2 Lignans and their biosynthetic enzymes

As mentioned before, aromatic amino acids phenylalanine and tyrosine are produced from shikimic acid pathway, and further metabolized in a series of cinnamic acid derivatives. The reduction of these acids forms three monolignols (p-coumaryl alcohol, coniferyl alcohol and sinalpyl alcohol) that are the precursors of lignans and lignin.

Monolignols are further oxidatively dimerized and lead to wide variety of natural compounds designated as lignans (**Fig. 1-1**). It is well known that, oxidative radical-radical coupling of monolignols cause to accumulate the phenylpropanoid polymer, lignin, which involved in structural support and water transportation in plants. Lignin shares same precursor with lignans and presents ubiquitously in plants kingdom, whereas, lignans including neolignans and norlignans are found in plants with various contents and compositions.

As shown in **Fig. 1-2,** the typical lignans are synthesized from derivatives of monolignols (hydroxycinnamic acids or hydroxycinnamyl alcohols) and possess two C_6-C_3 units linked by the central carbon of the 8-8′ position. Oxidative coupling of two monolignols are catalyzed with oxidative enzymes (e.g., peroxidase) and the enantio-specific coupling of them are controlled by dirigent proteins. On the next step, the enantiomer compounds which derived from monolignol coupling were further synthesized to various types of lignans catalyzed by pinoresinol-lariciresinol reductase (PLR) and other enzymes.

Based on the incorporation position of oxygen at the carbon skeleton and cyclization pattern of two monolignol moleculars, lignans are classified into eight groups which are furofurans (e.g., pinoresinol), furans (e.g., lariciresinol), dibenzylbutanes (e.g., secoisolariciresinol), dibenzylbutyrolactones (e.g.,

matairesinol), aryltetralins (e.g., podophyllotoxin), arylnaphthalenes (e.g., dehydropodophyllotoxin), dibenzocyclooctadienes (e.g., steganacin), and dibenzylbutyrolactols (e.g., dibenzylbutyrolactollignan) (Umezawa. 2003a; Umezawa. 2003b; Suzuki and Umezawa 2007). In addition, all lignans are classified into three categories that lignans with 9(9')-oxygen, lignans without 9(9')-oxygen, and dicarboxylic acid lignans (Umezawa. 2003a).

Lignans with 9(9')-oxygen are the most well-known lignans until now. They formed by dimerization of two coniferyl alcohol units where the dirigent proteins control enantioselectivity and give rise to pinoresinol (PR, furofuran). PR is then reduced by pinoresinol/ lariciresinol reductase, via lariciresinol (LR, furan), to secoisolariciresinol (SLR, dibenzylbutane), which is in turn oxidized to afford matairesinol (dibenzylbutyrolactone) by secoisolariciresinol dehydrogenase.

As mentioned above, dirigent proteins and PLRs are crucial enzymes in the lignans biosynthesis pathway. By 1997, Davin *et al.* isolated a dirigent protein which could control enantio-selectivity of coniferyl alcohols. Subsequently, dirigent proteins were discovered in many plant species, such as, two from *Frullania intermedia*, *Populus tremuloides* and *Tsuga heterophylla*, respectively, and eight from *Thuja plicata* (Gang *et al*. 1999a). Not only enantio-selective catalytic activities, dirigent proteins are accumulated by the abiotic or biotic stresses. For instance, expression levels of six dirigent proteins significantly increased in the stem bark and xylem of spruce when wounded or treated with weevils (Ralph *et al*. 2006).

Likewise, Dinkova-Kostova *et al.* first isolated the NADPH dependent oxidoreductase gene, named PLR. Polypeptide of this gene could reduce the PR) to SLR *via* LR. In addition, PLR could regulate the other lignan hinokinin

biosynthesis in *Linum corymbulosum* (Bayindir *et al.* 2008) and justicidin B biosynthesis in *Linum perenne* (Hemmatia *et al.* 2007). PLRs exhibited tissue-specific expression patterns in these plants species. Not only dirigent proteins, but also PLRs showed the enantioselective control on lignan biosynthetic pathways (von Heimendahl *et al.* 2005). Diversity of lignan structures may be due to the stereo-selective catalysis by dirigrnt proteins and PLRs.

In addition to dirigent proteins and PLRs, secoisolariciresinol dehydrogenase proteins which could catalyze the successive reaction of matairesinol synthesis from SLR also have been purified from several plant species (Umezawa *et al.* 1991; Okunishi *et al.* 2004).

Lignans are found in almost all the parts of plants, including stems, leaves, roots, flowers, fruits, and seeds. Lignans not only have important biochemical roles in plants, but also they have advantageous effects on human health. For example, (+)-PR, (+)-syringaresinol and herpetol indicate neuroprotective activity and inhibitory activity towards nitric oxide (NO) production (In *et al.* 2015). SLR is present in high levels in flax and possesses a detrimental effect on the aphids *Myzus persicae* (Saguez *et al.* 2013); Lignans of justicidins A, B, C and D, diphyllin, diphyllin apioside and diphyllin apioside 5-acetate exhibit antiviral activities (Asano *et al.* 1996); Podophyllotoxin is an active anticancer agent (Yousefzadi *et al.* 2010) and possesses antitumor and antihyperlipidemic activities (Farkya *et al.* 2004); Secoisolariciresinol diglucoside can decrease in serum cholesterol, prevent the lipid peroxidation and reserve the antioxidants (Prasad. 1999). In addition to these examples, lignans also have prevention of cancer activity (Huang *et al.* 2010), hepatoprotective activity (Negi *et al.* 2008)

and protective effects against breast cancer (Brooks *et al*. 2008).

The neolignans share same precursors with lignans. Compared to the biosynthesis pathway of lignans, the biosynthesis pathways of neolignans are not well understood. As shown in (**Fig. 1-3)**, the initial step of neolignans biosynthesis similar to that of lignans is catalyzed with oxidase enzyme (e. g., peroxidase). The 8-5′ and 8-*O*-4′-linked neolignans are most common in plant species, but biosynthetic pathways of these neolignans still remain unclear.

Phenylcoumaran benzylic ether reductase (PCBER) assumed to be a crucial biosynthetic oxidoreductase enzyme of 8–5′-linked neolignans, capable of catalyzing the NADPH-dependent reduction of various phenylcoumaran lignans to afford the corresponding diphenols, e.g. conversion of dehydrodiconiferyl alcohol (DDC) and dihydrodehydrodiconiferyl alcohol (DDDC) to isodihydrodehydrodiconiferyl alcohol (IDDDC) and tetrahydrodehydrodiconiferyl alcohol (TDDC), respectively. PCBER had been characterized in several plant species (Gang *et al*. 1997; Gang *et al*. 1999b; Shoji *et al*. 2002; Bayindir *et al*. 2008; Cheng *et al*. 2013).

In addition, Kasahara *et al.* (2006) first reported the phenylpropanoid double-bond reductase that converted both dehydrodiconiferyl and coniferyl aldehydes to dihydrodehydrodiconiferyl and dihydroconiferyl aldehydes using NADPH as cofactor.

Similar to lignans, neolignans also play certain roles in plant defense and are expected to have positive impacts on human health. For instance, a glucoside of typical 8-5'-linked neolignan DDC possesses a detrimental effect on the aphids *Myzus persicae* (Saguez *et al*. 2013). The DDC glucoside is known to affect cell division in tobacco suspension cells (Binns *et al*. 1987; Orr *et al*. 1991). 8-*O*-4′

neolignan showed cytotoxic activity against human tumor cells (Shu *et al*. 2015). In addition to these compounds, other neolignans also showed the antitumoral and anticancer effects (Apers *et al*. 2003; Lee and Xiao. 2003), anti-leishmania activity (Barata *et al*. 2000) and protective effects towards DNA damage (Hanusch *et al*. 2015).

By way of contrast, norlignans are formed with the C_6–C_5–C_6 carbon skeleton (Suzuki *et al*. 2007; Imai *et al*. 2006) and assumed to be biosynthesized from the phenylpropanoid pathway. Up to now, the biosynthesis pathway of norlignans is little known (**Fig. 1-4)**. It had been constructed that hinokiresinol, a typical norlignan, is formed from *p*-coumaryl CoA and *p*-coumarate (**Fig. 1-4**; Suzuki *et al*. 2001; Suzuki *et al*. 2002), and that sequirin D and sequosemperivirin A, which are also norlignans, share the same intermediate with lignans (Zhang *et al*. 2004). In addition, in 2006, Imai *et al.* deduced the biosynthesis pathway of agatharesinol from phenylalanine using ^{13}C labeled carbon. And, in 2009, Imai *et al.* demonstrated that the agatharesinol was further metabolized to sequirin C and metasequirin C, and this enzymatic step required both NAD(P)H and FAD as cofactors.

As shown in **Fig. 1-4**, norlignans possesse C7-C8', C8-C8' and C9-C8' linkage types and are mainly discovered in conifers and monocotyledons (Castro *et al*. 1996; Suzuki *et al*. 2007). Norlignans are assumed to have a crucial role in heartwood formation and coloration. Bito *et al* (2011) using GC-MS analysis demonstrated that *Cryptomeria japonica* heartwood samples were contained large amounts of norlignans, agatharesinol and sequirin C. Then, Takahashi and Mori (2006) indicated that, heartwood coloration (blackening phenomenon) and discoloration were particularly associated with norlignan, Sequirin C. The

norlignans are also considered to have an inhibitory activity towards the eating behavior of *Acusta despesta* (Chen *et al*. 2001) and an anticancer activity (Zhang *et al.* 2005).

Studies of lignans and their biosynthetic enzymes could bring valuable knowledge on the plant survive and human health. The atmosphere, soil and water environments have been polluted seriously and consequently. These would be the biggest threats to human health. Structural and functional studies of lignans may lead the way to effective drug discovery. In addition, pollution may bring plants a series of oxidative stresses that including increasing of ozone concentration, disastrous weather, UV irradiation and mechanical wounding. These oxidative stresses may be promoting plants to produce active oxygen species (e.g., H_2O_2) that may lead to cell death. The lignans biosynthesis pathways are initiated by catalyzing with the oxidative enzyme, and many NADPH dependent oxidoreductase enzymes are involved in lignan biosynthesis. Niculaes *et al.* (2014) concluded that lignan biosynthesis enzymes protect against oxidative damages in plants. Combined with those of experimental investigations described above, it is predicted that lignans and their biosynthesis enzymes protect plant cells against oxidative stresses.

Plant cell or tissue cultures have a good prospect on production of plant-based beneficial metabolites. Additionally, stress inductions applied in cell or tissue cultures also have been effective manners for improving the productivity of useful compounds. Recently, some researches also successfully produced the beneficial lignans using cell culture, such as DDC 4-β-D-glucoside (Attoumbre *et al*. 2005), justicidin B (Hemmati *et al*. 2007), LR diglucoside, DDC glucoside and guaicylglycerol-β-coniferyl ether glucoside (Beejmohun *et al*. 2007). On the

other hand, several studies tried to increase lignans in transformed plants with genes from other plant species. Ayella *et al.* (2007) successfully increasing the level of SLR diglucoside by over expressing PLR gene of *F. intermedia* in wheat. And in the same manner, the content of phyllanthin, a typical lignin, was significantly increased when PLR gene of *Linum usitatissimum* was heterologously and strongly expressed in *Phyllanthus amarus* (Banerjee and Chattopadhyay 2010). These exprimental studies further reinforced the importance of studies about lignans and their biosynthetic enzymes.

In recent years, numerous studies have focused on the biosynthesis pathways of the lignans. For examples, PLR and PCBER have attracted much attention. Consequentially, PLRs and PCBERs (**Fig. 1-5**) from many plant species were purified and characterized.

Due to their high sequence and structure similarities, PLR and PCBER have a close phylogenetic relationship between each other and also to isoflavone reductase (IFR), which was isolated firstly from a legume species and enzymatically catalyzed the NADPH-dependent reduction of isoflavonoids to corresponding reduced form, such as reduce 2′-hydroxyisoflavones to vestitone (**Fig. 1-5**; Vassão *et al*. 2007; Min *et al*. 2003).

On the other hand, both IFRs and PLRs indicated the specific enantioslective reduction. Such as, PLRs from *T. plicata* and *F. intermedia* catalyzed oppositely enantioslective conversions, respectively (Dinkova-Kostova *et al.* 1996; Gang *et al.* 1999b). Instead, PCBER from *Pinus taeda* catalyzes the conversion of the same amount of both enantiomers of substrate DDC to IDDDC. PLR functions had been characterized in many aspects. Compared to PLRs, the functions of PCBER have not been well understood.

Until now, histochemical localization of PCBER polypeptides and expression of the corresponding gene(s) have been characterized in some plant species. In *P. taeda*, PCBER localized to the axial and radial parenchyma cells of the secondary xylem in the stems (Kwon *et al.* 2001). In poplar, PCBER is one of the most abundant proteins in the woody tissue and localizes mainly in the young differentiating xylem, xylem parenchyma, and young differentiating phloem fibers (Vander Mijnsbrugge *et al.* 2000). High expressions of genes encoding for PCBERs were also detected in the stem of *Ginkgo biloba* (Cheng *et al*. 2013) and in leaves of *Coffea arabica* (Brandalise *et al.* 2009). These expression patterns were stimulated by the fungal infection, exposure to cadmium, mechanical damages, and phytohormone treatments (Sarry *et al*. 2006; Cheng *et al.* 2013). These results suggest that PCBER plays various roles in plant growth and development.

PCBERs, including purified polypeptides from plant tissues and recombinant enzymes derived from pine, ginkgo, and tobacco cDNAs, could reduce both DDC and DDDC to DDDDC and TDDC, respectively (Gang *et al*. 1999b; Shoji *et al*. 2002; Bayindir *et al*. 2008; Cheng *et al*. 2013; Niculaes *et al*. 2014). The purified PCBERs as well as PLR and pinoresinol reductase (PrR) could also reduce an 8–8′-linked lignan (PR), although the activities were relatively weaker compared to that of DDC (Gang *et al*. 1999b; Bayindir *et al*. 2008; Niculaes *et al*. 2014).

Except the PCBER localization and catalytic properties, the main roles of PCBERs in plants remain unclear. Recently, Dillon *et al*. (2010) revealed that single nucleotide polymorphisms (SNPs) in the PCBER gene exhibited significant associations with wood density of *P. radiata.* Moreover, although the

roles of PCBER in wood formation have not been well understood, it has been previously reported that down-regulation of PCBER expression caused reduction of the lignin content in the transgenic poplar (Boerjan *et al*. 2006). These results indicate that lignan and neolignan, in addition to genes for their biosynthesis, may play important roles in lignification and secondary cell wall formation.

In plants, especially in the xylem tissues, lignifying and nonlignifying cells live in a high concentration of hydrogen peroxide (H_2O_2) environment. Monolignols are exported to the apoplast and oxidized by peroxidases and then polymerized into lignin. Some monolignols are dimerized into lignans in the cytosol. Niculas with his coworker demonstrated that, in the absence of PCBER, H_2O_2 is consumed by the oxidation of monolignols, promoting the formation of cysteine adducts (Niculas *et al.* 2014). In addition, Matsuda (2010) with his coworkers demonstrated that reduced phenylpropanoid coupling products are generally better radical scavengers than nonreduced ones. Therefore, Niculas with his coworker suggest that, PCBER might increase the radical scavenging efficiency of the cell, and also suggest that when the reduced dilignols are radical scavengers, they must be oxidized back to the PCBER substrate (Niculas *et al.* 2014). It means, reduced neolignan catalyzed by PCBER enzyme could be cycled back to the original nonreduced neolignan under oxidative conditions. These reactions forming an antioxidant cycle which consume certain amounts of H_2O_2 to control oxidative balance of cells.

Although genes that encode polypeptides with sequences similar to identified PCBERs are found in the genome of *A. thaliana*, no functional characterization studies have been reported thus far in this species. In order to reveal the main role of PCBER in plants, we studied one of putative NADPH-dependent

oxidoreductase in *A. thaliana*, whose amino acid sequence is similar to those of identified PCBERs from various plant species.

1.3 Lignan biosynthetic enzymes in *A. thaliana*

In *A. thaliana*, two PLR candidate genes have been characterized, and namely *AtPrR1* and *AtPrR2*. Polypeptides encoded by them could reduce the PR to LR. AtPrR1 also could reduce the LR to SLR in the trace amount, but the reductive activity of AtPrR2 towards LR could not be detected *in vitro* (Nakatsubo *et al*. 2005). Functional characterizations have been performed on PCBERs in various plant species, no studies on putative PCBERs in *A. thaliana* have been reported so far.

Six genes whose polypeptides are similar to identified PCBERs from other plant species exist in the genome of *A. thaliana*. Among these genes, five genes (*AT1G75280*, *AT1G75290*, *AT1G75300*, *AT1G19540*, and *AT4G34540*) are documented to be homologs of isoflavone reductase or PLR in The Arabidopsis Information Resource database (https://www.arabidopsis.org/). By contrast, the gene studied in depth in this study, *AT4G39230*, is annotated as a putative gene for PCBER in The Arabidopsis Information Resource database. However, none of the studies has characterized the biochemical functions of the polypeptides encoded by these genes. In addition, the putative protein from *AT4G39230* shows high amino acid sequence identities (64% to 71%) with those of identified PCBERs, including from *L. corymbulosum* and *P. taeda*. In order to elucidate the in-depth roles of PCBERs in plant growth and development, we characterized the putative PCBER gene (*At4g39230*, designated *AtPCBER1*) in *A. thaliana*.

To review in more detail where *AtPCBER1* expresses, in addition to RT-PCR,

we fused the 2216 bp of *AtPCBER1* promoter sequence to the β-glucuronidase (GUS) reporter gene, *uidA*, and observe the blue staining tissues with 5-bromo-4-chloro-3-indolyl-beta-D-glucuronic acid (X-gluc.) in transgenic plants carrying this fusion construct.

To investigate the catalytic function of AtPCBER1, recombinant His-AtPCBER1 was produced in *E. coli* and purified by affinity chromatography. Catalytic properties of His-AtPCBER1 were characterized with three different substrates, DDC, PR, and LR.

To gain insight into the metabolic mechanisms controlled by *AtPCBER1*, we analyzed methanol-soluble metabolites prepared from the transgenic plants in which *AtPCBER1* was up- and down- regulated. In addition, for confirming the role of *AtPCBER1* expression in lignification process, we compared the lignin content profiles of our transgenic plants (with up- and down-regulated *AtPCBER1*) to that of wild-type *A. thaliana*.

1.4 Figures

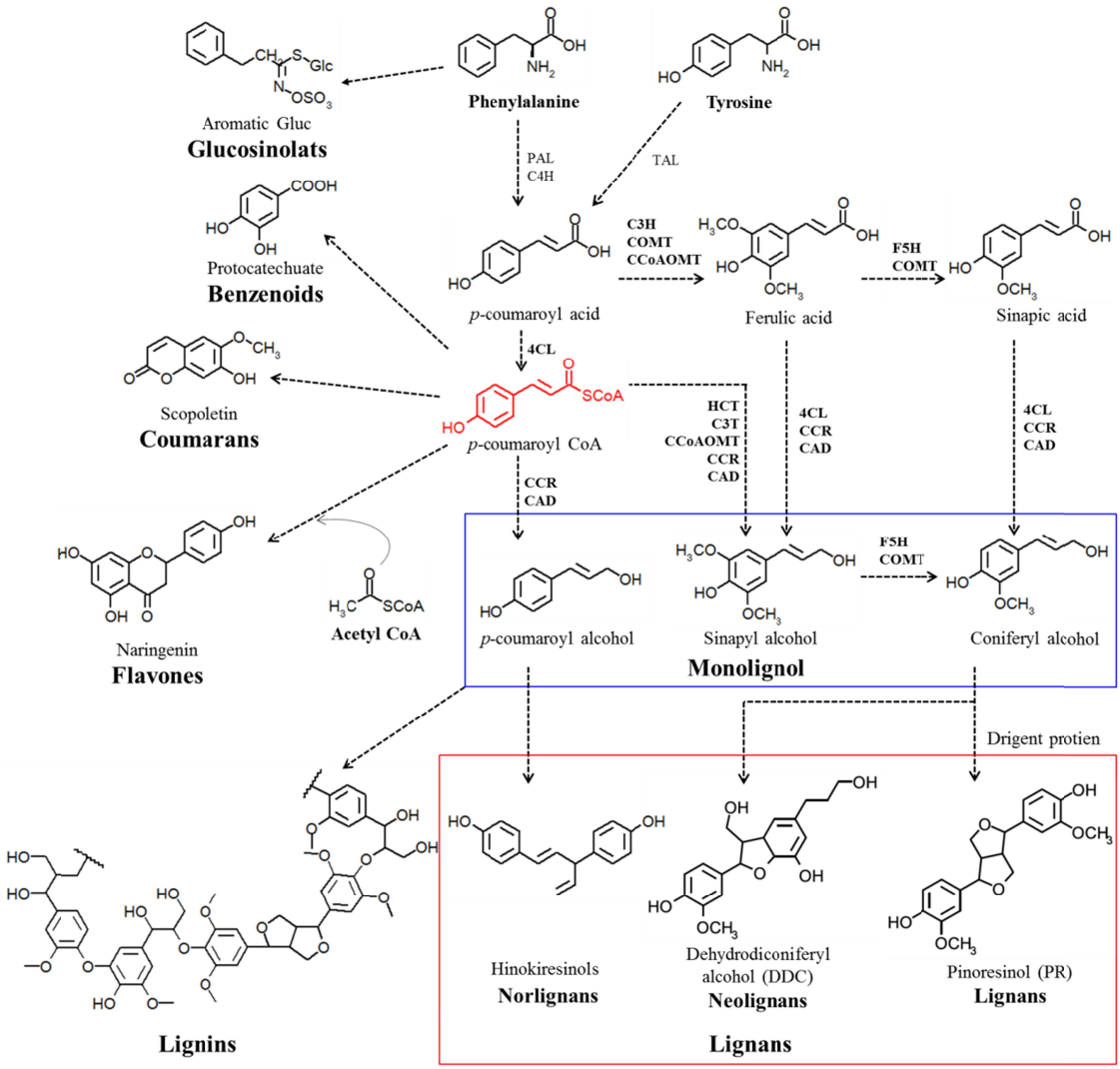

Figure 1-1 Common phenolics derived from phenylpropanoid pathways and some adjacent pathways. PAL: phenylalanine ammonia-lyase; C4H: cinnamate 4-hydroxylase; 4CL: 4-coumarate: CoA ligase; CCR: cinnamoyl-CoA reductase; HCT: hydroxycinnamoyl transferase; C3H: *p*-coumarate 3-hydroxylase; CCoAOMT: caffeoyl-CoA *O*-methyltransferase; CAD: cinnamyl alcohol dehydrogenase. COMT: caffeic acid 3-*O*-methyltransferase; CHS: chalcone synthase; CHI: chalcone isomerase; F5H: ferulate 5-hydroxylase.

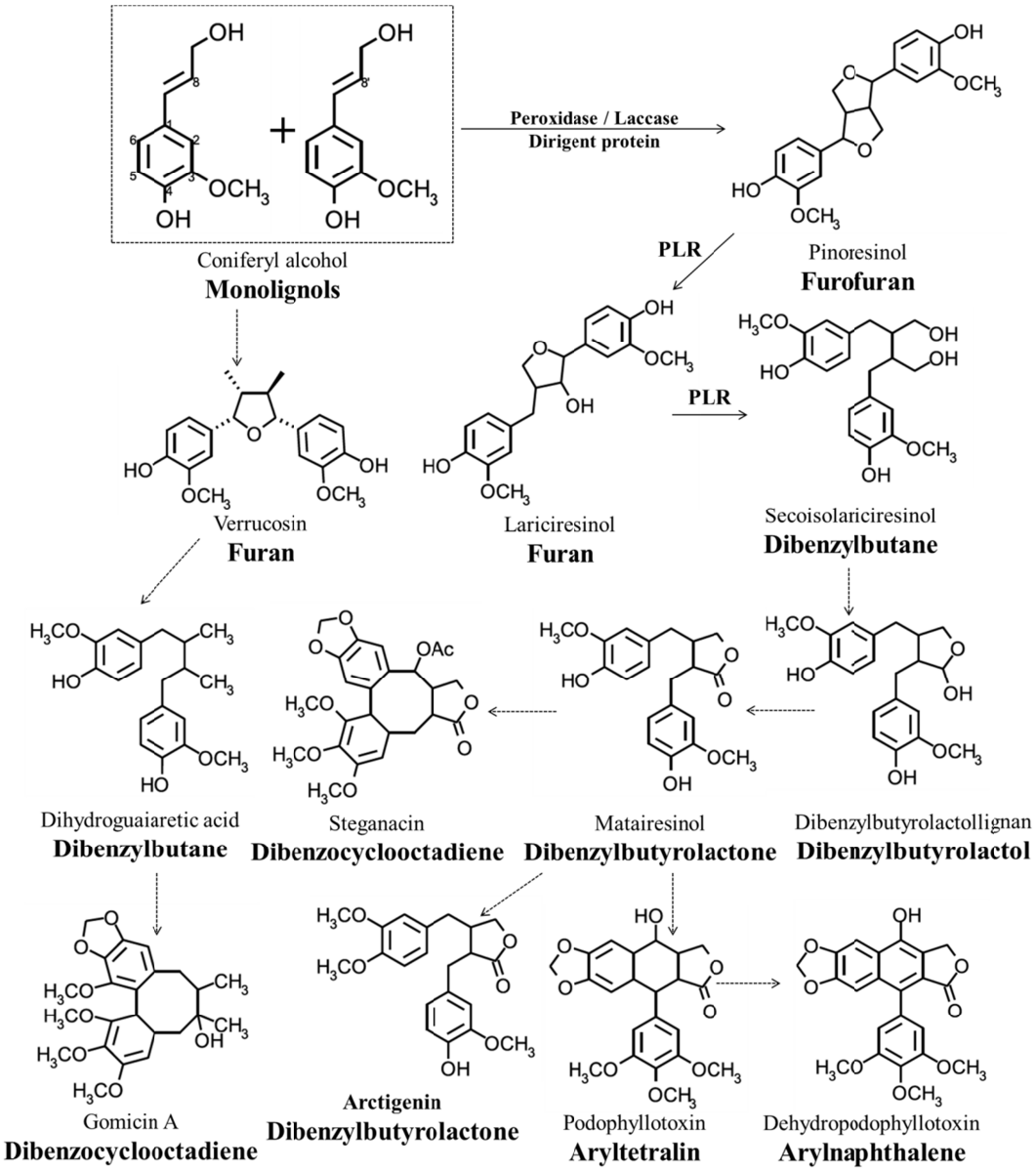

Figure. 1-2 The predicted biosynthesis pathway of monolignol-derived typical lignans.

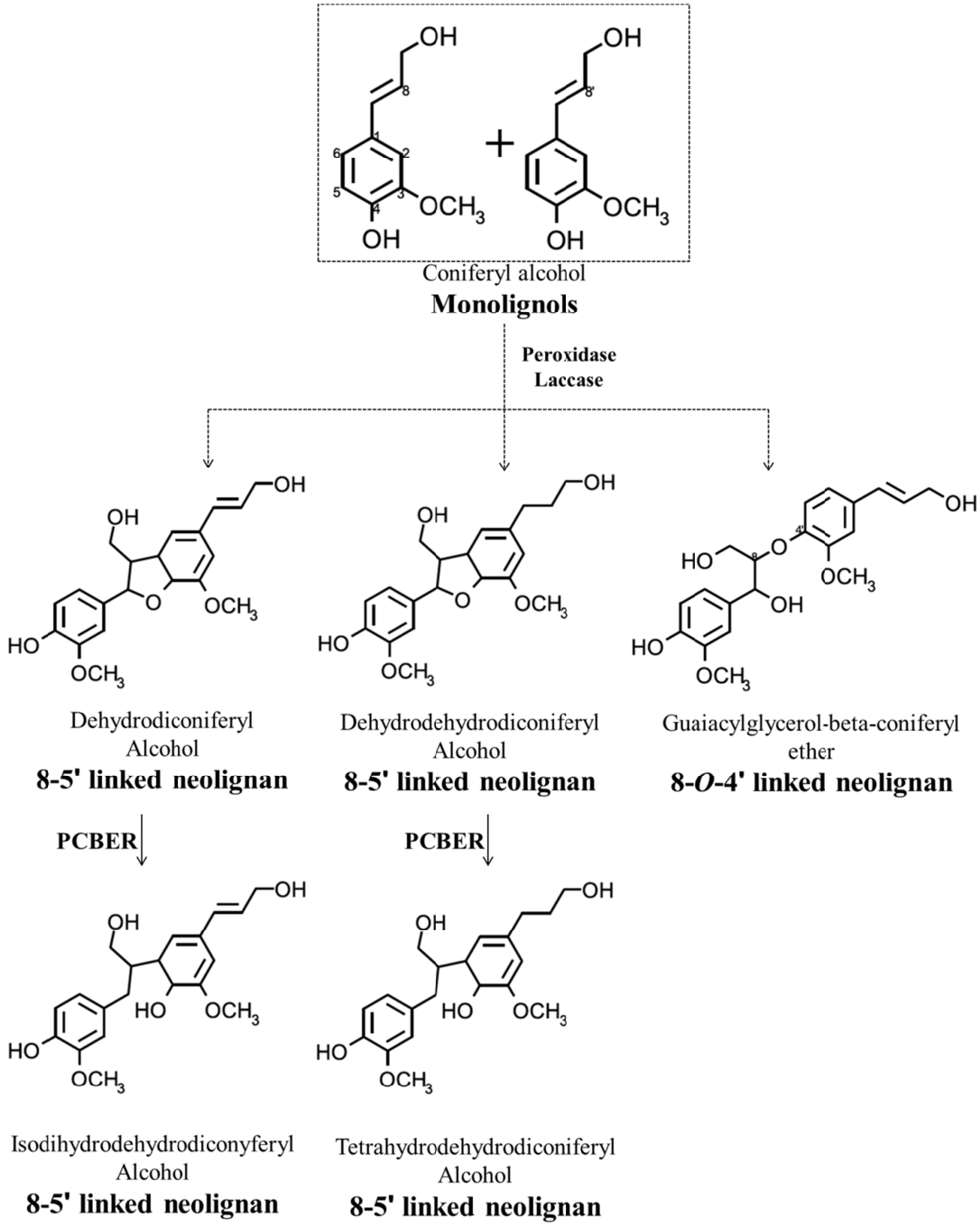

Figure. 1-3 The predicted biosynthesis pathway of monolignol-derived typical neolignans.

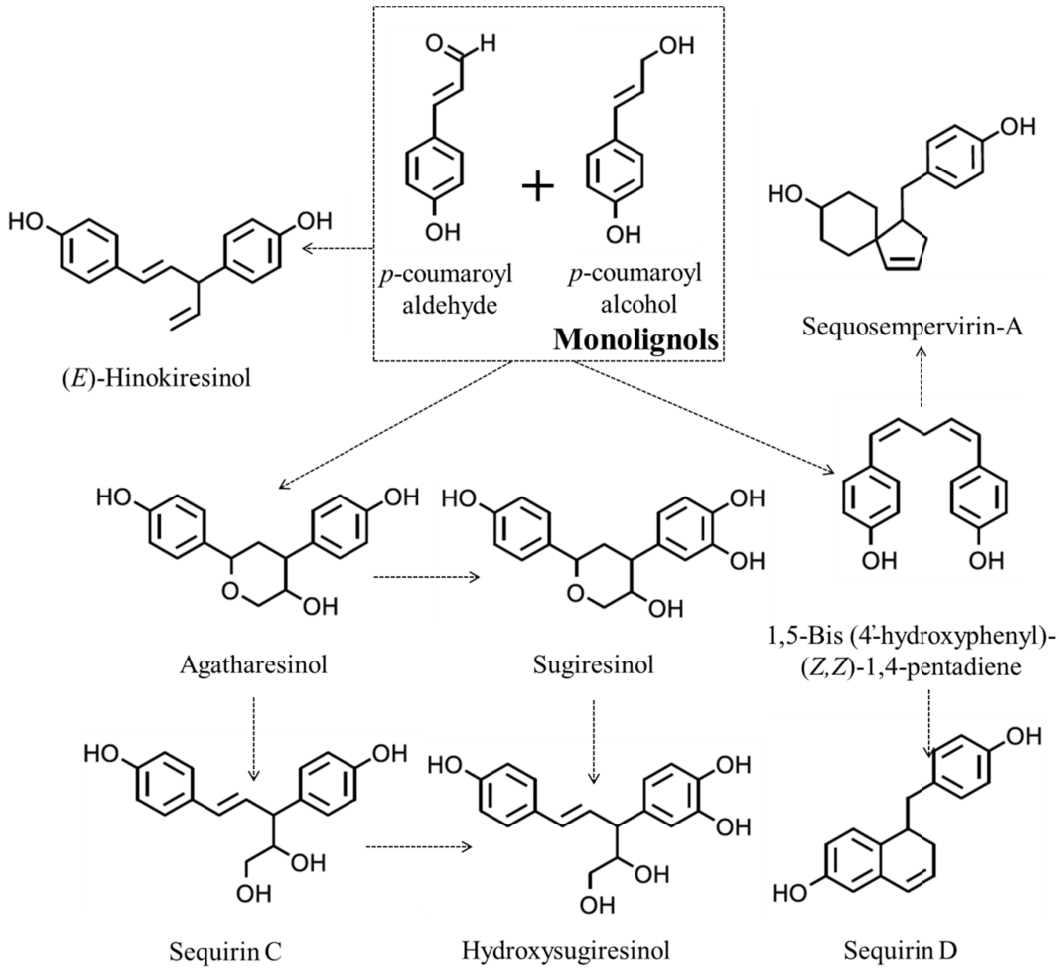

Figure. 1-4 The predicted biosynthesis pathway of monolignol-derived typical norlignans.

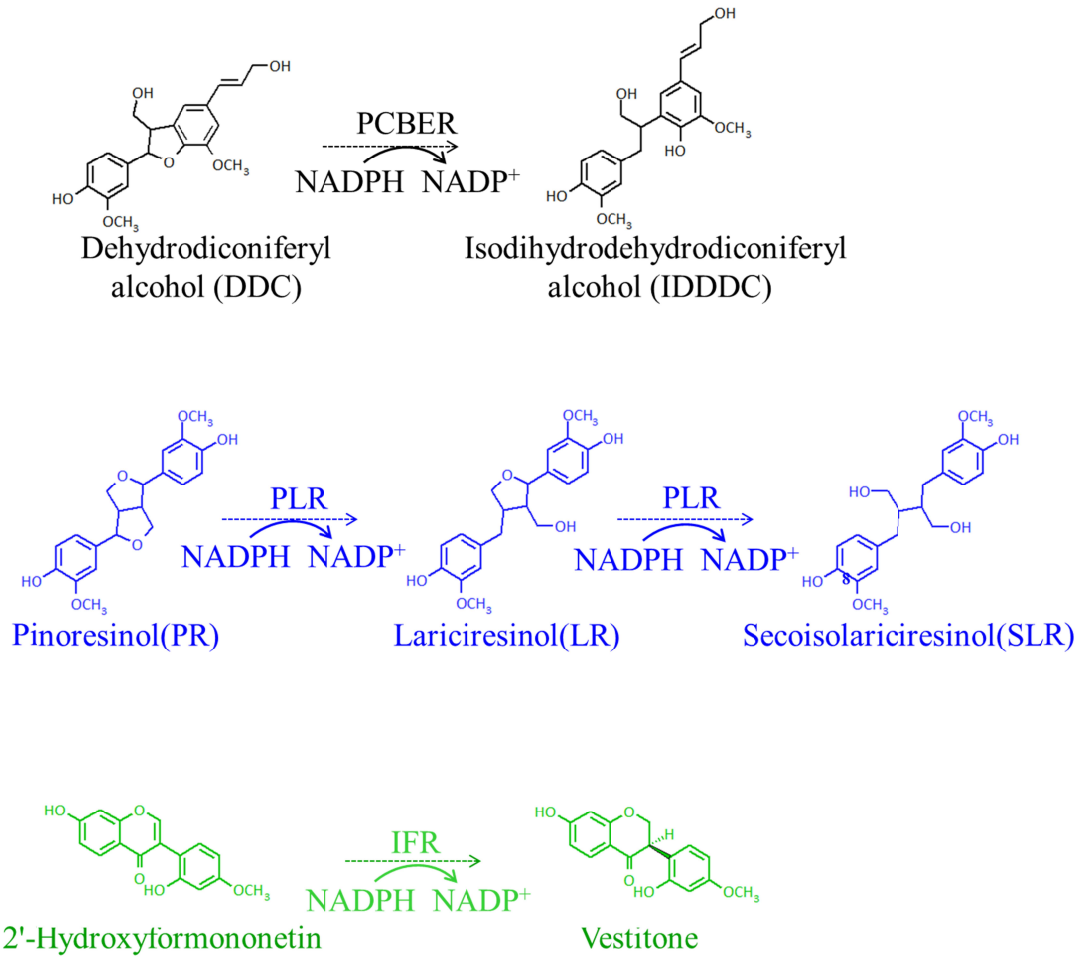

Fig. 1-5 Catalytic properties of NADPH-dependent reductases, PCBER, PLR and IFR.

PCBER: phenylcoumaran benzylic ether reductase

PLR: pinoresinol-lariciresinol reductase

IFR: isoflavone reductase

Chapter 2

Expression analysis of *AtPCBER1*

2.1 Introduction

AtPCBER1 exhibits the high similarity of its amino acid sequence with those of identified PCBERs. As mentioned in Chapter 1, *PCBER* genes are differentially expressed in various plant tissues. In poplar, PCBER was localized in the woody tissue and mainly in young differentiating xylem, xylem parenchyma, and young differentiating phloem fibers (Vander Mijnsbrugge *et al.* 2000). Similarly, PCBER was localized in the axial and radial parenchyma cells of secondary xylem of stems in *P. taeda*, (Kwon *et al.* 2001). High gene expression was also detected in the stem of *G. biloba* (Cheng *et al.* 2013), whereas, the high level of *PCBER* expression was detected in leaves of *C. arabica* (Brandalise *et al.* 2009) and petals of tobacco plants (Drews *et al.* 1992; Shoji *et al.* 2002). In addition, expression levels of some PCBERs were stimulated by fungal infection, exposure to cadmium, mechanical damage, and phytohormone treatment (Sarry *et al.* 2006; Cheng *et al.* 2013). These results suggest that PCBER plays various roles in plant.

To aim at illustrating the possible roles of *AtPCBER1* gene in Arabidopsis plant, we performed phylogenetic analysis of amino acid sequence of this enzyme, and expression analysis of the gene in different tissues. In order to reveal expression profile of the gene *in planta*, semi-quantitative reverse transcriptase-polymerase chain reaction (sqRT-PCR) with total RNA prepared

from different tissues and organs was performed. After cloning of the promoter region of *AtPCBER1* and subsequent construction of a fused construct with the promoter region and *uidA*, coding for β-glucuronidase (GUS), we also performed histochemical analysis of fused gene expression in transgenic plants harboring this gene construct. The expressions have been analyzed both under stress and non-stress conditions.

2.2 Materials and Methods

2.2. 1 Sequence analysis

Sequence information of *AtPCBER1* was obtained from The Arabidopsis Information Resource (TAIR). A multiple alignment of PCBER amino acid sequences from various plant species was generated using ClustalW (EMBL-EBI), and a rooted phylogenetic tree was constructed using ClustalW (http://www.genome.jp/tools/clustalw/). Sequence of the promoter region (2,216 bp) was analyzed *in silico* for *cis* regulatory sequences using PlantCare and PLACE (Lescot *et al.* 2002).

2.2.2 Isolation of genomic DNA and total RNA

To isolate total genomic DNA (gDNA), young rosette leaf tissue was placed in a microcentrifuge tube containing 200 μL of freshly prepared extraction buffer (200 mM Tris-HCl, 250 mM sodium chloride, 25 mM EDTA, and 0.1% sodium dodecyl sulfate) and homogenized with a mortar and pestle. The homogenized material was centrifuged and the supernatant was collected in a microcentrifuge tube. The total DNA remaining in the supernatant was precipitated with

isopropanol at room temperature. The pellet was washed twice using 70% ethanol and air dried before elution in 20 μL of sterile distilled water.

Total RNA was extracted from various tissues as described by Tamura *et al.* (2014). Briefly, the plants sample was homogenized with TRIzol® reagent and then 0.2 mL of chloroform per 1 mL of TRIZOL Reagent was added to the sample. After centrifugation, supernatant was transferred to new tube and the total RNA was precipitate by mixing with isopropyl alcohol. Further purification was performed using an RNeasy Plant Mini Kit (QIAGEN, Tokyo, Japan).

2.2.3 Construction of the promoter-GUS fused construct for generation of transgenic plants

To generate the vector with *uidA* coding for β-glucuronidase (GUS) under the control of the promoter of *AtPCBER1*, the promoter resion (2,216 nucleotides upstream from the start codon) was PCR-amplified using the two gene-specific primers (5′-GCTGCAGAAGCTTGATCTTCCTGACAAGCG-3′ and 5′-CGGGATCCTTTTAGACTCGGATTTTG-3′). Template gDNA was isolated from rosette leaf of wild-type plants and used for PCR amplification of the promoter. After the partial digestion of *AtPCBER1* promoter with *Hin*dIII and *Bam*HI and subsequent purification, the CaMV35S promoter of pBI121was replaced with the *AtPCBER1* promoter and fused transcriptionally to coding region of *uidA*. The resultant recombinant plasmid was designated pBI-pAtPCBER1 (**Fig. 2-4**) and then used for transformation of *A. thaliana* as described by Tamura *et al.* (2014).

2.2.4 Plant materials and growth conditions

Wild-type and transgenic *A. thaliana* used in this study were all in Columbia-0 background. Growth conditions of plants were reported in previously (Tamura *et al.*, 2014). Briefly, wild-type and transgenic plants seeds were surface-sterilized with 5% sodium hypochlorite and 0.3% Tween-20, and washed with sterilized water before sown on 0.8% (w/v) agar solidified Murashige and Skoog (MS) medium (**Table 2-1**) containing 30% (w/v) sucrose, 0.5 mg/L nicotinic acid, 100 mg/L *myo*-inositol, 2 mg/L glycine, 0.5 mg/L pyridoxine hydrochloride and 0.1 mg/L thiamine hydrochloride. After the sowing of the sterilized seeds, agar plates were placed under a 16 h light/8 h dark regime condition at 23°C for approximately 4 weeks. Then the germinated plants were removed from the plates and transplanted into soil.

2.2.5 Expression analysis of *AtPCBER1* using sqRT-PCR

Levels of *AtPCBER1* expression were quantified by sqRT-PCR analysis. Total RNA was isolated from flowers, stem, rosette leaf, root, leaf, and silique of 48-day-old wild type plants. Equal quantities of total RNA (2 μg) were used for synthesis of first-strand cDNA. Full length CDS was amplified with sequence-specific primers (PCBER-F, 5′-CGGGATCCGATGACGAGTAAAAGC-3′ and PCBER-R, 5′-TTGCGGCCGCTTCTGCAGTTAGACATATTGGTTG-3′). Semi-quantitative RT-PCR was performed with ExTaq DNA polymerase for 28 cycles. PCR products were separated by gel electrophoresis on a 1% agarose gel stained with ethidium bromide. Transcripts from *actin* gene were used as internal standard. The amplified DNA in the gel was quantified optically by ImageJ program.

2.2.6 Histochemical staining for GUS activity

Transgenic *A. thaliana* plants harboring the promoter-GUS construct were analyzed by histochemical staining for GUS activity using X-gluc. as substrate. Thirteen-day old seedlings, and flower, stem, and pollen of 48-day-old plants were immersed in staining solution (50 mM X-gluc., 10 mM EDTA, 0.1% Triton X-100, 50 mM $K_3[Fe(CN)_6]$, 50 mM $K_4[Fe(CN)_6]3H_2O$, 50 mM phosphate buffer pH 7.0) and incubation at 37 °C for 24–72 h. Then the staining solution was removed and the sample was washed with 70% ethanol until the tissue cleared. Whole samples were observed under an optical microscope (Leica Microsystems, Tokyo, Japan).

2.2.7 Abiotic stress treatment

Twenty eight day-old plants were used for mechanical wounding and ultraviolet (UV) radiation treatments. Mechanical damage was performed by punching holes in the rosette leaves and then treated leaves were incubated under a 16 h light/8 h dark regime condition at 23°C for for 1, 3 and 48 hours. Ultraviolet light exposure of leaves was performed in a clean bench for 1, 3 and 48 hours. Total RNA was isolated from the treated leaves and then used for RT-PCR analysis. The intact leaves without any stress treatments were used as the negative control samples.

2.3 Results

2.3.1 Sequence characterization of *AtPCBER1* gene

AtPCBER1 (*At4g39230*) gene was located on chromosome 4 of Arabidopsis,

and contained five exons and six introns. It contains 927 bp CDS and encodes a polypeptide of 308 amino acid residues with a predicted molecular mass of 34.7 kDa. The polypeptide contains a conserved NADPH binding domain, Gx(x)GxxG (positions 11 to 17), which is also common to other PCBERs (**Fig. 2-1**) and PLRs.

At the amino acid level, the sequence of AtPCBER1 shows high identities (64% to 71%) with those of previous identified PCBERs derived from other species, including *L. corymbulosum* and *P. taeda*. also shows high identities (52%-74%) with those of identified IFRs, but relatively low identities (37% to 44%) with PLRs derived from other species and low identities with AtPrR1 (38%) and AtPrR2 (37%). Furthermore, phylogenetic tree analysis indicated that *AtPCBER1* was clustered into the same clade with those of identified PCBERs from various species (**Fig. 2-1** and **2-2**). Without a doubt, AtPrR1 and AtPrR2 were clustered into the same clade with those of identified PLRs from various plant species.

The *cis*-acting regulatory elements on the cloned promoter region were analyzed by PlantCare (Lescot *et al.* 2002) and PLACE (Higo *et al.* 1999) programs. Some of the putative core sequences for response to biotic and abiotic stimuli such as phytohormones, wounding, and dehydration could be found in the promoter region (**Fig. 2-3**). Predicted *cis* elements for organ and tissue-specific expression in pollen and xylem have also been observed in the cloned sequence. Although the roles of these *cis* elements were not fully elucidated in this study, they likely function in part at least.

2.3.2 Expression analysis using semi-quantitative RT-PCR

To investigate expression of *AtPCBER1* in different tissues, semi-quantitative RT-PCR analysis was performed using gene-specific primers and total RNA from various tissues of 48-day-old plants. Amplified DNA from transcripts of the gene was detected in all of the tissues tested (**Fig. 2-5a**). According to digital image analysis of RT-PCR amplification, the highest expression was shown in whole flower and then followed by rosette leaf, root, stem, silique and cauline leaf (**Fig. 2-5b**).

2.3.3 Histochemical analysis of *AtPCBER1* gene using promoter GUS fusion system

In addition to RT-PCR, tissue-specific expression of *AtPCBER1* was monitored by histochemical analysis of GUS activity in the transgenic plants harboring the *AtPCBER1* promoter fused with *uidA* coding for β-glucuronidase (GUS).

The results of the histochemical GUS analysis of 13-day-old seedling and 48-day-old flower, stem, and root of the transgenic *A. thaliana* containing the construct indicated that *AtPCBER1* expressed mainly in vascular tissues of the leaf, root, petal and stem during different developmental stages (**Fig. 2-6a, b**, **c**, and **d**).

In young seedlings (**Fig. 2-6a**), relatively strong expression was observed in the tissues around the apical meristem in addition to cotyledon veins (**Fig. 2-6a**). In the root, GUS staining was detected with higher level in the root meristem and elongation zone where active cell expansion and elongation were occurring (**Fig. 2-6b**). In developing flowers of *A. thaliana*, high expression levels were also

detected in buds, sepals, petals, stigmas and filaments (**Fig. 2-6c** and **d**). In addition, strong GUS activity was observed in pollens. Interestingly, a brindled staining pattern was observed in stem inflorescences (**Fig. 2-6e**).

2.2.4 *AtPCBER1* was induced by abiotic stresses

Interestingly, the level of GUS expression markedly increased in the wounding stem and vascular tissue of leaves adjacent to the mechanical wound sites (**Fig. 2-7a** and **b**). But no significant increase in fold-expression could be detected in cells surrounding the wound sites. The increased expression has been also observed in leaves after UV irradiation (**Fig.2-7c** and **d**). Moreover, as shown in **Fig. 2-7**, expression responsible to mechanical wounding and UV irradiation increased with the treatment time when performing semi-quantitative RT-PCR analysis.

2.4 Discussion

Semi-quantitative RT-PCR analysis revealed that the highest expression of *AtPCBER1* was detected in flower and followed by rosette leaf and root. Pattern of this expression is nearly identical to the data deposited in the eFP Browser. In the eFP Browser (http://bar.utoronto.ca/efp/cgi-bin/efpWeb.cgi), microarray data indicate that *AtPCBER1* is in the highest levels expressed in pollen, followed by flower, shoot apex, hypocotyl, the first node, root and seed.

Furthermore, our GUS staining results adequately revealed that *AtPCBER1* was expressed in higher level in shoot apex (**Fig. 2-6a**), hypocotyl (**Fig. 2-6a**) and node (**Fig. 2-6e**), although the quantitative analysis for small parts of organs was not performed. To the best of our knowledge, this is the first report to

confirm the expression of an Arabidopsis homolog of *PCBER* by histochemical analysis of transgenic plants with the promoter region fused to *uidA*. Results also indicated that *AtPCBER1* was expressed in stem, leaf, and root tissues of different developmental stages, and tissues surrounding the apical meristem (**Fig. 2-6**), as well as in pollens. And *AtPCBER1* expressed in part of the elongation area, such as, in hypocotyl as well as in root apex (**Fig. 2-6)**. Menges *et al.* (2002) revealed that *AtPCBER1* expression was involved in cell division-related processes. All these results suggest that, *AtPCBER1* may have a particular role in plant growth and development. Clearly, *AtPCBER1* gene expression level and ubiquitous locations are a little bit different from those of other genes for PCBERs as mentioned above.

It is clear that, except *PCBER* mainly expressed in leaves of *C. arabica*, genes for PCBERs expressed in stems in all tested plants including poplar (Vander Mijnsbrugge *et al*. 2000), *P. taeda* (Kwon *et al*. 2001), *G. biloba* (Cheng *et al*. 2013) and tobacco (Drews *et al.* 1992) as well as in Arabidopsis, although the expression levels were different upon plant species. In addition, *PCBER* is the most abundant gene in poplar woody tissues (Vander Mijnsbrugge *et al*. 2000). It is predicted that *PCBER* might be involved in active lignification.

Previously characterized PLR candidate genes *AtPrR1* and *AtPrR2* exhibited strong expressions in the root and relatively lower expression in the stem (Nakatsubo *et al.* 2008). These data were also in accordance with microarray data in eFP Browser. That is to say, neither of them expressed in flowers as well as in pollens, or expressed at the detective level. *AtPCBER1* at the high level expressed in flower organs as well as pollens. These tissue-specific expression patterns of *AtPCBER1*, *AtPrR1* and *AtPrR2* may be related to their corresponding

functions in plants.

Previous studies demonstrated that, *cis*-acting elements controlled by *trans*-transcriptional factors are involved in stress inducible gene expressions (Boter *et al.* 2004; Dubouzet *et al.* 2003). However, except the one of MBS motif, which considered to be a MYB binding site involved in drought response, we not found those of potential *cis*-acting motifs for ABRE, MYC, and DRE/CRT in the 2016 bp long 5'-upstream sequence of *AtPCBER1* gene. *Cis*-acting elements for pollen specific expression, found in the tomato *lat52* gene (Bate and Twell 1998), were identified in the promoter region of *AtPCBER1* (**Fig. 2-3**). Correspondingly, our GUS staining results indicate that *AtPCBER1* was high level expressed in pollen in Arabidopsis. Predicted AC elements for xylem-specific expression also could be observed in the promoter region of *AtPCBER1* (**Fig. 2-3**). In accordance to this result, *AtPCBER1* expression was highly concentrated in vascular tissues of root, petal, cauline and rosette leaves (**Fig. 2-6a**, **b**, **c**, and **f**). Although this expression pattern in the stem was not as clear as in these organs, *AtPCBER1* expression was also observed in the vascular tissue of the stem (**Fig. 2-6e**).

As mentioned before, PCBER polypeptides have been reported as allergenic pollen proteins (Karamloo *et al.* 2001; Jimenez-Lopez *et al.* 2013) and their expressions were induced by fungal infection and mechanical injury and oxidative stresses (Brandalise *et al.* 2009; Cheng *et al.* 2013). Here, *AtPCBER1* expression was significantly induced by mechanical wounding and ultraviolet-light treatment. Interestingly, core *cis*-acting elements that regulate expression of the gene in response to wounding responses were identified within the promoter region of *AtPCBER1*. These results, including the analysis of cis-acting regulatory elements on the cloned promoter region suggest that,

AtPCBER1 expression may be also induced by ethylene, salicylic acid and pathogen infection and drought stress. Furthermore, methyl jasmonate, gibberellin and auxin may affect transcription level of *AtPCBER1* in Arabidopsis.

Taken together these results indicate that *AtPCBER1* contributes, at least in part, to *A. thaliana* biotic and/or abiotic stress responses, particularly in vascular (xylem) tissue, as shown in other plant species.

2.5 Tables and Figures

Table 2-1 Composition of Murashige and Skoog medium

Major salts	
Potassium phosphate (KH_2PO_4)	170 mg/L
Magnesium sulphate ($MgSO_4 \cdot 7H_2O$)	370 mg/L
Calcium chloride ($CaCl_2 \cdot 2H_2O$)	440 mg/L
Ammonium nitrate (NH_4NO_3)	1,650 mg/L
Potassium nitrate (KNO_3)	1,900 mg/L
Minor salts	
Ferrous sulphate ($FeSO_4 \cdot 7H_2O$)	27.8 mg/L
$Na_2EDTA \cdot 2H_2O$	37.2 mg/L
Boric acid (H_3BO_3)	6.2 mg/L
Cobalt chloride ($CoCl_2 \cdot 6H_2O$)	0.025 mg/L
Cupric sulphate ($CuSO_4 \cdot 5H_2O$)	0.025 mg/L
Manganese sulphate ($MnSO_4 \cdot 4H_2O$)	22.3 mg/L
Potassium iodide (KI)	0.83 mg/L
Sodium molybdate ($Na_2MoO_4 \cdot 2H_2O$)	0.25 mg/L
Zinc sulphate ($ZnSO_4 \cdot 7H_2O$)	8.6 mg/L
Vitamins and amino acid	
myo-Inositol	100 mg/L
Nicotinic acid	0.5 mg/L
Pyridoxine · HCl	0.5 mg/L
Thiamine · HCl	0.1 mg/L
Glycine	2 mg/L
Sucrose	30 g/L
pH	5.8

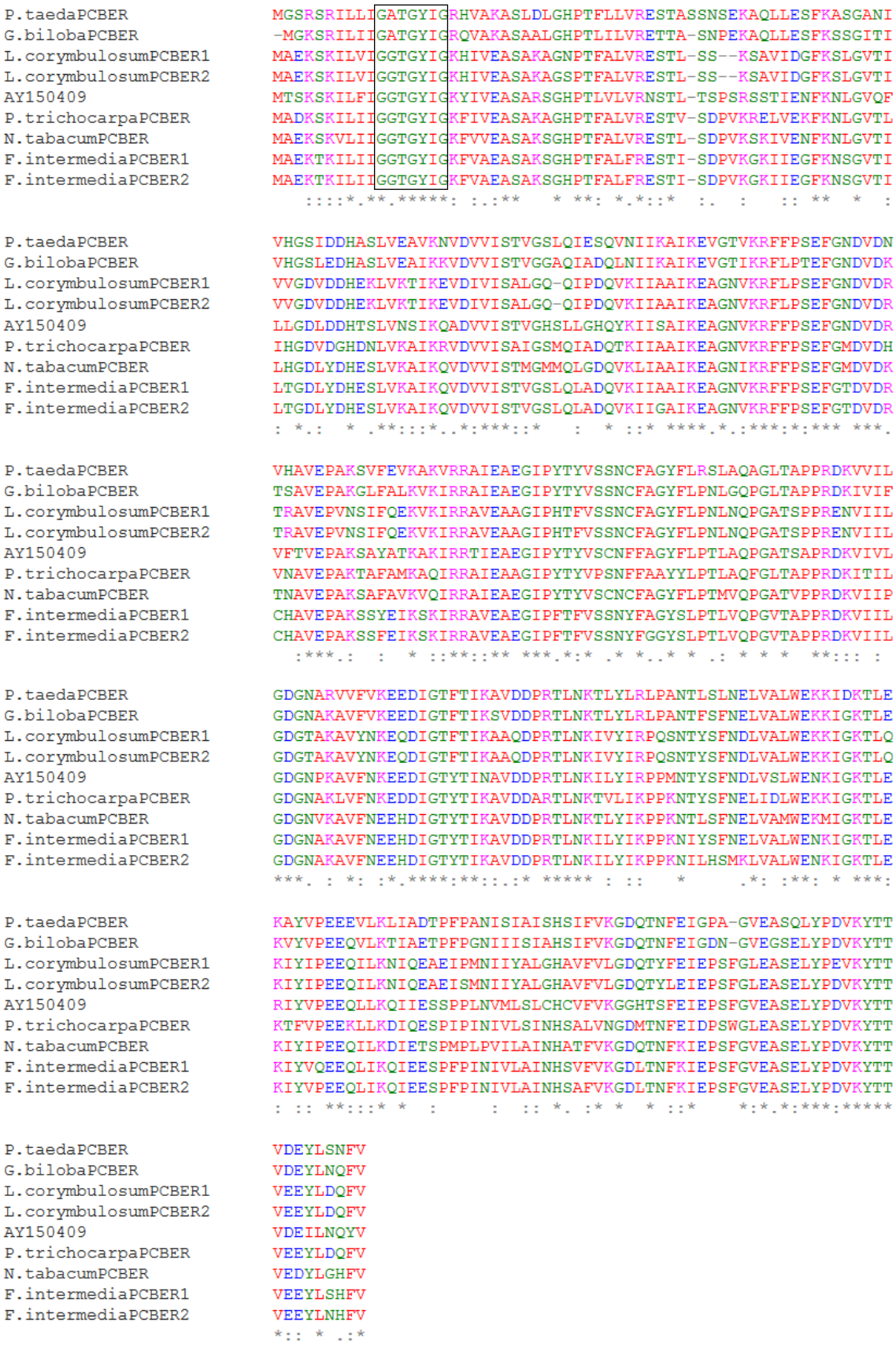

Figure. 2-1 Alignment of amino acid sequences of AtPCBER1 (accession number: AY150409) and

other PCBERs from various species of plants. Color indicates the structurally similar amino acid residues as follows: red: A, V, F, P, M, I, L, W; blue: D and E; magenta: R and K; green: S, T, Y, H, C, N, G and Q; grey: others unusual amino acid. Black box indicates the putative NAD(P)H binding motif.

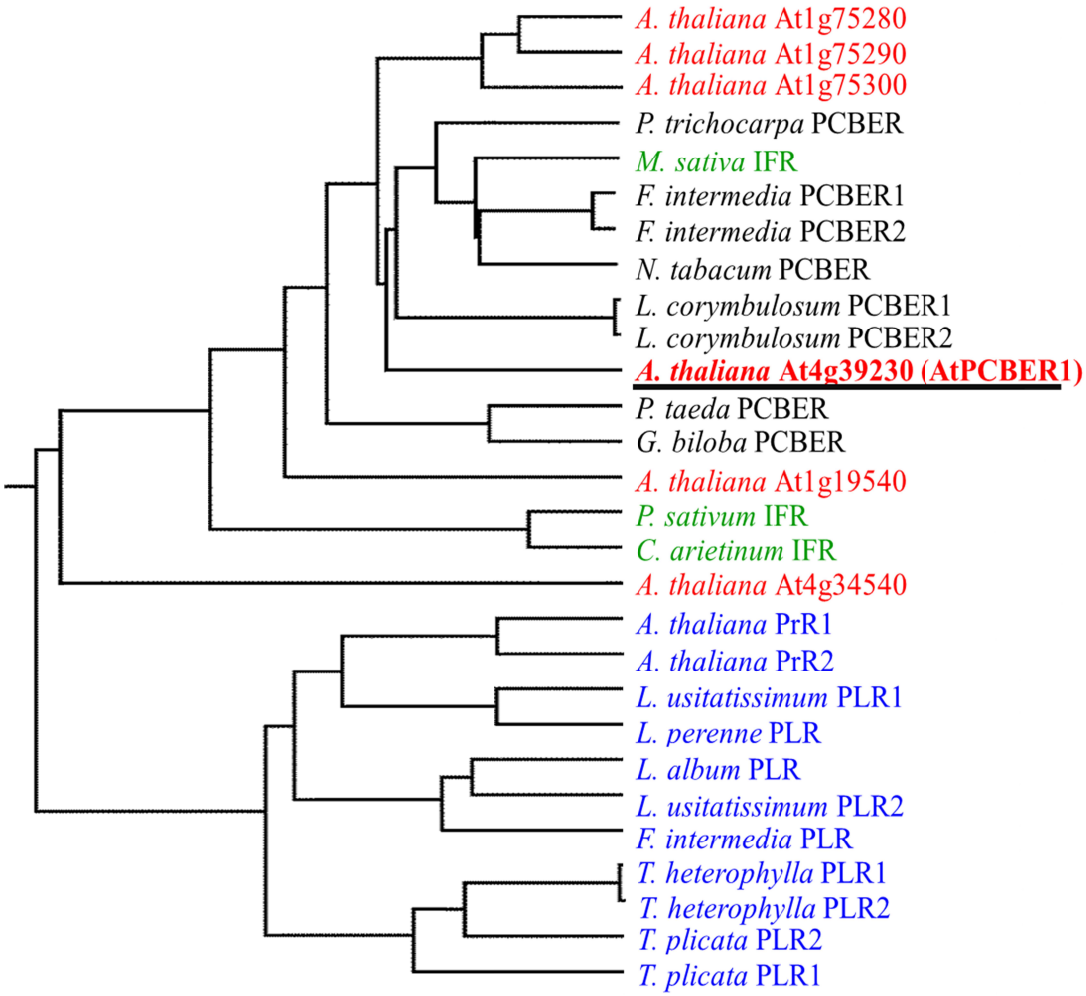

Figure. 2-2 Phylogenetic relationships of NADPH-dependent reductases PCBERs (black), PLRs (blue), and IFRs (green) derived from various plant species. ClustalW (Japanese GenomeNet Service, http://www.genome.jp/tools/clustalw/) was used for the multiple sequence alignment and phylogenetic tree construction. The protein sequences for PCBERs, PLRs, and IFRs were obtained from the National Centre for Biotechnology Information (NCBI) Gene bank. The sequence accession numbers are as follows: *A. thaliana* (At4g39230), AY150409; *A. thaliana* (At1g75280), AY117175; *A. thaliana* (At1g75290), BT033106; *A. thaliana* (At1g75300), BT008345; *A. thaliana* (At1g19540), BT024779; *A. thaliana* (At4g34540), NM_119619; *A. thaliana* (AtPrR1), AY096520 (Nakatsubo *et al.* 2008); *A. thaliana* (AtPrR2), BT004406 (Nakatsubo *et al.* 2008); *Populus trichocarpa* (PCBER),

AJ005803 (Gang *et al.* 1999b); *L. corymbulosum* (PCBER1), EU360968 (Bayindir *et al.* 2008); *L. corymbulosum* (PCBER2), EU360969 (Bayindir *et al.* 2008); *P. taeda* PCBER1, AF242490 (Gang *et al.* 1999b); *F. intermedia* PCBER1, AF242491 (Gang *et al.* 1997); *F. intermedia* PCBER2, AF242492 (Gang *et al.* 1997); *Nicotiana tabacum* PCBER, AB445398 (Shoji *et al.* 2002); *G. biloba* PCBER, KC244282 (Cheng *et al.* 2013); *Linum album* PLR, AJ849358 (Heimendahl von Heimendahl *et al.* 2005); *L. usitatissimum* PLR1, AJ849359 (Banerjee and Chattopadhyay 2010); *L. corymbulosum* PLR1, EU107358 (Bayindir *et al.* 2008); *L. perenne* PL), EF050530 (Hemmatia *et al.* 2007); *T. plicata* PLR1, AF242503 (Fujita *et al.* 1999); *T. plicata* PLR2, AF242504 (Fujita *et al.* 1999); *T. heterophylla* PLR1, AF242501 (Gang *et al.* 1999b); *T. heterophylla* PLR2, AF242502 (Gang *et al.* 1999b); *F. intermedia* PLR, U81158 (Dinkova-Kostova *et al.* 1996); *Pisum sativum* IFR, S72472 (Paiva *et al.* 1994); *Cicer arietinum* IFR, X60755 (Tiemann *et al.* 1991); and *Medicago sativa* IFR, X58078 (Paiva *et al.* 1991).

GATCTTCCTGACAAGCGTGATGGCTCGAGAATGTCGAATCTCGGGGGAAATCTTGCG

ATTATGTTTAACCTTGAGAAGGGTTCAACCAAAATCTGTTGCACGGAGATCAGATTG

GAAAGGAGGGAAGGAGGAAAGATTTGGGGGACGGTCCTGTGGTCTAATATTGTCATT

ACCTTGAAAGAACCTTCCACCATTGTACGATGTCTAACTGTAACAGTTTGATAAAGGT

ATGCTCCCGACTCCAATGACATTGGCTTTGTGATGAATTCATAATATTAATTTTGGATT

GATACTTGTTCTGGTATGTCTTGTAACAATGGCATTCAGATATTATCCTGCTTAGATTA

AGTGTGATGGTATATTTTTGTTGAGATGGGCATTCATAAGTCATGTTCTTGTATGTTGC

AGCTTCAAGCTTGAAAATCATATCTGTAAACGTGTACCGGAGCAGCTTGTTCTGTTCA

AGATGAAACAAACAACATACGAGGCTTTATTGGATATTGGTATCCAGAACCTAATATA

GATATCTTTTGGAACTTTGGGCTAAGTTATGCAATATATTTCTCTTGTTTCTTTGTTGTA

CGACTCTTATGTATGCAAGTATATTGTATGATTAATAGAAACTATGTTACCAGCTGTTT

GTTTAACAAAGATCAAACCAATAACATTTGAAATGTTTGAATTCAAATCTGGTCTCTA

GGTCGGAAAAGTTGATTTACAAAGAAACTTATATGTGATGTTAAACAAGAGAAACGA

CATCAAACGCAGAAGGAAAGAAGCTAGTCTTTACTCCGAGACTGTCGTCTGAAGAG

GCAATTGACTCTCGACTCCCTTTGCCTCCACAGCTTGCTTCTCTGCGACCGCCTTTGA

CAATCCAAACATCTGAAATCAACATACATAAGCTTAAGTTTAGGAGACAGATGATCA

CCAAATGGAGCTGTAAAGAGCAAATTGATTGACGCCAGAAATCACAATTTGTAGCAA

GTGTATTCAACAATCTCCTATGAGTGAGTACATGGGGTCTGAAACATTGAATACCAGC

TAAGAGAGTTTATTCGAGGACTAAATCTAAAAAAAAAAAAAAAAAAAAAAAAAAAA

AAAAAAAAAAAAATCTAAGCTATAATAAGAGAGTTGAGAAAGAACCTTTTTGATGGT

CTTTTGGAAACAGGACTTGTGTTCATCCATTGAGGCATGTATAAAGTCATCAATGTGA

TCTTTCACGTCCTCAAAGAAAGTGGCATCATCCTTTACCTTCTTCCTACATGAAGTCA

TGGCCGGTTTCGGACTTTGATTTGTCTGGGTCTCCATTTGTACCTGCAAAATAATTGA

ACAAGAAATTCAACCCAAGTAAACGACACTTAGCAACCAGAAAATTCATAATCCCAA

AATGCACATTCAATATTATAAAAGAGTAGAGATAATTGTTTACAAACTAGAACAAAAA

CCGAAATGAATCGTCGGGTGTTGTTGTTCAGGTTCAGCAGCACATCCAAAACAATAA

AGTACACAATCAAATTGTCAAAGTAGAACCCTAAACAAAAAAAAACTCAACGATTCC

AAACAAAATTCTTTCAAATCCTGAACTGAACATCACCATCCATTATCCGTATCCACCT

AACTACAAGCAAGGAAAGAGATCGAAGAACAAGAATAAGAGCTTCATGATTAATTTT

ACCTCTACGAGATCTTTCAATTCGTCTCCTTCTTCTTCTTCTTCTAAACGAGAAGAGG

AGGTTCTAGACTTGTTTAGTTTTAGTAATCAGCTACAACGAGAAGACGCTGTTAATCC

TTGCAGAACAAGTGGTGAAAAACGCATCGTTTTATTATAATAATGTTAACAATATGGG

CCTTTCACGATGGCCCAATAAAAACATTATTACAACGTCTATTAGGATAACAGCCCAC

GTCTCAAAGAAAGTTGAGTCATAAAAAGCCGCCAATTTCACCAACCACGTCTCAACT

TTTGACTAAAAAGTAAACGTAAGTGTTGACTACAGAGGGTATTATTGTCAGATTCTCC

ATAAGCCTCTTCTCTCTCTCTCAGAGTGTGGTGGTTTCATACTATTTATGTAAAAGGA

AGCAACGGGTGAGAAGAATTAAAAAGCCGCAATTTTGGGATCATAAGAGTTCTCTTC

TTCATCTGTGATTCATTCCGTTGTTACCCGCCAGGCACCAGCCACCGTACTTTTTCTC

TCTCCGGCAAAATCCGAGTCTAAAA**ATG**

ATG: translational initiation codon

AC-I element: restricted expression in xylem

AC-II element: enhanced expression in xylem; enhancement of petal expression

GCC box: wounding and pathogen responses

TCA element: salicylic acid response element

TGA element: auxin response

TGACG motif: response to methyl jasmonate

Box-S: wounding and pathogen responses

***lat52* element**: pollen specific activation

CCGTCC box: meristem specific activation

ERE motif: ethylene-responsive element

GARE motif: gibberellin-responsive element

MBS: MYB binding site for drought response

Figure 2-3 The cloned sequence of the promoter region of *AtPCBER1* (*At4g39230*) and predicted *cis*-regulatory elements. *In silico* analyses were performed using the online tools of PlantCare (http://bioinformatics.psb.ugent.be/webtools/plantcare/html/) and PLACE (http://www.dna.affrc.go.jp/PLACE/).

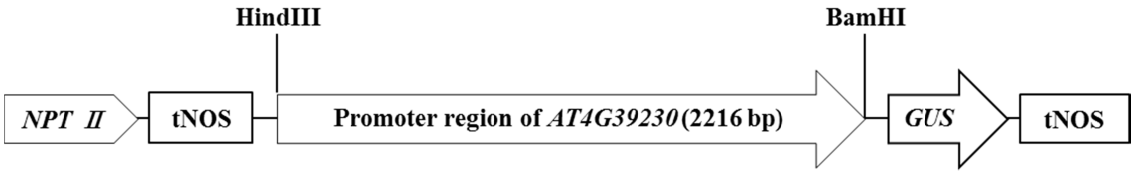

Figure 2-4 Representative structure of promoter-GUS fusion cassette.

NPTII: Kanamycin resistence gene

tNOS: Terminater sequence of nopaline synthase gene (from the Ti plasmid of *Agrobacterium tumefaciens*)

GUS: β-glucuronidase gene, *uidA*

HindIII: Restriction enzyme, *Hin*dIII, recognition site

BamHI: Restriction enzyme, *Bam*HI, recognition site

a

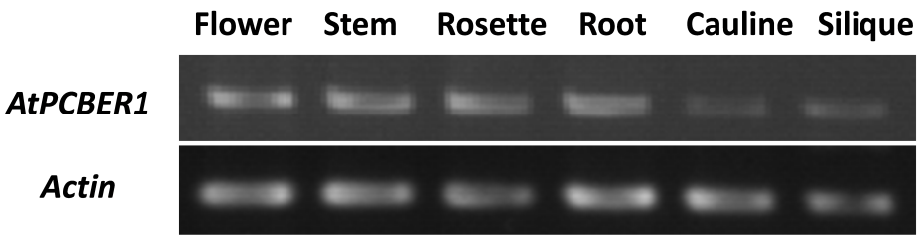

b

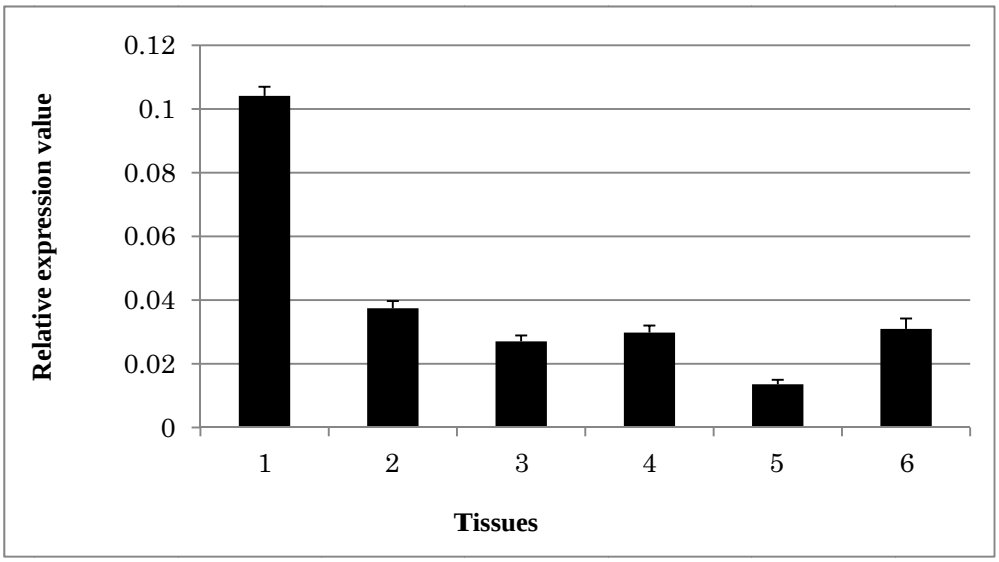

Figure 2-5 Expression profiles of *AtPCBER1* in 48-day-old *A. thaliana* organs measured by semi-quantitative RT-PCR analysis. Equal quantities of total RNA (2 μg) was isolated from 48-day-old wild type plant's flowers (1), rosette leaf (2), stem (3), root (4), cauline leaf (5) and sillique (6). And the gene *AtPCBER1* was amplified with the full length CDS primer pairs and RT-PCR products were analyzed by 1% agarose gel electrophoresis and stained with ethidium bromide. Transcripts of *actin* gene were used as the internal control. a. Semi-quantitative RT-PCR analysis. b. The density of DNA electrophoresis band was quantified by ImageJ Program. Each value is the mean of three independent replicates, and error bars indicate SD.

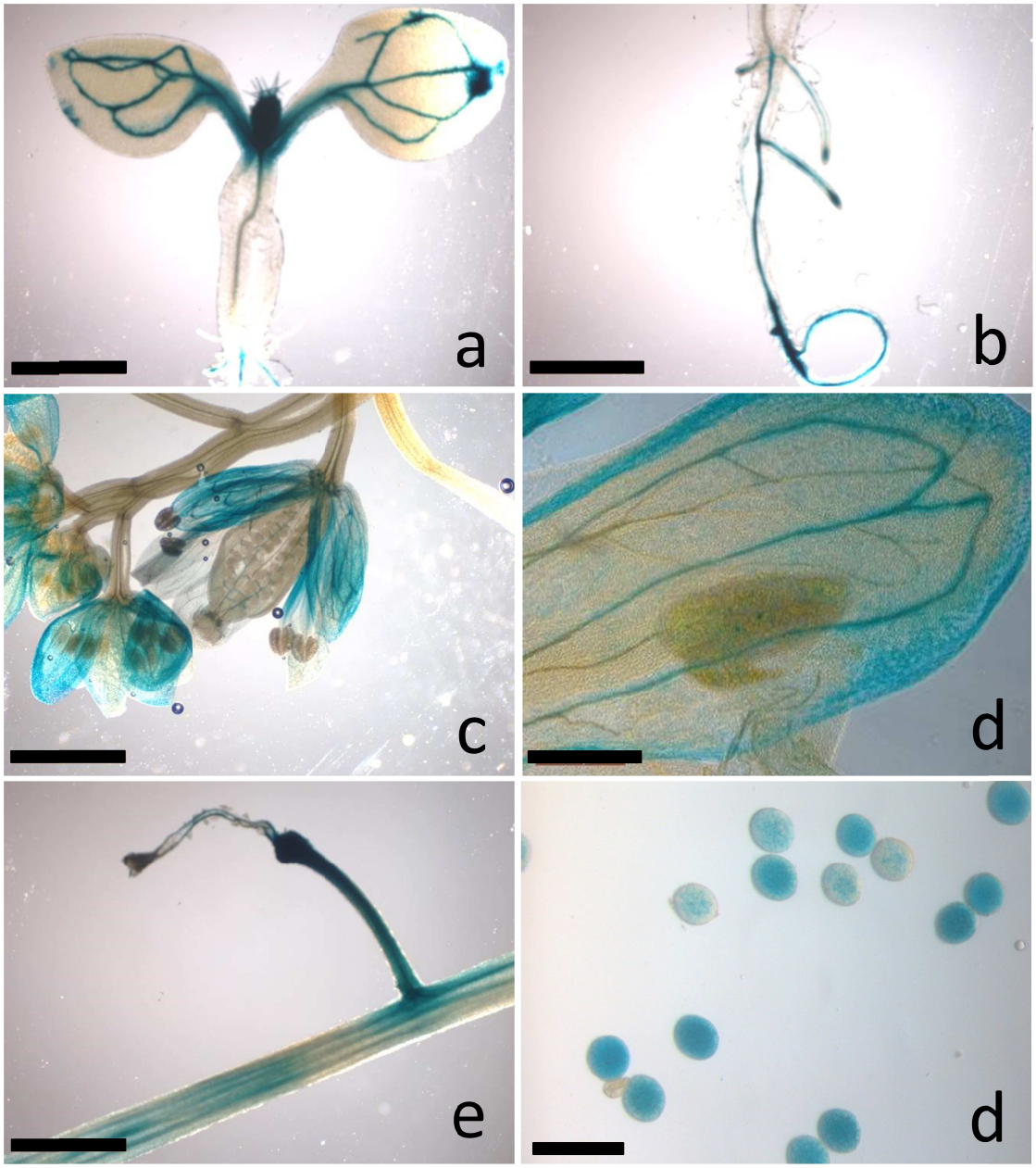

Figure 2-6 Histochemical localization of *uidA* gene expression driven by the promoter of *AtPCBER1*. **a**, Seedling with fully developed cotyledon; **b**, root; **c**, flower bud; **d**, petal; **e**, stem; and **f**, pollen. Scale bars: 500 μm (a, b, c, and e); 50 μm (d); 1 mm (f).

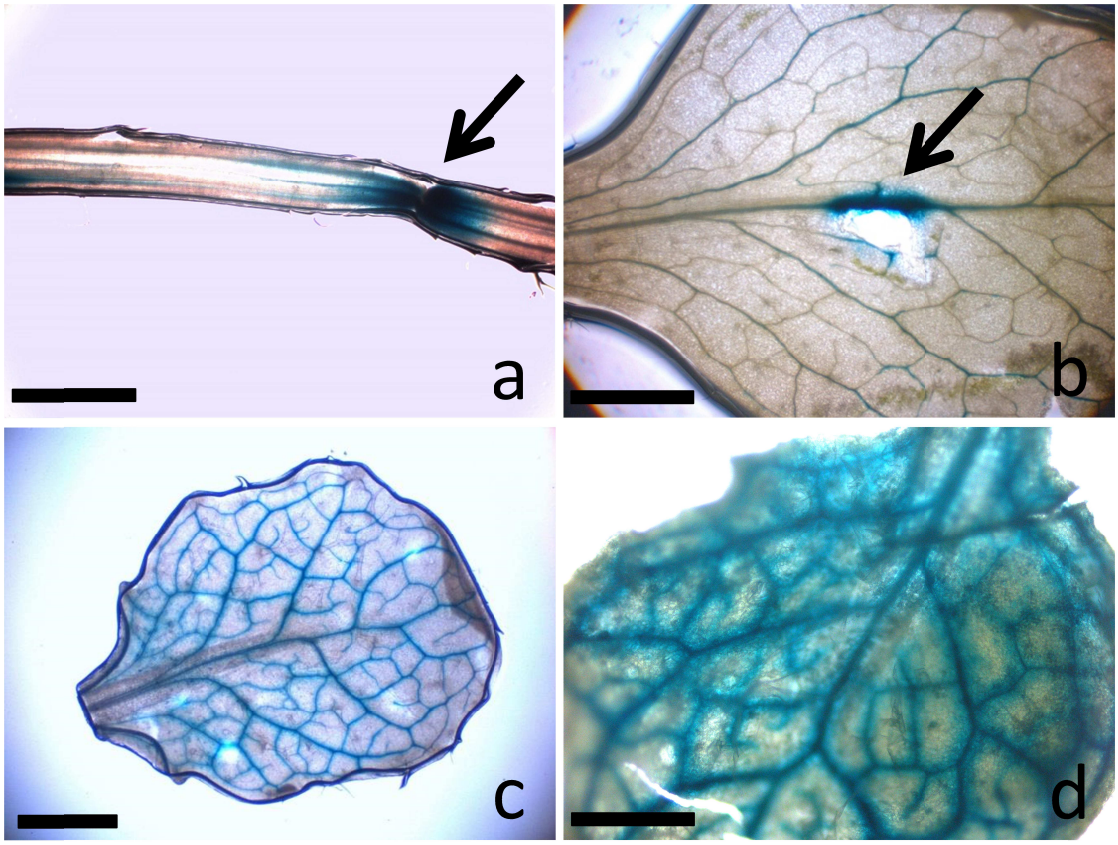

Figure 2-7 Histochemical staining of transgenic plants harboring the promoter:***uidA*** contruct after mechanical wounding and exposure to ultraviolet (UV) radiation. **a**, wounded stem; **b**, wounded leaf; **c**, and **d,** UV-irradiated leaf. Scale bars: 1 mm. Arrows, wounded sites in stem (a) and leaf (b).

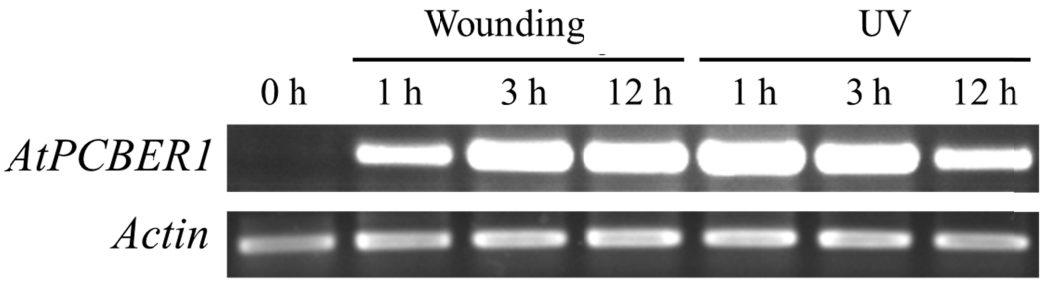

Figure 2-8 RT-PCR investigation of *AtPCBER1* gene expression in wild type plants treated with the stresses. Analysis was performed with total RNA prepared from leaves of wild-type plants (28 days old) after wounding or UV irradiation. Mechanical damage was performed by punching with a thumbtack. The total RNA was extracted from the leaves before and 1-, 3-, 12-h after the stress treatments. RT-PCR products were separated in 1% agarose gel and the resultant gel was stained with ethidium bromide. Expression of *actin* was also monitored as an internal standard.

Chapter 3

Catalytic analysis of recombinant AtPCBER1

3.1 Introduction

Both lignans and neolignans are synthesized from one of monolignols, coniferyl alcohol. Especially, PR and LR (**Fig. 1-2**) as lignans and DDC as a neolignan (**Fig. 1-3**), are composed with similar aryl-dihydrobenzofuran and diaryl-furofuran rings. PCBER is one of the key enzymes for biosynthesis of 8-5′-linked neolignans, capable of catalyzing the NADPH-dependent reduction from various phenylcoumaran type neolignans to the corresponding diphenols.

In previous reports, purified PCBERs and recombinant enzymes derived from cDNAs of PCBER genes from pine, ginkgo, and tobacco, could reduce both DDC and DDDC to DDDDC and TDDC, respectively (Gang *et al*. 1999b; Shoji *et al*. 2002; Bayindir *et al*. 2008; Cheng *et al*. 2013; Niculaes *et al*. 2014). The purified PCBERs could also reduce an 8–8'-linked lignan (PR), as do PLR and pinoresinol reductase (PrR), although the activity was relatively weak compared to that of DDC (Gang *et al*. 1999b; Bayindir *et al*. 2008; Niculaes *et al*. 2014).

In Arabidopsis, AtPrR1 and AtPrR2 phylogenetically close to those of PLRs which can reduce PR to SLR via LR from other plant species. Whereas, the recombinant AtPrR1 and AtPrR2 tended to show substrate preference toward PR and show only weak or no activity toward LR (Nakatsubo *et al*. 2008). In addition, it is interesting that the expression property of *AtPCBER1* was a little bit different from those of previously characterized lignan reductase genes, as well as *AtPrR1* and *AtPrR2*. The *AtPCBER1* highly expressed in flowers as well

as pollens.

For a better understanding of the AtPCBER1 biochemical properties, a fusion protein His-AtPCBER1, including an N-terminal 6x histidine tag, was overexpressed in *E. coli* and purified by affinity chromatography. Catalytic properties of His-AtPCBER1 were characterized using three different lignans DDC, PR and LR as substrates. Kinetic analysis of His-AtPCBER1 was characterized using DDC and PR as substrates.

3.2 Materials and Methods

3.2.1 Cloning of cDNA of *AtPCBER1*

Total RNA was extracted from rosette leaves of wild-type Arabidopsis plants using the method described in Chapter 2 (**2.2.2**).

To construct the expression vector for His-AtPCBER1 production, the coding sequence (CDS) of *AtPCBER1* was amplified with reverse transcription polymerase chain reaction (RT-PCR) using total RNA from leaves and sequence-specific primers (PCBER-F, 5′-CGGGATCCGATGACGAGTAAAAGC-3′ and PCBER-R, 5′-TTGCGGCCGCTTCTGCAGTTAGACATATTGGTTG-3′). After synthesis of first-strand cDNA from isolated total RNA, the CDS was amplified in a reaction mixture containing 0.2 mM of each dNTP, 1 μM of each primer, and 0.125 units of KOD FX Neo polymerase (Toyobo Co. Ltd., Tokyo). The RT-PCR product was then subcloned into the expression vector pETDuet-1 (with the nucleotide sequence for an N-terminal 6× histidine tag) at the site between the *Bam*HI and *Pst*I sites (**Fig. 3-1**). Accuracy of DNA sequence was confirmed by restriction

enzyme cutting and sequencing analysis. Transformed *E. coli* with the empty vector (no insert) was used as a negative control.

3.2.2 Heterologous expression in *E. coli* and purification of the recombinant protein

The recombinant expression vector harboring the His-AtPCBER1 construct was introduced into *E. coli* strain BL-21(DE3). The recombinant strain, which was pre-cultured overnight, was inoculated into 10 mL of fresh LB medium (**Table 3-1)** at 37 °C. When the optical density (OD_{600}) reached 0.6, isopropyl-D-thiogalactopyranoside (final concentration 100 μM) was added to induce expression of the recombinant protein. After further 4 h incubation, the bacteria were harvested by centrifugation at 15,000 rpm for 15 min at 4 °C. Pellets were resuspended in 600 μL binding buffer (**Table 3-2**), and the suspensions were sonicated on ice to break the cells. The sonicated cell lysate was centrifuged at 15,000 rpm for 30 min at 4 °C, and His-AtPCBER1 in the supernatant was purified by affinity chromatography (His Spin Trap Column, GE Healthcare Japan, Tokyo). Buffer exchange to remove salts from the solution containing the purified protein was performed using Amicon Ultra-15 Centrifugal Filter Units (Millipore - Merck, Germany). Then the purified His-AtPCBER1 fusion protein was quantified by the Bradford method using Bio-Rad Protein Assay Kit (Bio-Rad Laboratories Inc., CA), with bovine serum albumin as the standard. Purification was confirmed by sodium dodecyl sulfate- polyacrylamide gel electrophoresis (SDS-PAGE, **Table 3-2**) with a 12.5% polyacrylamide gel.

3.2.3 Enzymatic assay

Catalytic properties of His-AtPCBER1 were characterized with three different substrates DDC, PR, and LR. Enzyme assays were designed according to Gang *et al*. (1999b). The reaction mixture (200 μL final volume) contained 20 mM PBS buffer (pH 7.0), 1.5 mM β-NADPH, 5 mM dithiothreitol, 100 μg/mL of purified His-AtPCBER1, and various concentrations of three substrates: DDC, PR and LR. Reactions were performed at 37°C for 1 h, 8 h, and 12 h for DDC, PR, and LR, respectively. Each reaction was stopped by adding ethyl acetate (500 μL). After shaking the mixture, the organic layer was recovered. This extraction procedure was repeated three times, and the combined organic phase was evaporated to dryness. Identification of the reaction products was performed using a high performance liquid chromatograph equipped with a mass spectrometer (LC-MS) as described previously (Tamura *et al*. 2014) by comparison of their MS spectra with those of authentic standards.

3.2.4 Kinetic analysis of His-AtPCBER1

To analyze kinetics of His-AtPCBER1 toward different substrates, we set up a series of tubes with the same amount of His-AtPCBER1 and different substrate concentrations. After a 1 h incubation, the reduction products were quantified by LC (LC-2000, JASCO Corporation, Tokyo, Japan) equipped with a C18 column (250 mm × 4.6 mm) and UV detector (UV-2075, JASCO International CO., LTD, Tokyo, Japan), using methanol-water (40:60) with a flow rate of 0.5 mL/min. Standard curves for each compound were generated for the authentic compounds. V_{max} and K_m were calculated using the Michaelis-Menten equation.

3.3 Results

3.3.1 Amplification of cDNA of *AtPCBER1* and purification of the recombinant enzyme prepared with the cDNA

AtPCBER1 was amplified with RT-PCR and sub-cloned into an expression plasmid pETDuet-1. Then, The fusion enzyme with an N-terminal 6x histidine tag (His-AtPCBER1) was purified by immobilized metal ion affinity chromatography. Distribution of the purified His-AtPCBER1 in SDS-PAGE (12.5% polyacrylamide) showed that His-AtPCBER1 was efficiently purified with the expected size of polypeptide (**Fig. 3-2**, lane 3). The crude extracts from *E. coli* strain BL-21(DE3) harboring plasmid pETDuet-1 (no insertion) was used as a negative control (**Fig. 3-2,** lane 1).

3.3.2 Catalytic analysis of the recombinant AtPCBER1

As mentioned above, Catalytic properties of His-AtPCBER1 were characterized with three different substrates, DDC, PR, and LR (**Fig. 1-5**). HPLC analysis of reaction mixtures revealed that His-AtPCBER1 reduced DDC (**Fig. 3-3**). Relative weak activity could be also detected towards PR (**Fig. 3-4**). Although AtPCBER1 did not reduce LR in the same reaction time as for DDC and PR, a small amount of a reductive product, SLR, was detected when the reaction time was extended to 12 h (**Fig. 3-5**). This is the first report to confirm the catalytic function of a putative PCBER of *A. thaliana* and its ability to reduce PR and LR, in addition to DDC.

Further quantitative analysis also confirmed that His-AtPCBER1 exhibited significant differences of kinetic parameters towards these substrates (**Table 3-5**).

Reduction activity towards DDC (12.1 nmol min^{-1} mg^{-1}) was 18 times higher than towards PR (0.67 nmol min^{-1} mg^{-1}). Reduction activity towards LR could not be determined because it was likely under the detectability threshold. These results indicate that AtPCBER1 shows activity as expected for PCBERs identified in the other plant species.

3.4 Discussion

The specific activity (V_{max}) of recombinant PCBERs toward DDC vary among flax (0.78 pmol min^{-1} mg^{-1}, PCBER-Lc1), poplar (0.88 nmol min^{-1} mg^{-1}, PCBER-Pop1), pine (1.74 nmol min^{-1} mg^{-1}, PCBER-Pt1) (Gang et al. 1999; Bayindir et al. 2008) and Arabidopsis (12.1 nmol min^{-1} mg^{-1}, AtPCBER1). This might be due to different experimental conditions for measurement of specific activity and/or different original kinetic parameters. Based on these results, we propose that *AtPCBER1* encodes the PCBER of *A. thaliana*.

The enantiomer selectivity of AtPCBER1 was not investigated here, enzymatic analysis indicated that His-AtPCBER1 reduced not only DDC (12.1 nmol mim^{-1} mg^{-1}), but also PR (0.35 nmol mim^{-1} mg^{-1}) and LR with lower levels. It is obvious that His-AtPCBER1 shows significantly lower relative activity towards PR (0.35 nmol mim^{-1} mg^{-1}) than those of AtPrR1 (35.5 nmol mim^{-1} mg^{-1}) and AtPrR2 (5.9 nmol mim^{-1} mg^{-1}) (Nakatsubo *et al*. 2008).

As His-AtPCBER1, recombinant PCBERs of flax and poplar also reduced 8–8′-linked lignan, in addition to 8–5′-linked neolignan, although the substrate preferences of the polypeptides toward the 8–8′-linked compounds were variable between AtPCBER1 and poplar PCBER (Niculaes *et al*. 2014). Overlap in the substrate specificities of PCBER and PLR should be responsible for their close

phylogenetic relationship and structural similarities of the substrates between aryl-dihydrobenzofuran and diaryl-furofuran rings.

3.5 Tables and Figures

Table 3-1 Composition of Lysogeny broth (LB) medium

Tryptone	10 g/L
Yeast extract	5 g/L
Sodium chloride	10 g/L

Table 3-2 Composition of buffers for histidine-tagged protein purification

Binding buffer (pH 7.4)	
Sodium phosphate buffer	50 mM
Sodium chloride	500 mM
Washing buffer ((pH 7.4))	
Sodium phosphate buffer	50 mM
Sodium chloride	500 mM
Imidazole	25 mM
Elution buffer (pH 7.4)	
Sodium phosphate buffer	20 mM
Sodium chloride	500 mM
Imidazole	200 mM

Table 3-3 Compositions of SDS-PAGE gel and loading buffer

Separating gel composition	
30% (w/v) Acrylamide	12.5% (w/v)
1.5 M Tris-HCl, pH 8.8	375 mM
10% (w/v) SDS	0.1% (w/v)
10% (w/v) Ammonium persulfate (APS)	0.1% (w/v)
N,*N*,*N*',*N*'-Tetramethylethylene diamine (TEMED)	0.01% (v/v)
Staking gel composition	
30% (w/v) Acrylamide	6% (w/v)
0.5 M Tris-HCl, pH 6.8	125 mM
10% (w/v) SDS	0.1% (w/v)
10% (w/v) Ammonium persulfate (AP)	0.1% (w/v)
N,*N*,*N*',*N*'-Tetramethylethylene diamine (TEMED)	0.01% (v/v)
2X Sample buffer	
SDS	4% (w/v)
β-mercaptoethanol	10% (v/v)
Sucrose	10% (w/v)
Tris-HCl, pH 6.8	0.2 M
Bromophenol blue	0.005% (w/v)

Table 3-4 Compositions of 0.2 M sodium phosphate buffer (pH 5.8–8.0) used in this study

0.2 M NaH_2PO_4 (mL)	0.2 M Na_2HPO_4 (mL)	Final pH
87.7	12.3	6.0
68.5	31.5	6.5
51.0	49.0	6.8
39.0	61.0	7.0
16.0	84.0	7.5
6.8	93.2	8.0

Table 3-5 Kinetic parameters of recombinant AtPCBER1 measured toward two different substrates.

	DDC	**PR**
K_m **(μM)**	**333 ± 24**	**684 ± 39**
V_{max} **(nmol min^{-1} mg^{-1})**	**12.1 ± 0.42**	**0.67 ± 0.04**
K_{cat} **(min^{-1})**	**0.42 ± 0.01**	**0.01 ± 0.00**

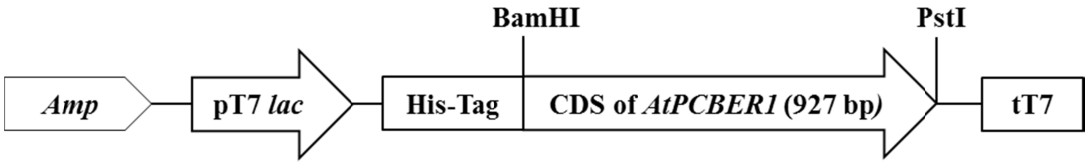

Figure 3-1 Representative structure of expression vector for production of His-AtPCBER1.

Amp: Ampicillin resistant gene

pT7 *lac*: Hybrid promoter, combined with the T7 promoter (strong promoter from T7 bacteriophage) and *lacO*, the operator of *lac* (*lactose*) operon

tT7: T7 Terminator

His-tag: The nucleotide sequence for N-terminal 6x histidine tag

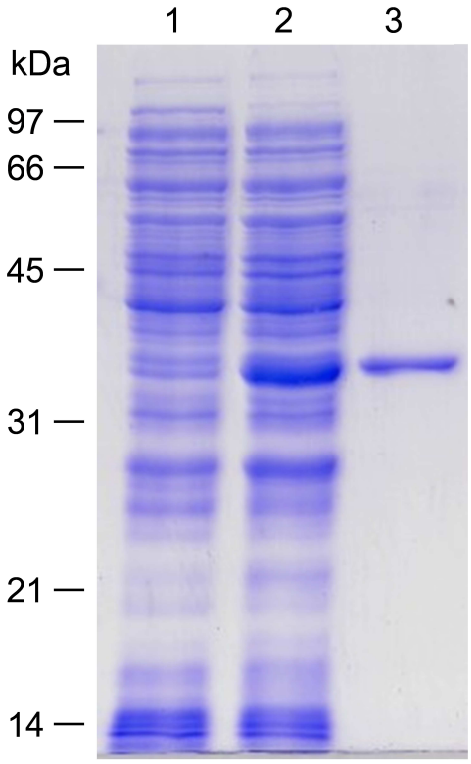

Figure 3-2 Sodium dodecyl sulfate-polyacrylamide gel electrophoresis analysis of protein derived from transgenic *E. coli*. Two μg of protein was loaded in each lane and the gel was stained with Coomassie Brilliant Blue.

Lane 1. Crude proteins from *E. coli* transformed with an empty vector (pETDuet)

Lane 2. Crude proteins from *E. coli* transformed with pETDuetAT4G39230.

Lane 3. Purified recombinant protein (polypeptide derived from the candidate gene for PCBER)

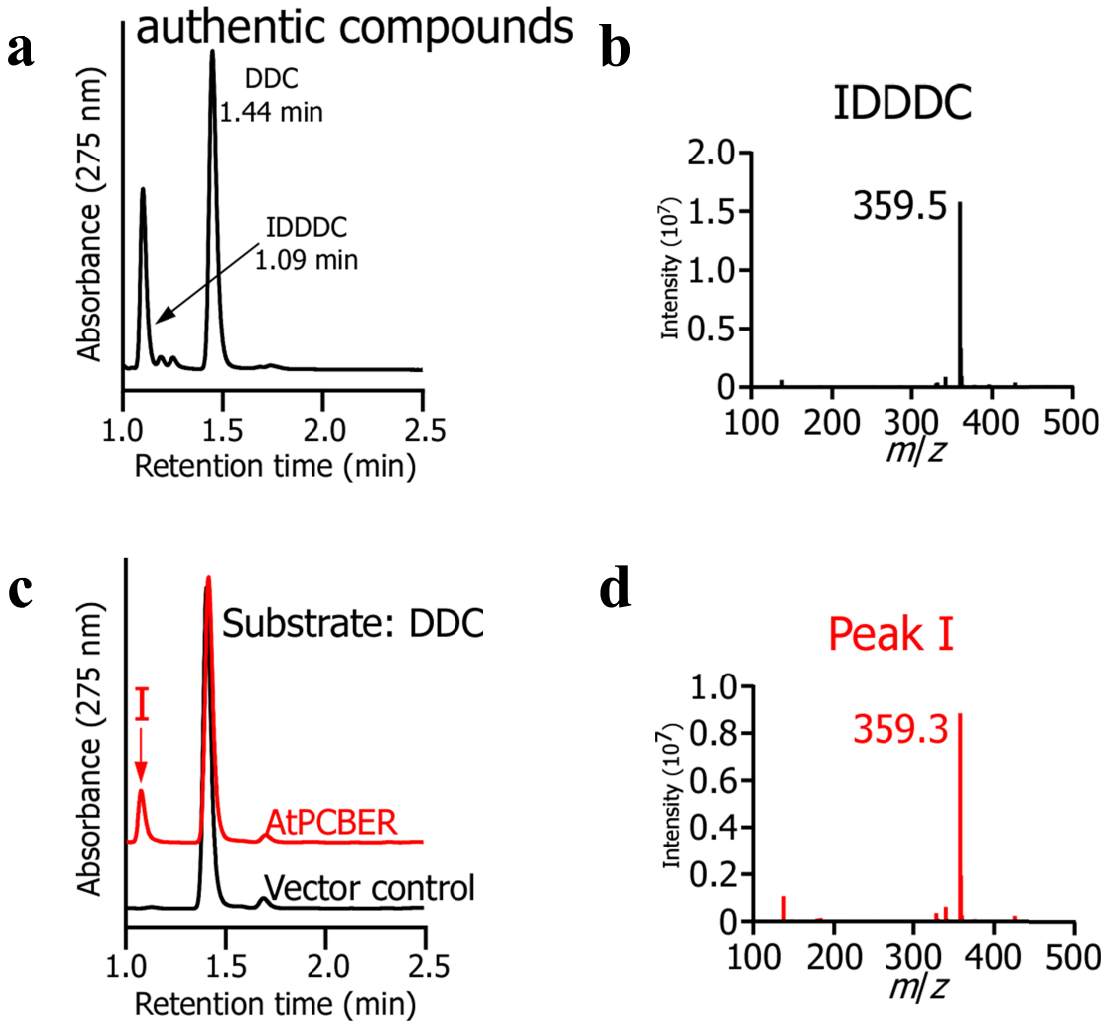

Figure 3-3 Characterization of recombinant His-AtPCBER1 using substrates DDC. **a** and **b**, chromatogram and mass spectra of authentic compounds DDC and IDDDC; **c**, **a**nalysis of reaction mixture with purified His-AtPCBER1 and DDC. The reaction product (Peak I) was identified as IDDDC; **d**, crude extract from *E. coli* transformed with an empty vector was used as the negative control.

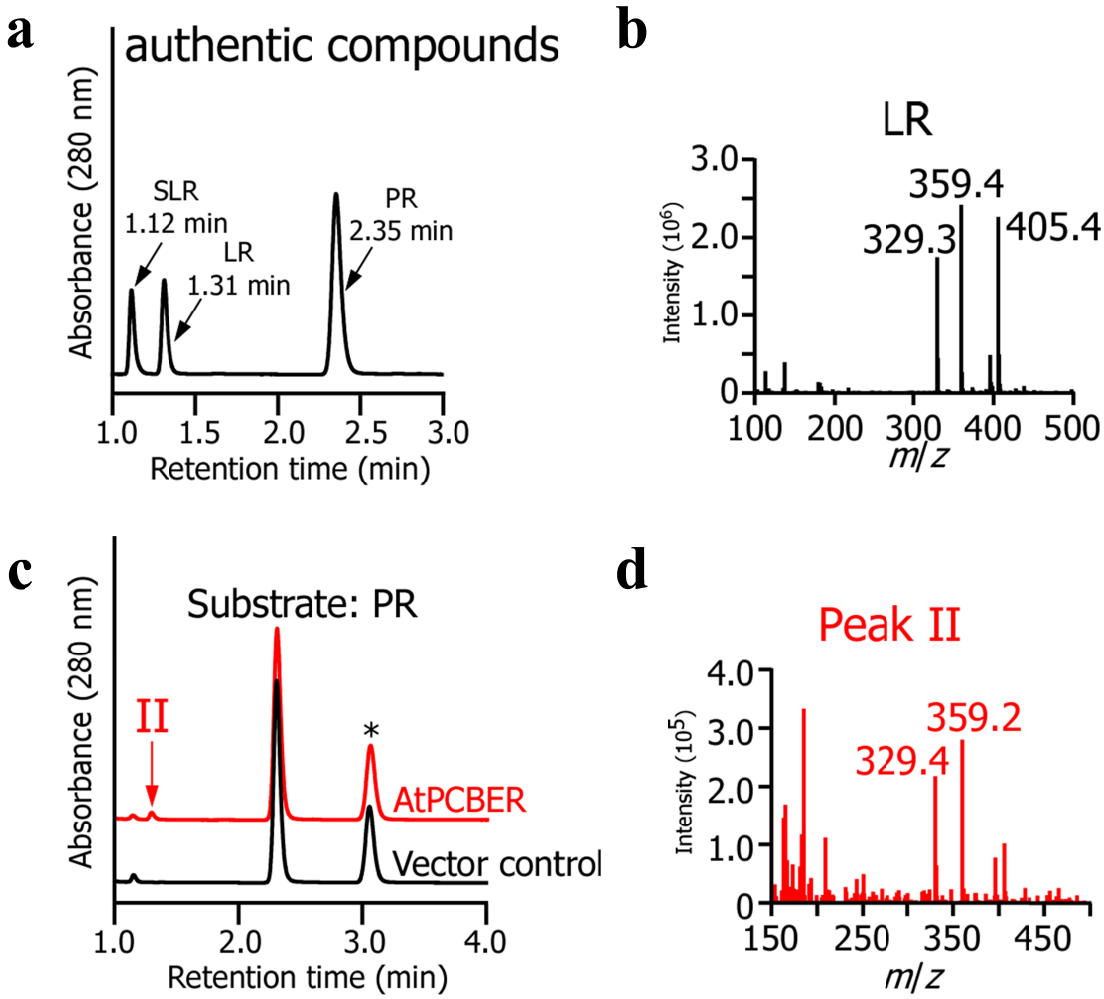

Figure 3-4 Characterization of recombinant His-AtPCBER1 using a substrate, PR. **a** and **b**, chromatogram of authentic compounds, PR, LR, and SLR and mass spectra of authentic compounds LR; **c**, analysis of reaction mixture with purified His-AtPCBER1 and PR. Peak **II** were detected as reaction product. A peak marked with asterisk was derived from reaction buffer; **d**, Crude extract from *E. coli* transformed with an empty vector was used as the negative control.

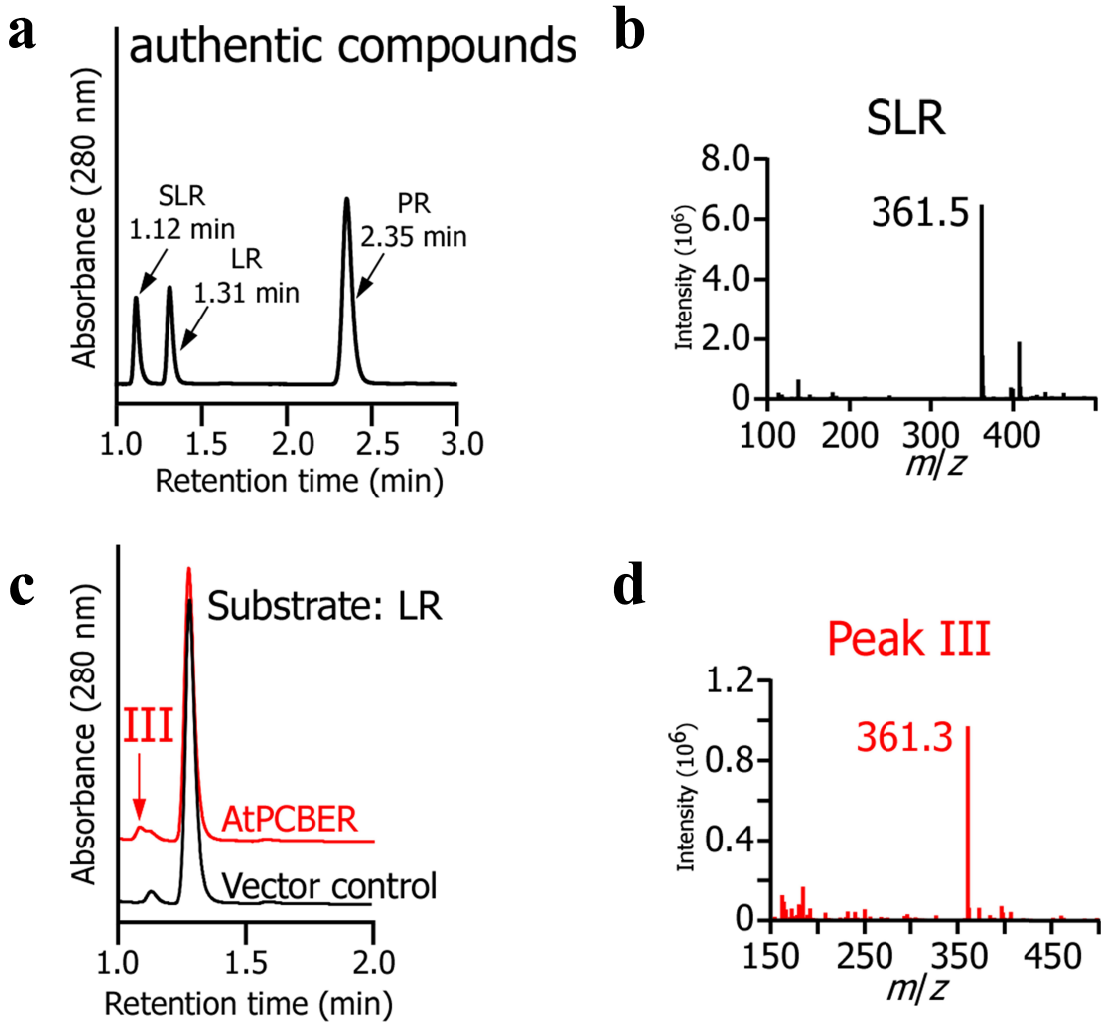

Figure 3-5 Characterization of recombinant His-AtPCBER1 using a substrate, LR. **a** and **b**, chromatogram of authentic compounds, PR, LR, and SLR and mass spectra of authentic compounds SLR; **c**, analysis of reaction mixture with purified His-AtPCBER1 and LR. Trace amounts of SLR (Peak III) were detected as reaction product. A peak marked with asterisk was derived from reaction buffer. **d**; Crude extract from *E. coli* transformed with an empty vector was used as the negative control.

Chapter 4

Analysis of transgenic plants with up- or down-regulated *AtPCBER1* gene

4.1 Introduction

Monolignols are assumed to be the common precursors of lignins and lignans, whose biosynthesis pathways also connected with many other secondary metabolites biosynthesis pathways, such as, flavonoids biosynthesis (**Fig. 1-1**). The mechanisms how these natural compounds coexist in plants remain unknown. The plausible relationship of them has been previously discussed in some studies. In *G. biloba*, contents of both lignins and flavonols are influenced by the expression level of PCBER gene (Cheng *et al*. 2013). Single nucleotide polymorphisms (SNPs) in *PCBER* related to wood density of *P. radiata* (Dillon *et al*. 2010). Moreover, down-regulation of *PCBER* expression induced reduction of lignin content in transgenic poplar (Boerjan *et al*. 2006). Studies have also shown that reduced expression of another lignan biosynthesis gene, *AtPrR1*, impacted thickness and distribution of the secondary cell wall in *A. thaliana* (Ruprecht *et al.* 2011; Zhao *et al*. 2014). These results indicate that lignans and neolignans, in addition to genes for their biosynthesis, may play important roles in lignification and secondary metabolite accumulation.

According to previous references and this study, recombinant PCBER polypeptides could reduce 8–5′-linked neolignan, in addition to 8–8'-linked lignan, although the substrate preference of the polypeptides toward 8–8′-linked compounds was variable between AtPCBER1 and other PCBERs. In addition, some of previous researches have investigated natural substrates of lignan

biosynthesis enzymes in plants. For instance, in flax cell culture, content of DDC 4-β-D-glucoside (DCG) decreased and expression level of *PCBER* increased simultaneously when elicited by fungal extracts (Attoumbre *et al*. 2005). In cell culture, PLR from *L. album* catalyzed only (+)-PR into (-)-SLR. In contrast, PLR in *L. usitatissimum*, which was different a few amino acid residues from that of PLR in *L. album* converted only (-)-PR to (+)-SLR (von Heimendahl *et al*. 2005). Chromatography–mass spectrometry (GC–MS) analysis to transgenic Arabidopsis in which the expression of the *AtPrR1* gene was perturbed indicated that the concentration of the 8-8'-linked lignan, PR, was 4.8-fold higher in the transgenic plants than in wild type plants (Zhao *et al*. 2014). In addition, Nakatsubo *et al.* suggested that, AtPrR1 and AtPrR2 prefer to reduce (+)-PR in Arabidopsis plants when chiral HPLC analysis were performed with hot methanol extract of transgenic Arabidopsis in which *AtPrR1* and *AtPrR2* genes were perturbed. Recently, a study revealed that a 8–5'-linked compound coupled between sinapyl alcohol and guaiacylglycerol ($S(8–5)G^{glycerol}$) is a possible natural substrate of poplar PCBER. By the down-regulation of PCBER activity in transgenic poplar, the level of $S(8–5)G^{glycerol}$ was increased more than four times compared to the wild-type. In contrast, the reduction product of this compound was more than seven times less abundant in the same transgenic line (Niculaes *et al*. 2014).

In our result above, the amino acid sequences of AtPCBER1 phylogenetically closely related to those of identified PCBERs, IFRs and PLRs (**Fig. 2-2**). The highest expression level of *AtPCBER1* was shown in flower, and vascular parts of petal, leaf, root and stem, and the expression was induced by mechanical wounding and UV irradiation. Furthermore, catalytic analysis indicated that

His-AtPCBER1 reduced not only DDC (12.1 nmol mim^{-1} mg^{-1}), but also PR (0.35 nmol mim^{-1} mg^{-1}) and LR with lower levels (**Table 3-5**). These results indicated that expression properties of *AtPCBER1* and catalytic properties of His-AtPCBER1 are a little bit different from those of other PCBERs.

To gain further insights into contribution of *AtPCBER1* gene in plants, we performed analyses for the metabolites and lignin contents in the transgenic plants in which *AtPCBER1* gene expression was up- and down- regulated.

4.2 Materials and Methods

4.2.1 Plant materials and transgenic selection

Wild and transgenic *A. thaliana* plants used in this study were all in Columbia-0 background and the growth conditions were same as described in Chapter 2.

Transgenic Arabidopsis line (stock number Salk-013209) with a T-DNA-insertion in *AtPCBER1* was purchased from the Arabidopsis Biological Resource Center (OH, USA). We isolated the homozygous line using primer pairs: RB (corresponding to the right border of the T-DNA, 5′-TCATCTACGGCATTGATTGTG-3′), LB (corresponding to the left border of the T-DNA, 5′-GTCGACTCCACCATCGAGAATTTCAAG-3′), and LBa1 (corresponding to the left border of the T-DNA, 5′-TGGTTCACGTAGTGGGCCATCG-3′). Genomic PCR was performed with ExTaq DNA polymerase (TAKARA BIO INC., Otsu, Japan). To identify the exact position and orientation of the T-DNA in the genome, Sanger sequencing of the PCR product amplified by LB and LBa1 was performed after subcloning.

In order to generate the *AtPCBER1* over-expression construct, full-length CDS of *AtPCBER1* was inserted into plant expression plasmid (pBF2). The resultant recombinant plasmid was named pBF-AtPCBER1 (**Fig. 4-1**), and *Agrobacterium tumefaciens* was transformed by this plasmid, and then the T-DNA region was introduced into Arabidopsis as described by Tamura *et al.* [1]. Introduction of the transgene constructs into genomes of the transgenic plants were confirmed by genomic PCR and RT-PCR. Wild-type Arabidopsis (ecotype Columbia-0) was used as the negative control for all experiments.

4.2.2 Metabolomic analysis of wild-type and transgenic plants

Plants sample preparation and subsequent analyses were performed as described previously (Tamura *et al.* 2014) and briefly as follows. Organ samples (stems, roots, and flowers) from 48-day-old plants were freeze-dried and used for extraction of metabolites. The samples (each from four individual plants) were extracted with 50 μL of 80% methanol containing 2.5 μM lidocaine and 10-camphorsulfonic acid per mg dry weight and analyzed by LC-QTOF-MS (LC, Waters Acquity UPLC system; MS, Waters Xevo G2 Q-Tof). Values of *m/z* were set for precursor ions ($[M+H]^+$ or $[M-H]^-$), and then, we searched for matching value of references with tolerance 0.01 Da. For lignan standards, we searched for matches with retention time values with tolerance 0.2 min.

4.2.3 Quantification of lignin in stem

Lignin content was measured quantitatively using the acetyl bromide method according to Kajita *et al.* (1997) and Kim *et al.* (2014). Briefly, methanol-extracted cell residue (5 mg) was incubated at 70°C for 30 min after

25% acetyl bromide (v/v in glacial acetic acid) were added. After complete digestion, the sample was mixed with 0.9 mL of 2 M NaOH, 0.1 mL of 5 M hydroxylamine-HCl, and a volume of glacial acetic acid sufficient for complete solubilization of the lignin extract (total 50 mL). The absorbance of the resultant mixture was measured at 280 nm and lignin contents were represented as g lignin g^{-1} cell wall (ε) value obtained as 23.35 g L^{-1} cm^{-1}(Kim *et al*. 2014).

4.3 Results

4.3.1 Metabolomic analysis of wild-type plants and transgenic plants

The transgenic Arabidopsis line, in which *AtPCBER1* was disrupted by T-DNA insertion, was generated. The first step, PCR analysis were performed using primer pairs described in Materials and Methods (LP with RP and LBa1 with RP). Genomic DNAs of transgenic plants and wild type plants were used as PCR template. At this step, we could select the transgenic homozygous knock-outed lines successfully by using their genomic DNAs as template to perform PCR. In which there was no PCR product when using primer pairs LP and RP, whereas expected PCR products were obtained when using primer pairs LBa1 and RP. This result confirmed T-DNA insertion into *AtPCBER1* of the genome. However, when performing RT-PCR analysis with these transgenic plants, trace amount of *AtPCBER1* were detected (**Fig. 4-2**). It is may be due to the fact that the T-DNA insertion is into an intron, and a small percentage of insertions in introns produce a reduced level of wild type transcript, the rest are spliced out with the intron sequence. The same phenomena also occurred in previous studies (Xue *et al*. 2012). The transgenic Arabidopsis lines, in which *AtPCBER1* was up-regulated,

were successfully selected by RT-PCR method. These transgenic plants exhibited no significant phenotypic and apparent differences with wild-type plants (**Fig. 4-3**).

With the aim to gain insight into metabolic mechanisms controlled by *AtPCBER1* gene, we analyzed methanol-soluble metabolites prepared from the 48-day-old wild-type and *AtPCBER1* up- and down-regulated plants. The metabolomic profiling of these transgenic plants was performed using LC-Q-TOF-MS with negative and positive ion modes. In positive ion mode, there were 1757, 1422 and 1097 unique compounds were detected in flower, root and stem samples, respectively. And there were 1049, 1065, 657 unique compounds were detected in flower, root and stem samples respectively when using negative ion mode. Principal components analysis (PCA) of all detected components in stem (**Fig. 4-4a**, **b, c,** and **d**) and root (**Fig. 4-4e**, **f, g,** and **h**) revealed significant variation in contents between wild-type and transgenic plants, however, no evident differences were observed in flowers (**Fig. 4-4i**, **j, k,** and **l**)..

Chemical assignment of the detected components was performed by comparing mass spectra with those of compounds previously documented in the literature (Song *et al*. 2005; Tohge *et al*. 2005; Böttcher *et al*. 2008; Yonekura-Sakakibara *et al*. 2008; Morreel *et al*. 2014) and listed in databases KNApSAcK (http://kanaya.naist.jp/KNApSAcK/)(Afendi *et al*. 2012).

We identified 36 independent components most of that were secondary metabolites at MSI level 2 (Sumner *et al*. 2007) with MS/MS analysis (**Table 4-1**). Among these components, levels of 9, 14, and 17 components were significantly altered in flower, stem, and root of up- and/or down-regulated plants compared to the wild-type plants.

LR hexoside, a major lignan in Arabidopsis plants, was detected in all samples, and was markedly elevated in roots of *AtPCBER1* down-regulated plants. Although a neolignan, guaiacylglycerol 8–*O*–4-feruloyl malate ether, tended to be elevated in flower and reduced in stem and root of transgenic lines, only levels in the root of down-regulated plants were significant compared to the wild-type.

Unfortunately, DDC, PR, and related neolignan and lignan components were not identified in extracted metabolites at MSI level 2 and were below detectable levels as reported in our previous study (Tamura *et al*. 2014).

Interestingly, content of several flavonoids and glucosinolates were also altered. Four cyanidin derivatives could be identified only in the root and they were reduced in transgenic roots. Some of kaempferol and quercetin derivatives were decreased in the root of down-regulated plants and tended to be increased in flower and stem of down-regulated plants. Some glucosinolates such as 8-methylsulfinyloctyl glucosinolate and glucoraphanin were also tended to be increased in stem and root of transgenic plants.

In addition to all the compounds mentioned above, the coumarin scopoletin, hydrophobic amino acid, valine, and the common primary metabolites, citric acid (or isocitric acid), are also altered in contents in the transgenic plants compared to the wild type plants.

Nevertheless, these results indicate that AtPCBER1 plays an important role in the biosynthesis of secondary metabolites in *A. thaliana*.

4.3.2 Measurement of lignin contents toward wild-type plants and transgenic plants

Stems of 56-day-old wild type plants and transgenic plants were used to

quantifying lignin content, as shown in **Fig. 4-8**, lignin contents in cell wall measured by acetyl bromide method using wild-type plants, *AtPCBER1* up-regulated plants and *AtPCBER1* down- regulated plants, respectively. There were no significant differences in lignin contents between wild-type plants and transgenic plants.

4.4 Discussion

PCBER is an NADPH-dependent oxidoreductase and a crucial enzyme for lignan biosynthesis in plants. In order to reveal the potential role of *AtPCBER1* gene expression in Arabidopsis, methanol extracts from flower, stem and root of transgenic and wild type plants were identified using LC-QTOF-MS. In our metabolomic analyses, structures of 36 components were resolved by MS/MS analysis (**Table 4-1**).

Interestingly, almost one third of these components, derivatives of kaempferol, quercetin, and cyanidin were flavonoids. According to the data shown in **Table 4-1,** these flavonoids decreased and increased in PCBER up- and down-regulated plants, respectively. In a previous study, Cheng *et al*. (2013) analyzed the relationship between annual changes of flavonoid contents and *GbIRL1* (a gene for PCBER in *G. biloba*) expression in leaves. Their levels, while not completely synchronous, showed a close positive relationship. Previously, several researches have indicated that the flavonoids were accumulated after UV-light irradiation (Caldwell *et al*. 1983; Krizek *et al*. 1998). Interestingly, the *AtPCBER1* expression was also stimulated by UV light irradiation. These results suggest that, *AtPCBER1* expression and/or lignan biosynthesis somehow have influence on the flavonoids biosynthesis. As shown in **Fig. 4-5**, flavonoids are initially

biosynthesized from *p*-coumaroyl CoA, which is synthesized from phenylalanine, an aromatic amino acid, by phenylpropanoid synthetic pathway. In the results of our metabolomic analyses, the flavonoids, especially kaempferol and quercetin derivatives decreased and increased in PCBER up- and down-regulated plants. Thus, we made the presumption that Level of *AtPCBER1* expression may have an impact on adjacent metabolic pathway. Kaempferol (and/or quercetin) derivatives conversion may be directly catalyzed by AtPCBER1. To reveal the second possibility, catalytic properties of His-AtPCBER1 towards flavones were measured using four different flavones derivatives as substrates, including kaempferol, quercetin, kaempferol 7-*O*-β-D-glucoside and quercetin 3-β-D-glucoside. Results of LC-Q-TOF-MS analysis of reaction mixture indicate that, two new peaks were observed in reaction mixture only when quercetin was used as substrate. The two compounds were both eluted at the retention times near the retention time of authentic quercetin (**Fig. 4-6**). We further analyzed the compounds of both peaks by MS/MS analysis (**Fig. 4-7**). Results indicate that none of them are in accordance with the authentic compounds that reduced forms of quercetin. In addition, based on the comparison of fragmentation pattern of these candidate reaction products with substrate quercetin (**Fig. 4-7**), both candidate reactants 1 and 2 were considered to be generated by enzymatic reaction catalyzed by AtPCBER1. These results suggest that quercetin could be converted or modified in other ways by AtPCBER1 enzyme.

As mentioned in Chapter 1, aromatic amino acids are produced through the shikimic acid pathway, and as shown in **Fig. 1-1** these aromatic amino acids are partly involved in glucosinolate biosynthesis and lead to accumulate the aromatic glucosinolates. In our metabolomic analysis, except for the flavonoids, some

glucosinolates, such as aromatic glucosinolate glucobrassicin, were quantitatively altered in transgenic plants. Similar results were also reported in transgenic Arabidopsis harboring a bacterial PLR gene (Tamura *et al*. 2014). It is suggested that the expression level of lignan biosynthetic genes may have impact on glucosinolates accumulation.

Except for several flavonoids, the changing trend of all characterized compounds in **Table 4-1** was varied in flower, root and stem. These results suggest that *AtPCBER1* expression level or lignan biosynthesis may have different impact on different plant organs.

It has been investigated that 8–5′-linked neolignans are abundantly present in tracheophyte plants and woody tissues of various tree species (Weng and Chapple. 2010; Davin and Lewis. 2003; Holmborn *et al*. 2003; Kwon *et al*. 2001; Ribeiro *et al*. 2005), and that DDC and its derivative compound, DDDC, appear in many plants species, such as pine (Nose *et al*. 1995) and tobacco (Binns *et al*. 1987), whereas, DDC accumulated in small amounts in leaves of *C. japonica* (Su *et al*. 1995). In flax stem, IDDDC hexoside was detected in either inner or outer stem tissues but IDDDC was not. In addition, Nakatsubo *et al.* suggested that treating with glucosidase might increase the extraction efficiency of lignans. In our metabolomic results, DDC and the derived compounds were not detectable in all samples. This may be due to the small level existence of DDC in Arabidopsis. It is also possible to think that DDC or derived compounds may present in complex-glucosylated form in Arabidopsis.

It is significantly that the lariciresinol hexoside and 8-*O*-4' type lignans quantitatively increased in *AtPCBER1* down-regulated plants, as well as some flavonoids and glucosinolates. It suggests that AtPCBER1 may have no catalytic

functions towards 8-8'-linked lignans and that *AtPCBER1* down-regulation may facilitate the other oxidative reactions, such as PLR-dependent oxidative reactions. And it is from another standpoint that increasing of 8-*O*-4' type lignans may imply the role of AtPCBER1 in lignin accumulation. However, the lignin contents in transgenic plants were not altered (**Fig. 4-8**).

As mentioned above, it is had been confirmed that, levels of PCBER expression in plant tissues and an intronic SNP in its nucleotide sequence could influence the lignin biosynthesis and wood density (Dillon et al. 2010), respectively. Cheng et al. (2013) indicate that the lignin content exhibited a linear correlation with the level of GbIRL1 transcript (R2 = 0.517) in various organs of ginkgo. The investigation of relationships between stem hypolignification and phenolic accumulation in stem of *L. usitatissimum* suggested that PLR and PCBER abundantly existed in flax inner stem tissues, their data also suggested that MYB transcription factors might be regulate monolignol production and lignin polymerization as well as neolignans dimerization (Huis *et al*. 2012). In addition, a gene encodes the pinoresinol reductase *AtPrR1* in *A. thaliana* and highly co-expressed with cell wall biosynthesis genes. Loss of function of *AtPrR1* gene in Arabidopsis could influence content of lignin and shape of xylem cell (Ruprecht *et al.* 2011; Zhao *et al.* 2014). As shown in **Fig. 4-8**, no differences could be detected in lignin content between wild-type and the transgenic plants in our result, suggesting that *AtPCBER1* has no significant role regulating lignin levels in *A. thaliana.* Here, we constructed co-expression networks of *AtPCBER1* by using gene co-expression database, ATTED-II (**Fig. 4-9**). *AtPCBER1* was directly co-expressed with the cinnamoyl CoA reductase gene, ARM repeat superfamily protein gene (important in transducing WNT signals during

embryonic development) and with LYS/HIS transporter 7 gene (amino acid transmembrane transporter gene). In addition, *AtPCBER1* was closely co-expressed with genes involved in biosynthesis of secondary metabolites (**Fig. 4-9**, marked with red ball), phenylpropanoid metabolism(**Fig. 4-9**, marked with yellow ball), starch and sucrose metabolism (**Fig. 4-9**, marked with green ball), and cyanoamino acid metabolism (**Fig. 4-9**, marked with blue ball). This result again emphasizes the importance of *AtPCBER1* gene in biosynthesis of phenylpropanoids as well as other secondary metabolites.

Moreover, quantities of scopoletin (one of coumarins) and L-glutathione were significantly influenced by *AtPCBER1* down-regulation (**Table 4-1**), suggesting that, *AtPCBER1* expression might influence the other enzymatic processes for formation of secondary metabolites. This phenomenon also was observed in metabolomic analysis of *PCBER* down-regulated transgenic poplar reported by Niculaes *et al.* (2014) and metabolomic analysis of transgenic *A. thaliana* overexpressing bacterial pinoresinol reductase gene reported by Tamura *et al.* (2014).

Taken together, all results indicate that, AtPCBER1 is a crucial enzyme in *A. thaliana* and have a considerable role in formation of secondary metabolites.

4.5 Table and Figures

Table 4-1. Untargeted metabolomic analysis of the wild-type and transgenic plants in which *AtPCBER1* was up- or down-regulated.

Detection mode	*m/z*	Assigned compound	Flower		Stem		Root		References
			Fold change[1]		Fold change		Fold change		
			Up-regulated plant	Down-regulated plant	Up-regulated plant	Down-regulated plant	Up-regulated plant	Down-regulated plant	
Positive ion mode	268.1048	Adenosine	1.23	0.99	**0.31**	**0.14**	0.69	0.53	a
	202.1267	9-(Methylsulfinyl)nonanenitrile	1.04	1.40	1.97	2.21	3.20	4.17	a
	188.1109	8-(Methylsulfinyl)octanenitrile	1.36	1.14	0.58	**0.46**	**1.07**	1.67	a
	202.1266	9-(Methylsulfinyl)nonanenitrile	**1.34**	1.12	0.56	0.48	1.11	1.62	a
	757.2192	Quercetin 3-*O*-[6"-*O*-(rhamnosyl) glucoside] 7-*O*-rhamnoside	0.84	**1.24**	0.62	1.65	0.65	0.57	b
	741.2241	Kaempferol 3-*O*-[6"-*O*-(rhamnosyl) glucoside] 7-*O*-rhamnoside	0.86	1.09	0.79	**1.37**	0.73	0.66	b

Positive ion mode	611.1615	Quercetin 3-*O*-glucoside 7-*O*-rhamnoside	0.80	1.16	0.74	**2.88**	0.91	0.88	b
	595.1665	Kaempferol 3-*O*-glucoside 7-*O*-rhamnoside and Quercetin 3-O-rhamnoside 7-O-rhamnoside	0.85	**1.19**	0.79	**1.88**	0.73	0.61	b
	625.1769	Isorhamnetin 3-*O*-rhamnoside 7-*O*-glucoside	0.87	1.12	0.84	2.83	0.63	**0.46**	b
	579.1716	Kaempferol 3-*O*-rhamnoside 7-*O*-rhamnoside	**0.88**	**1.13**	0.76	**1.41**	0.54	0.57	b
	743.2051	Cyanidin 3-*O*-[2"-*O*-(xylosyl) glucoside] 5-*O*-glucoside	ND	ND	ND	ND	**0.28**	**0.24**	b
	829.2047	Cyanidin 3-*O*-[2"-*O*-(xylosyl) glucoside] 5-*O*-(6"'-*O*-malonyl) glucoside	ND	ND	ND	ND	**0.24**	**0.20**	b
	1137.2930	Cyanidin 3-*O*-[2"-*O*-(xylosyl) 6"-*O*-(*p*-*O*-(glucosyl) *p*-coumaroyl) glucoside] 5-*O*-[6"'-*O*-(malonyl) glucoside]	ND	ND	ND	ND	**0.23**	**0.41**	b
	975.2394	Cyanidin 3-*O*-[2"-*O*-(xylosyl)-6"-*O*-(p-coumaroyl) glucoside] 5-*O*-malonylglucoside	ND	ND	ND	ND	**0.35**	**0.43**	b
	118.0867	Valine	1.10	0.98	1.41	1.59	2.00	2.63	c
	193.0502	Scopoletin isomer	0.97	1.22	1.11	**2.94**	**1.13**	1.60	c
	193.0500	Scopoletin	1.19	0.92	**0.26**	**0.33**	0.73	0.72	c

	287.0557	Kaempferol	0.76	0.89	ND	ND	**0.35**	0.39	c
	308.0920	L-Glutathione	ND	ND	2.37	**4.47**	1.32	1.07	c
Negative ion mode	447.0529	Glucobrassicin	0.93	1.31	1.76	**2.45**	**1.45**	**2.09**	c
	477.0636	4-Methoxyglucobrassicin	0.59	0.98	0.80	0.63	1.20	1.10	c
	477.0637	Neoglucobrassicin	0.98	1.51	2.87	1.76	1.19	**1.45**	c
	338.0875	6-hydroxyindole 3-carboxylate hex	1.24	0.84	0.56	0.66	0.83	0.78	d
	755.2034	Quercetin 3-*O*-[2"-*O*-(rhamnosyl) glucoside] 7-*O*-rhamnoside	0.76	1.22	0.68	1.38	0.64	**0.55**	d
	577.1556	Kaempherol 3-*O*-rhamnosyl 7-*O*-rhamnoside	**0.86**	1.09	0.79	**1.30**	0.54	**0.58**	d
	385.1134	*cis*-sinapoyl glcoside or *trans*-sinapoyl glcoside	**0.51**	1.28	4.19	3.31	1.01	1.54	d
	521.2026	Lariciresinol hexoside	0.72	0.81	1.00	1.57	1.23	**2.15**	d
	339.0715	*cis*-sinapoyl malate or *trans*-sinapoyl malate	0.92	**1.15**	1.24	1.38	1.09	1.42	d
	505.1346	Guaiacylglycerol 8–*O*–4 feruloyl malate ether	1.21	1.29	0.31	0.86	0.60	**0.48**	d
	500.1406	6-hydroxyindole 3-carboxylate dihex	ND	ND	ND	ND	0.90	0.80	d
	551.1770	Guaiacylglycerol 8–*O*–4 ferulic acid ether hexoside	ND	ND	ND	ND	1.21	1.47	d

Negative ion mode	450.0563	5-Methylsulfinylpentyl glucosinolate	0.79	1.33	1.85	**3.05**	1.06	1.83	e
	191.0190	Citric acid or Isocitric acid	1.14	1.01	1.02	1.52	**3.77**	2.35	f
	191.0189	Citric acid or Isocitric acid	1.09	0.98	1.71	3.26	**1.70**	1.29	f
	436.0405	Glucoraphanin	0.74	1.14	1.56	**2.80**	1.12	1.47	f
	420.0456	Glucoerucin	0.61	1.48	0.83	1.02	1.34	**3.93**	f
	492.1029	8-Methylsulfinyloctyl glucosinolate	0.98	**1.49**	2.11	2.51	2.43	**4.97**	g
	476.1079	8-Methylthio-octyl glucosinolate	0.75	3.49	2.37	0.94	**2.52**	2.24	g

Five or six biological replicates prepared from each organ (stem, root and flower) were analyzed. All components have been identified at MSI level 2 based on the descriptions developed under the Metabolomics Standards Initiative (Sumner *et al*. 2007).

[a] Mass and mass/mass spectra of each detected component were compared with data observed in the following references: a, Böttcher *et al*. (2008); b, Tohge *et al*. (2005); c, In house database; d, Morrel *et al*. (2014); e, Song *et al*. (2005); f, MassBank Japan; g, RIKEN tandem mass spectral database (ReSpect), Riken, Japan.

[b] Fold changes of signal intensity were calculated with each transgenic line versus the wild-type. Data are given as the arithmetic average of five or six independent experiments with five or six biological replicates. Significant differences were assessed by Tukey's HSD test ($P < 0.05$). Bold font indicates a significant difference between the wild-type and transgenic line. ND, not detected.

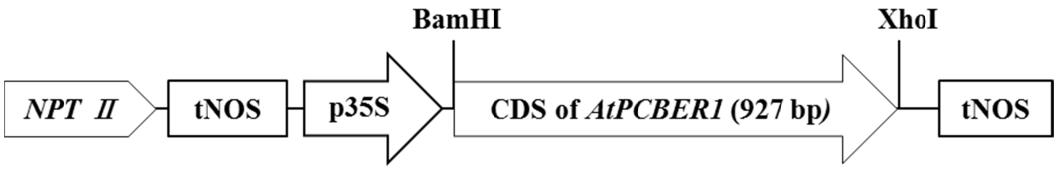

Figure 4-1 Expression cassette of expression vector for over expression of *AtPCBER1* gene in plants

tNOS: *nos* terminator

p35S: cauliflower mosaic virus (CaMV) 35S promoter

BamHI: restriction enzyme, *Bam*HI, recognition site

XhoI: restriction enzyme, *Xho*I, recognition site

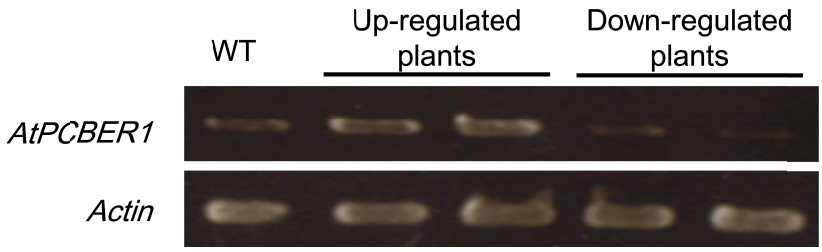

Figure 4-2 Analysis of *AtPCBER1* transcripts in wild-type (WT) and *AtPCBER1* up- and down-regulated plants by RT-PCR. The same amounts of RNA (2 μg) were isolated from rosette leaves of 48-day-old wild-type and the transgenic plants. The full-length CDS of *AtPCBER1* was amplified, and RT-PCR products were analyzed by gel electrophoresis on 1% agarose and stained with ethidium bromide.

Figure 4-3 *AtPCBER1* up- (middle) and down- (left) regulated transgenic Arabidopsis and wild type plants (right).

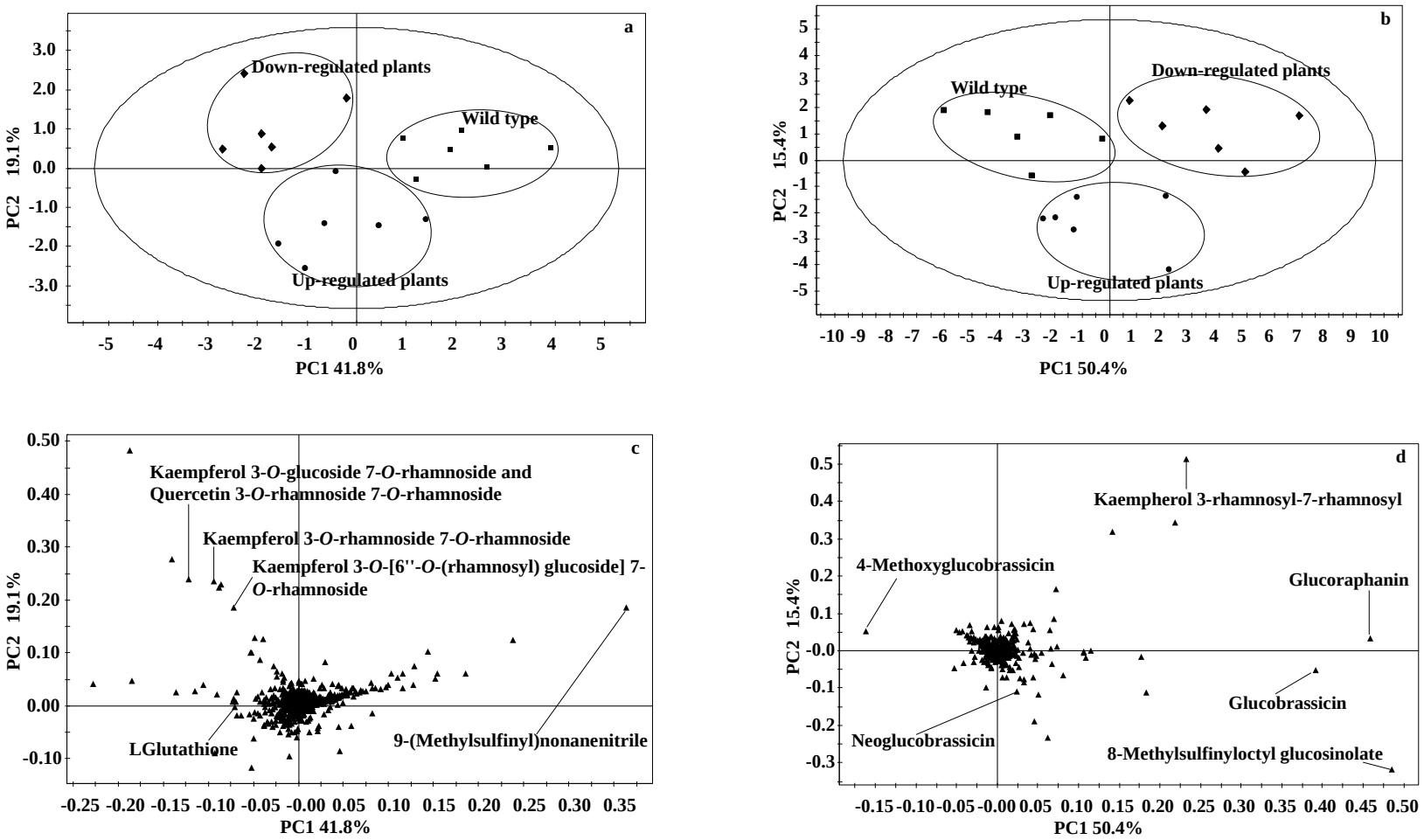

Figure. 4-4 Principal component analysis (PCA) of metabolites detected in untargeted metabolomic analysis of stem from wild-type and *AtPCBER1* up- and down-regulated plants. (Continued to next page)

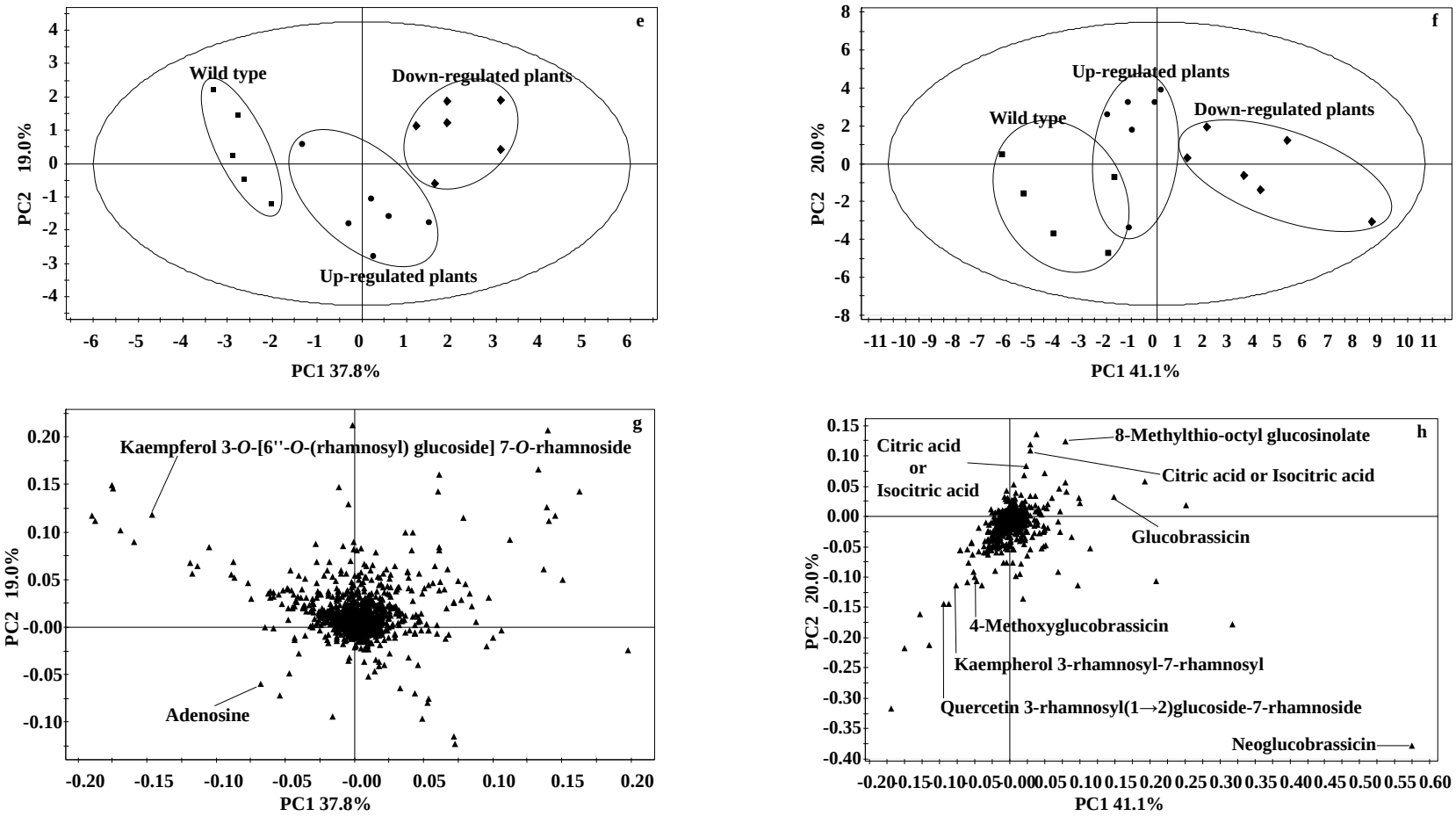

Figure. 4-4 Principal component analysis (PCA) of metabolites detected in untargeted metabolomic analysis of root from wild-type and *AtPCBER1* up- and down-regulated plants. (Continued to next page)

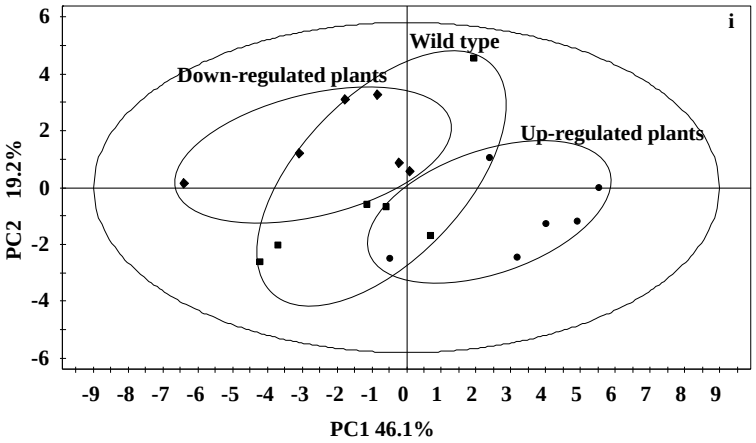
i
Wild type
Down-regulated plants
Up-regulated plants
PC2 19.2%
PC1 46.1%

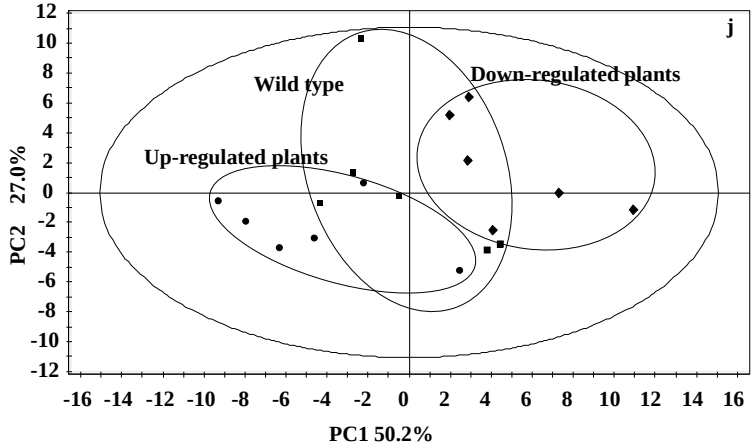
j
Wild type
Down-regulated plants
Up-regulated plants
PC2 27.0%
PC1 50.2%

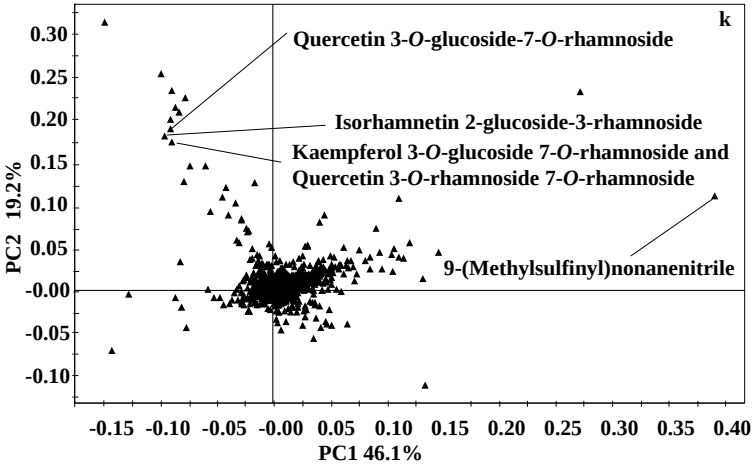
k
Quercetin 3-O-glucoside-7-O-rhamnoside
Isorhamnetin 2-glucoside-3-rhamnoside
Kaempferol 3-O-glucoside 7-O-rhamnoside and
Quercetin 3-O-rhamnoside 7-O-rhamnoside
9-(Methylsulfinyl)nonanenitrile
PC2 19.2%
PC1 46.1%

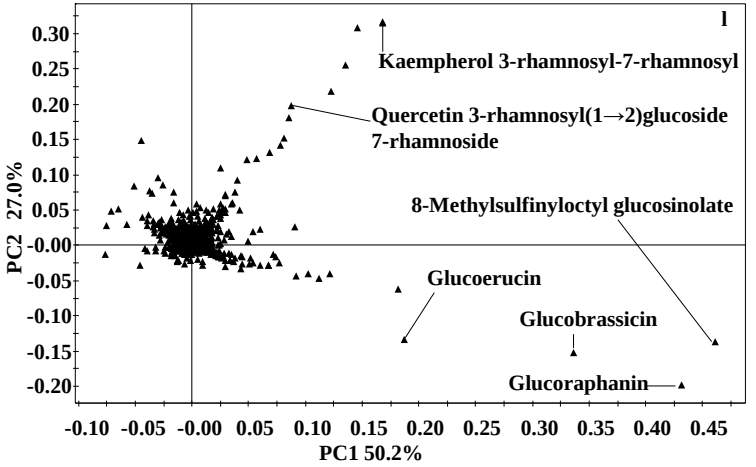
l
Kaempherol 3-rhamnosyl-7-rhamnosyl
Quercetin 3-rhamnosyl(1→2)glucoside
7-rhamnoside
8-Methylsulfinyloctyl glucosinolate
Glucoerucin
Glucobrassicin
Glucoraphanin
PC2 27.0%
PC1 50.2%

Figure 4-4 Principal component analysis (PCA) of metabolites detected in untargeted metabolomic analysis of flower from wild-type and *AtPCBER1* up- and down-regulated plants. **a**, **e** and **i** (score plots) and **c**, **g** and **k** (loading plots) were detected with negative ion modes, and **b**, **f** and **j** (score plots) and **d**, **h** and **l** (loading plots) was detected with positive ion modes. The annotated components indicate the significant differences between wild type plants and transgenic plants. The analysis was performed with five or six independent biological replicates for each organ.

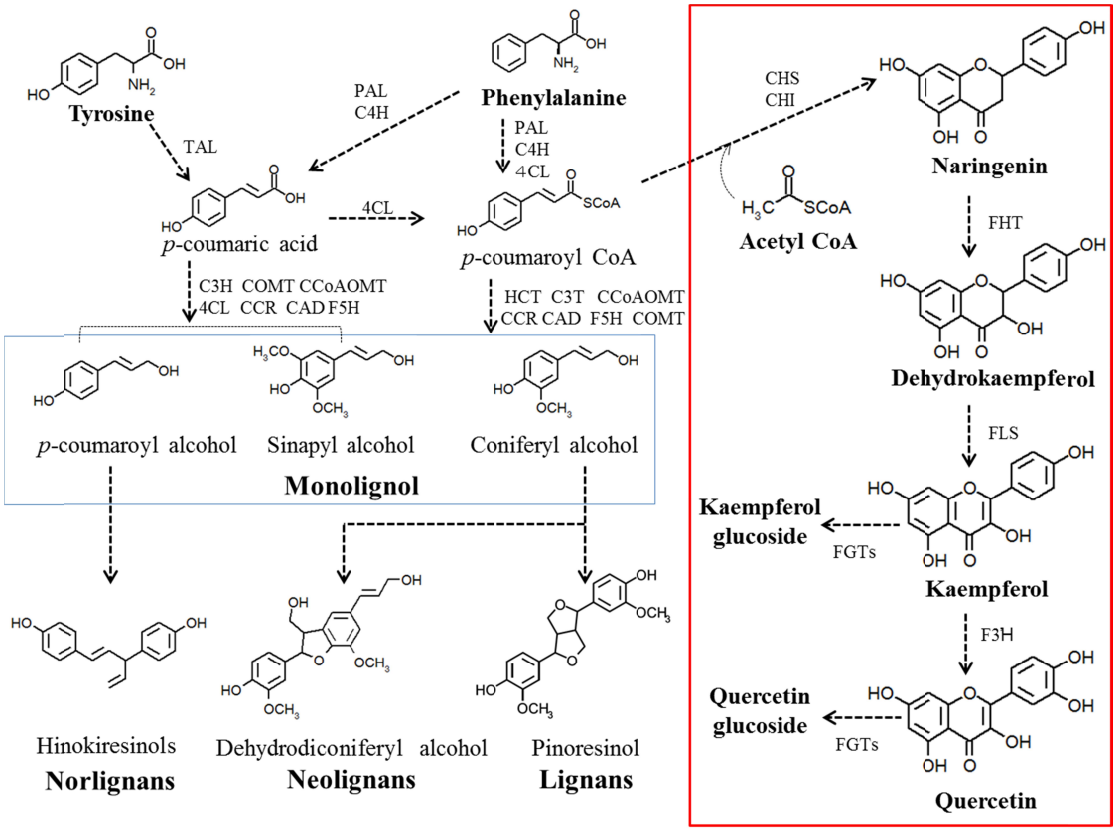

Figure 4-5 Biosynthetic pathway of lignans and flavones . PAL: phenylalanine ammonia-lyase; C4H: cinnamate 4-hydroxylase; 4CL: 4-coumarate: CoA ligase; CCR: cinnamoyl-CoA reductase; HCT: hydroxycinnamoyl transferase; C3H: *p*-coumarate 3-hydroxylase; CCoAOMT: caffeoyl-CoA *O*-methyltransferase; CAD: cinnamyl alcohol dehydrogenase. COMT: caffeic acid 3-*O*-methyltransferase; CHS: chalcone synthase; CHI: chalcone isomerase; F5H: ferulate 5-hydroxylase. FHT: Flavanone 3β-hydroxylase; FLS: Flavonol synthase; F3H: Flavanone 3-hydroxylase; FGTs: Flavonoid glycosyltransferases.

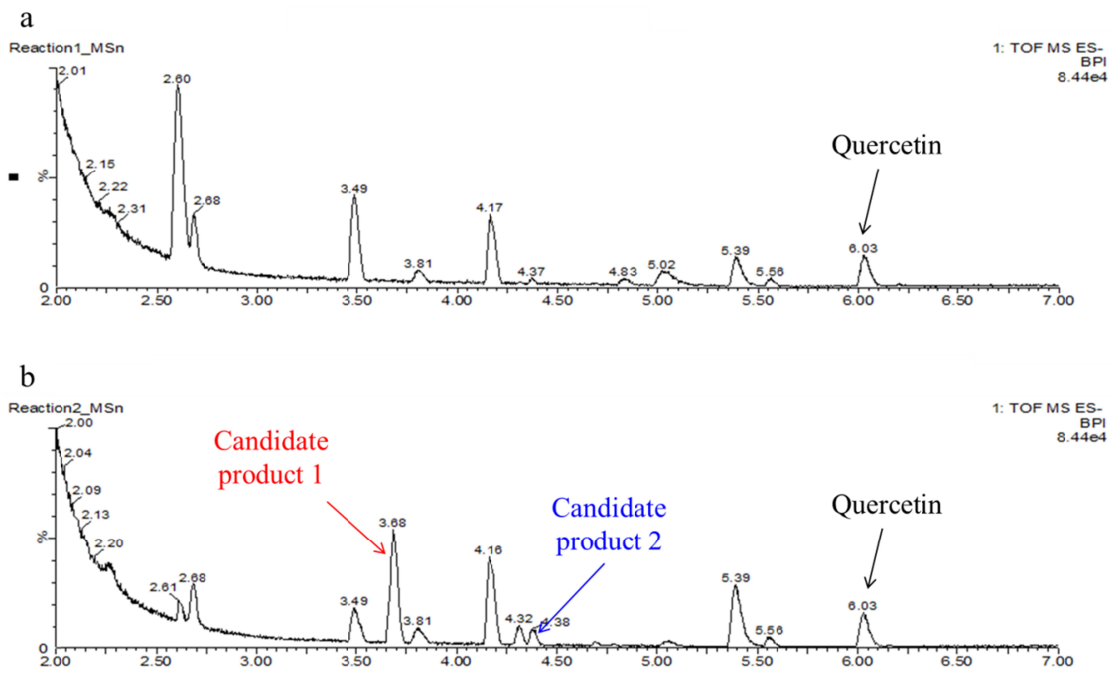

Figure 4-6 Characterization of recombinant His-AtPCBER1 with quercetin as substrate using LC-Q-TOF-MS analysis. **a** chromatogram of reaction mixture in which purified His-AtPCBER1was not added. **b**, chromatogram of reaction mixture with purified His-AtPCBER1 (100 ug/mL) and quercetin. The peaks of candidate product 1 and candidate product 2 could be observed only in Figure 4-6b.

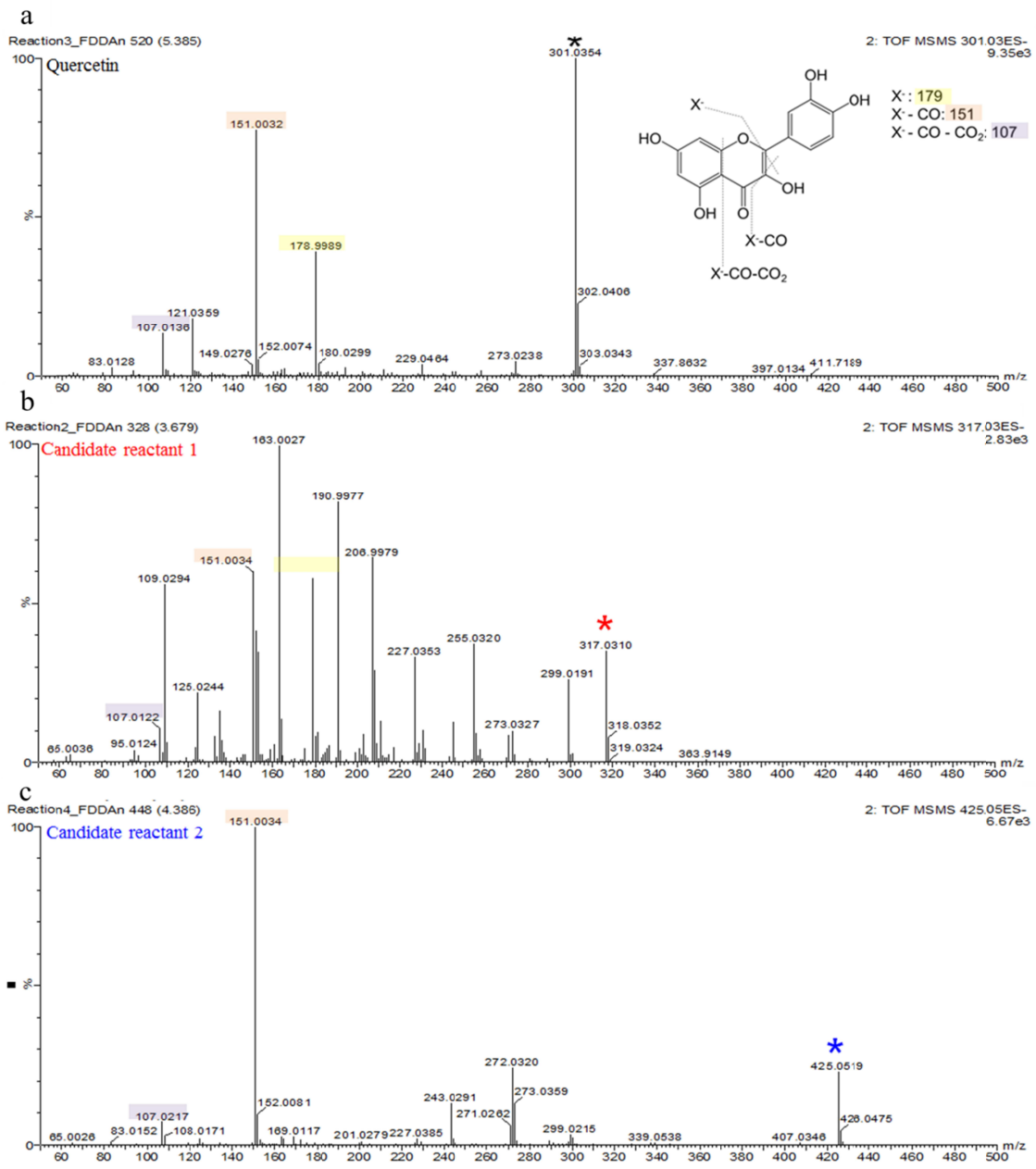

Figure 4-7 MS/MS characterization of reaction product in reaction mixture containing recombinant His-AtPCBER1 and quercetin. **a** MS spectrum of authentic compound quercetin; **b** and **c**, MS spectrum of candidate product 1 and candidate product 2.

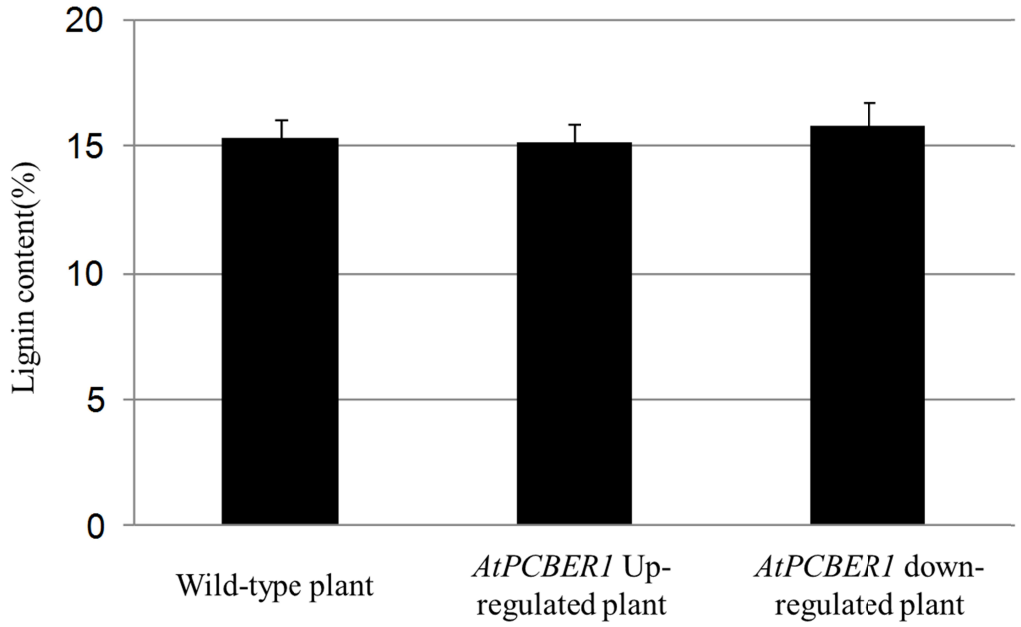

Figure 4-8 Lignin contents in stems of wild-type and transgenic lines. Levels of lignin in stems were measured using the acetyl bromide method. Values expressed as the percentage of lignin in extract-free samples (%, w/w).

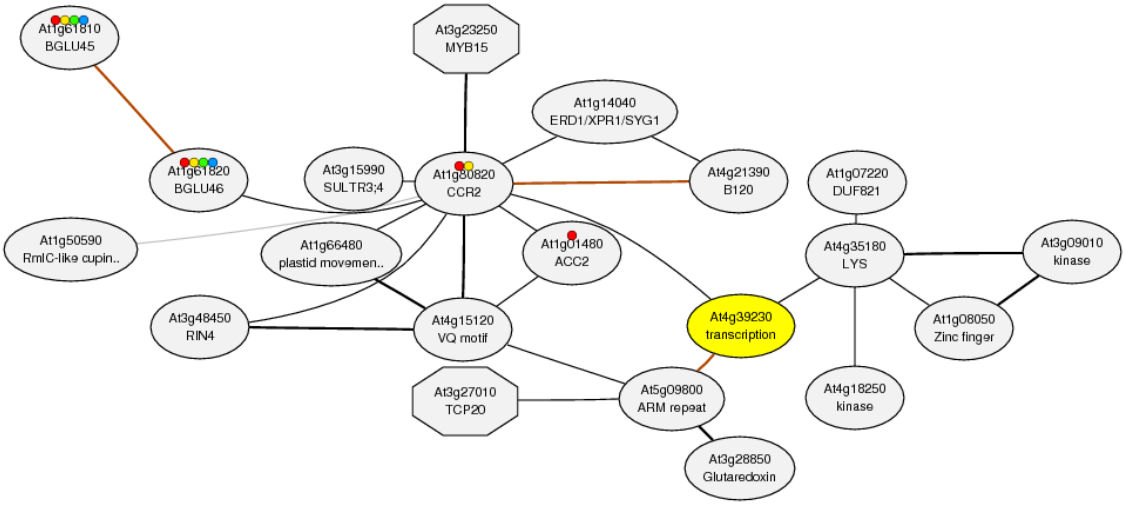

Figure 4-9 *AtPCBER1* (*AT4G39230*) gene co-expression networks.

The red ball indicates the gene involved in biosynthesis of secondary metabolites.

The yellow ball indicates the gene phenylpropanoid biosynthesis.

The green ball indicates the gene starch and sucrose metabolism.

The blue ball indicates the gene cyanoamino acid metabolism.

ARM repeat: ARM repeat superfamily protein, important in transducing WNT signals during embryonic development.

CCR: Cinnamoyl CoA reductase.

LYS: LYS/HIS transporter 7, amino acid transmembrane transporter activity.

Chapter 5

Final conclusions

Several genes that encode polypeptides with sequences similar to previously identified PCBERs are found in the genome of *A. thaliana*, no functional characterization studies have been reported thus far in this species. In order to reveal the main role of PCBER in plants, we studied one of putative NADPH-dependent oxidoreductase (At4g39230, named AtPCBER1) in *A. thaliana*, whose amino acid sequence is similar to those of identified PCBERs from various plant species.

The AtPCBER1 polypeptide contains a conserved NADPH binding domain, Gx(x)GxxG (positions 11 to 17), which is also common to other PCBERs, PLRs and IFRs. At the putative amino acid level, the sequences of AtPCBER1 shows high identities (64% to 71%) with those of previous identified PCBERs derived from other species, also shows high identities (52%-74%) with those of identified IFRs, but relatively low identities (37% to 44%) with PLRs derived from other species.

Expression analyses of *AtPCBER1* by reverse transcriptase-polymerase chain reaction and histochemical analysis of transgenic plants harboring the promoter region of *AtPCBER1* linked with *uidA* coding sequence indicated that expression is induced by wounding and UV irradiation (**Fig. 2-7** and **2-8**) and *AtPCBER1* was expressed in most organs, including flower, stem, leaf, and root.

Interestingly, In the putative promoter region of *AtPCBER1*, some of the putative core sequences for response to biotic and abiotic stimuli could be found, including *cis*-acting motifs for auxin response, wounding and pathogen responses, drought response, and pollen and meristem specific activation. In addition,

methyl jasmonate, ethylene and gibberellin responsive element also could be found in the promoter region of *AtPCBER1* (**Fig. 2-3**). Correspondingly, our GUS staining results indicate that *AtPCBER1* was high level expressed in pollen (**Fig. 2-6d)** and vascular tissues of root, petal, cauline and rosette leaves (**Fig. 2-6a**, **b**, **c**, and **f**). Although this expression pattern in the stem was not as clear as in these organs, *AtPCBER1* expression was also observed in the vascular tissue of the stem (**Fig. 2-6e**). And *AtPCBER1* expressed in part of the elongation area, such as, in hypocotyl as well as in root apex (**Fig. 2-6)**. Furthermore, *AtPCBER1* expression was significantly induced by mechanical wounding and ultraviolet-light treatment. Although the roles of *cis* elements were not fully elucidated in this study, these results suggest that the *cis*-acting regulatory elements on promoter region likely function in part at least.

PCBERs, including purified polypeptide from plant tissues and recombinant enzymes derived from other plant species indicate that substrate preferences of the PCBER toward the 8–5′ and 8–8′-linked lignans are variable upon plant species. In this article, we firstly isolated and cloned *AtPCBER1* from *A. thaliana* and successfully purified AtPCBER1 as a fusion protein with an N-terminal 6x histidine tag. According to previous research (Gang *et al*. 1999b; Bayindir *et al*. 2008) and result of this study, the specific activities (V_{max}) of recombinant PCBERs toward DDC vary among flax (0.78 pmol min^{-1} mg^{-1}, PCBER-Lc1), poplar (0.88 nmol min^{-1} mg^{-1}, PCBER-Pop1), pine (1.74 nmol min^{-1} mg^{-1}, PCBER-Pt1) and Arabidopsis (12.1 nmol min^{-1} mg^{-1}, AtPCBER1). This might be due to different experimental conditions for measurement of specific activity and/or different original kinetic parameters. Based on comparison of these catalytic properties, we concluded that *AtPCBER1*/*At4g39230* encodes the

PCBER of *A. thaliana*. In addition to tissue-specific expression pattern of PCBERs and comparison of these kinetic parameters of PCBERs from various plant species suggest that PCBER play various roles in *planta*.

The natural substrate of PCBER in *A. thaliana* or in other plant species has not been fully characterized. Put in another way, the exact role of PCBER in plant still remain unclear. To investigate further, we performed metabolomic analyses of transgenic plants in which the target gene was up- or down- regulated.

The transgenic plants in which the gene *AtPCBER1* was up- or down-regulated show normal phenotype. In our metabolomic analyses, structures of 36 components were resolved by MS/MS analysis (**Table 4-1**). Levels of 31 components were significantly different between the wild-type and *AtPCBER1* up- and/or down-regulated plants (**Table 4-1**). Interestingly, 12 of the 31 components, derivatives of kaempferol, quercetin, and cyanidin were flavonoids. Also, results indicate that significant changes in the levels of glucosinolates were detected in *AtPCBER1* up- and/or down-regulated transgenic plants compared to the wild-type (**Table 4-1**).

It is significantly that the lariciresinol hexoside and 8-*O*-4' type lignans quantitatively increased in *AtPCBER1* down-regulated plants. It suggests that AtPCBER1 may have no catalytic functions towards 8-8'-linked lignans and that *AtPCBER1* down-regulation may facilitate the other oxidative reactions, such as PLR-dependent oxidative reactions. And it is from another standpoint that increasing of 8-*O*-4' type lignans may imply the role of AtPCBER1 in lignin accumulation. However, the lignin contents in transgenic plants were not altered (**Fig. 4-8**). Unfortunately, DDC and the derived compounds were not detectable in all tested samples. This may be due to the small level existence of DDC in

Arabidopsis. It is also possible to think that DDC or derived compounds may present in complex-glucosylated form in Arabidopsis.

As mentioned in Chapter 1, biosynthesis of some glucosinolates is closely related to aromatic amino acids metabolites. In our metabolomic analysis, some glucosinolates, such as aromatic glucosinolate (glucobrassicin), were quantitatively altered in transgenic plants. It is suggested that the *AtPCBER1* expression level may have impact on glucosinolates accumulation.

In addition, quantities of scopoletin (one of coumarins) and L-glutathione were significantly influenced by *AtPCBER1* down-regulation (**Table 4-1**), it also suggested that, *AtPCBER1* expression might influence the other enzymatic processes for formation of secondary metabolites. This phenomenon also was observed in metabolomic analysis of *PCBER* down-regulated transgenic poplar reported by Niculaes *et al.* (2014) and metabolomic analysis transgenic *A. thaliana* overexpressing bacterial pinoresinol reductase gene reported by Tamura *et al.* (2014).

Except for several flavonoids, the changing trend of all characterized compounds in **Table 4-1** was varied in flower, root and stem. These results suggest that *AtPCBER1* expression level or lignan biosynthesis may have different impact on different plant organs.

Among these components, derivatives of kaempferol and quercetin decreased and increased in PCBER up- and down-regulated plants, respectively. It is well known that, flavonoids are the stress responsible compounds in plants, such as, response to UV-irradiation. Interestingly, the *AtPCBER1* expression was also stimulated by UV light irradiation. These results suggest that, *AtPCBER1* expression and/or lignan biosynthesis somehow have influence on the flavonoids

biosynthesis. In addition, based on linear correlation of *ATPCBER1* expression level and flavonoids contents, we made the presumption that conversion of kaempferol (and/or quercetin) derivatives may be directly catalyzed by AtPCBER1. And this possibility was determined by using four different flavonoid derivatives as substrates. As shown in **Fig. 4-6** and **4-7,** the quercetin could be converted or modified in other ways by AtPCBER1 enzyme. These results also suggest the possibility that *AtPCBER1* gene involved in flavones biosynthesis.

Taken together, all results indicate that, AtPCBER1 is a crucial enzyme in *A. thaliana* and have a considerable role in formation of secondary metabolites.

References

Afendi FM, Okada T, Yamazaki M, Hirai-Morita A, Nakamura Y, Nakamura K, Ikeda S, Takahashi H, Altaf-Ul-Amin M, Darusman L, Saito K, Kanaya S (2012) KNApSAcK family databases: Integrated metabolite-plant species databases for multifaceted plant research. Plant Cell Physiol 53:e1. doi: 10.1093/pcp/pcr165

Apers S, Vlietinck A, Pieters L (2003) Lignans and neolignans as lead compounds. Phytochem Rev 2:201–217. Doi: 10.1023/B:PHYT.0000045497.90158.d2

Asano J, Chiba K, Tada M, Yoshii T (1996) Antiviral activity of lignans and their glycosides from *Justicia procumbens*. Phytochemistry 42: 713-717. doi: 10.1016/0031-9422(96)00024-6

Attoumbre J, Hano C, Mesnard F, Lamblin F, Bensaddek L, Grandic SRL, Laine É, Fliniaux MA, Baltora-Rosset S (2005) Identification by NMR and accumulation of a neolignan, the dehydrodiconiferyl alcohol-4-β-D-glucoside, in *Linum usitatissimum* cell cultures. C R Chimie 9:420–425. doi: 10.1016/j.crci.2005.06.012

Ayella AK, Trick HN, Wang WQ (2007) Enhancing lignan biosynthesis by over-expressing pinoresinol lariciresinol reductase in transgenic wheat. Mol Nutr Food Res 51: 1518-1526. doi: 10.1002/mnfr.200700233

Banerjee A, Chattopadhyay S (2010) Effect of over-expression of *Linum*

usitatissimum pinoresinol lariciresinol reductase (LuPLR) gene in transgenic *Phyllanthus amarus.* Plant Cell Tiss Organ Cult 103:315–323. doi: 10.1007/s11240-010-9781-x

Bayindir Ü, Alfermann AW, Fuss E (2008) Hinokinin biosynthesis in *Linum corymbulosum* Reichenb. Plant J 55:810-820. doi: 10.1111/j.1365-313X.2008.03558.x

Brandalise M, Severino FE, Maluf MP, Maia IG (2009) The promoter of a gene encoding an isoflavone reductase-like protein in coffee (*Coffea arabica*) drives a stress-responsive expression in leaves. Plant Cell Rep 28:1699–1708. doi: 10.1007/s00299-009-0769-0

Barata LES, Santos LS, Ferri PH, Phillipson JD, Paine A, Croft SL (2000) Anti-leishmanial activity of neolignans from *Virola* species and synthetic analogues. Phytochemistry 55: 589-595. doi: 10.1016/S0031-9422(00)00240-5

Bate N and Twell D (1998) Functional architecture of a late pollen promoter pollen-specific transcription is developmentally regulated by multiple stage-specific and co-dependent activator elements. Plant Mol Biol 37:859-869. doi: 10.1023/A:1006095023050

Beejmohun V, Fliniaux O, Hano C, Pilard S, Grand E, Lesur D, Cailleu D, Lamblin F, Laine E, Kovensky J, Fliniaux MA, Mesnard F (2007) Coniferin dimerisation in lignan biosynthesis in flax cells. Phytochemistry 68: 2744-2752.

doi: 10.1016/j.phytochem.2007.09.016

Binns AN, Chen RH, Wood HN and Lynn DG (1987) Cell-division promoting activity of naturally-occurring dehydrodiconiferyl glucosides - do cell-wall components control cell-division. Proc Natl Acad Sci USA 84:980–984. doi: 10.1073/pnas.84.4.980

Bito N, Nakada R, Fukatsu E, Matsushita Y, Fukushima K, Imai T (2011) Clonal variation in heartwood norlignans of *Cryptomeria japonica*: evidence for independent control of agatharesinol and sequirin C biosynthesis. Ann For Sci 68: 1049-1056. doi: 10.1007/s13595-011-0118-7

Boerjan W, Polle A, Mijnsbrugge KV (2006) Role in lignification and growth for plant phenylcoumaran benzylic ether reductase. US patent application US 20060015967 A1

Boter M, Ruiz Rivero O, Abdeen A, Prat S (2004) Conserved MYC transcription factors play a key role in jasmonate signaling both in tomato and Arabidopsis. Genes Dev 18, 1577–1591. doi: 10.1101/gad.297704

Böttcher C, von Roepenack-Lahaye E, Schmidt J, Schmotz C, Neumann S, Scheel D, Clemens S (2008) Metabolome analysis of biosynthetic mutants reveals a diversity of metabolic changes and allows identification of a large number of new compounds in Arabidopsis. Plant Physiol 147:2107–2120. doi: 10.1104/pp.108.117754

Brooks JD, Ward WE, Lewis JE, Hilditch J, Nickell L, Wong E, Thompson LU (2008) Supplementation with flaxseed alters estrogen metabolism in postmenopausal women to a greater extent than does supplementation with an equal amount of soy. AM J Clin Nutr 79: 318-325.

Burchard P, Bilger W, Weissenböck G (2000) Contribution of hydroxycinnamates and flavonoids to epidermal shielding of UV-A and UV-B radiation in developing rye primary leaves as assessed by ultraviolet-induced chlorophyll fluorescence measurements. Plant Cell Environ 23:1373-1380. doi: 10.1046/j.1365-3040.2000.00633.x

Caldo RA, Nettleton D, Wise RP (2004) Interaction-dependent gene expression in Mla-specified response to barley powdery mildew. Plant Cell 16: 2514–2528. doi: 10.1105/tpc.104.023382

Caldwell M, Robberecht R, Flint S (1983) Internal filters: Prospects for UV-acclimation in higher plants. Physiol Plant 58(3):445-450.

Castro MA, Gordaliza M, Miguel del Corral J, San Fericiano A (1996) The distribution of lignanoids in the order Coniferae. Phytochemistry 41:995–1011. doi: 10.1016/0031-9422(95)00512-9

Chen XH, Kim CS, Kashiwagi T, Tebayashi S, Horiike M (2001) Antifeedants against *Acusta despesta* from the Japanese cedar, *Cryptomeria japonica* II. Biosci Biotechnol Biochem 65:1434–1437. doi:10.1271/bbb.65.1434

Cheng H, Li LL, Xu F, Wang Y, Yuan HH, Wu CH, Wang SB, Liao ZQ, Hua J, Wang YP, Cheng SY, Cao FL (2013) Expression patterns of an isoflavone reductase-like gene and its possible roles in secondary metabolism in *Ginkgo biloba*. Plant Cell Rep 32:637–650. doi: 10.1007/s00299-013-1397-2

Davin LB, Wang HB, Crowell AL, Bedgar DL, Martin DM, Sarkanen S, Lewis NG (1997) Stereoselective bimolecular phenoxy radical coupling by an auxiliary (dirigent) protein without an active center. Science 275:362-366. doi: 10.1126/science.275.5298.362

Davin LB, Lewis NG (2003) An historical perspective on lignan biosynthesis: monolignol, allyphenol and hydroxycinnamic acid coupling and downstream metabolism. Phytochem Rev 7: 257–288. Doi:10.1023/B:PHYT.0000046175.83729.b5

Dillon SK, Nolan M, Li W, Bell C, Wu HX, Southerton SG (2010) Allelic variation in cell wall candidate genes affecting solid wood properties in natural populations and land races of *Pinus radiata*. Genetics 185:1477-1487. doi: 10.1073/pnas.84.4.980

Dinkova-Kostova AT, Gang DR, Davin LB, Bedgar DL, Chu A, Lewis NG (1996) (+)-Pinoresinol/ (+)-Lariciresinol reductase from *Forsythia intermedia* - Protein purification, cDNA cloning, heterologous expression and comparison to isoflavone reductase. J Biol Chem 271:29473–29482

Dixon RA, Paiva Nl (1995) Stress-induced phenylpropanoid metabolism. Plant cell 7:1085-1097. doi: 10.1105/tpc.7.7.1085

Drews GN, Beals TP, Bui AQ, Goldberg RB (1992) Regional and cell-specific gene expression patterns during petal development. Plant Cell 4: 1383–1404.

Dubouzet JG, Sakuma Y, Ito Y, Kasuga M, Dubouzet EG, Miura S, Seki M, Shinozaki K, Yamaguchi-Shinozaki K (2003) *OsDREB* genes in rice, *Oryza sativa* L., encode transcription activators that function in drought-, high salt- and cold- responsive gene expression. Plant J. 33: 751–763. doi: 10.1046/j.1365-313X.2003.01661.x

Edwards K, Cramer CL, Bolwell GP, Dixon RA, Schuch W, Lamb CJ (1985) Rapid transient induction of phenylalanine ammonia-lyase mRNA in elicitor-treated bean cells. Proc Natl Acad Sci. 82: 6731-6735

Farkya S, Bisaria VS, Srivastava AK (2004) Biotechnological aspects of the production of the anticancer drug podophyllotoxin. Appl. Microbiol. Biotechnol. 65: 504-519. doi: 10.1007/s00253-004-1680-9

Fujita M, Gang DR, Davin LB, Lewis NG (1999) Recombinant Pinoresinol-Lariciresinol Reductases from Western Red Cedar (*Thuja plicata*) catalyze opposite enantiospecific conversions. J Biol Chem 274: 618–627. doi: 10.1074/jbc.274.2.618

Gang DR, Costa MA, Fujita M, Dinkova-Kostova AT, Wang HB, Burlat V, Martin W, Sarkanen S, Davin LB, Lewis NG (1999a) Regiochemical control of monolignol radical coupling: a now paradigm for lignin and lignan biosynthesis. Chem Biol 6: 143-151. doi: 10.1016/S1074-5521(99)89006-1

Gang DR, Dinkova-Kostova AT, Davin LB, Lewis NG (1997) Phylogenetic links in plant defense systems: Lignans, isoflavonoids, and their reductases. Am Chem Soc Symp Ser 658:58–89.

Gang DR, Kasahara H, Xia ZQ, Mijnsbrugge KV, Bauw G, Boerjan W, Montagu MV, Davin LB, Lewis NG (1999b) Evolution of plant defense mechanisms. Relationships of phenylcoumaran benzylic ether reductases to pinoresinol-lariciresinol and isoflavone reductases. J Biol Chem 274(11):7516–7527. doi: 10.1074/jbc.274.11.7516

Gomes GLGC, Carbonari CA, Velini ED, Trindade MLB, Silva JRM (2015) Extraction and simultaneous determination of glyphosate, ampa and compounds of the shikimic acid pathway in plants. Planta daninha 33: 295-304. doi: 10.1590/0100-83582015000200015

Hanusch AL, de Oliveira GR, de Saboia-Morais SMT, Machado RC, dos Anjos MM, Chen LC (2015) Genotoxicity and cytotoxicity evaluation of the neolignan analogue 2-(4-nitrophenoxy)-1 phenylethanone and its protective effect against DNA damage. PLOS ONE 10. doi: 10.1371/journal.pone.0142284

Hartmann T (2007) From waste products to ecochemicals: Fifty years research of plant secondary metabolism. Phytochemistry 68: 2831-2846. doi: 10.1016/j.phytochem.2007.09.017

Hemmatia S, Schmidtb TJ, Fussa E (2007) (+)-Pinoresinol/(-)-lariciresinol reductase from *Linum perenne* Himmelszelt involved in the biosynthesis of justicidin B. FEBS Lett 581:603–610. doi: 10.1016/j.febslet.2007.01.018

Herrmann KM, Weaver LM (1999) The Shikimate Pathway. Annu Rev Plant Physiol Plant Mol Biol 50: 473–503. doi:10.1146/annurev.arplant.50.1.473

Higo K, Ugawa Y, Iwamoto M, Korenaga T (1999) Plant *cis*-acting regulatory DNA elements (PLACE) database: 1999. Nucleic Acids Res 27:297-300. doi: 10.1093/nar/27.1.297

Holmborn B, Eckerman C, Eklund P, Hemming J, Nisula L, Reunanen M, Sjöholm R, Sundberg A, Sundberg K, Willför S (2003) Knots in trees: a new rich source of lignans. Phytochem Rev 2: 331–340

Huang WY, Cai YZ, Zhang Y (2010) Natural phenolic compounds from medicinal herbs and dietary plants: potential use for cancer prevention. Nutrition and Cancer 62:1532-7914

Huis R, Morreel K, Fliniaux O, Lucau-Danila A, Fenart S, Grec S, Neutelings G, Chabbert B, Mesnard F, Boerjan W, Hawkins S (2015) Natural hypolignification

is associated with extensive oligolignol accumulation in flax stems. Plant physiol 158: 1893-1915. doi: 10.1104/pp.111.192328

Imai T, Nomura M, Fukushima K (2006) Evidence for involvement of the phenylpropanoid pathway in the biosynthesis of the norlignan agatharesinol. J. Plant Physiol 163:483-487. doi: 10.1016/j.jplph.2005.08.009

Imai T, Asai K, Takino M, Fukushima K (2009) In vitro hydroxylation of a norlignan: from agatharesinol to sequirin C and metasequirin C with a microsomal preparation from *Cryptomeria japonica*. Phytochem Lett 2:196–200. doi:10.1016/j.phytol.2009.07.002

In SJ, Seo KH, Song NY, Lee DS, Kim YC, Baek NI (2015) Lignans and neolignans from the stems of *Vibrunum erosum* and their neuroprotective and anti-inflammatory activity. Arch Pharm Res 38: 26-34. doi: 10.1007/s12272-014-0358-9

Jimenez-Lopez JC, Kotchoni SO, Hernandez-Soriano MC, Gachomo EW, Alché JD (2013) Structural functionality, catalytic mechanism modeling and molecular allergenicity of phenylcoumaran benzylic ether reductase, an olive pollen (Ole e 12) allergen. J Comput Aided Mol Des 27:873–895. doi: 10.1007/s10822-013-9686-y

Kajita S, Hishiyama S, Tomimura Y, Katayama Y, Omori S (1997) Structural characterization of modified lignin in transgenic tobacco plants in which the

activity of 4-Coumarate:Coenzyme a ligase is depressed. Plant Physiol 114:871-879

Karamloo F, Wangorsch A, Kasahara H, Davin LB, Haustein D, Lewis NG, Vieths S (2001) Phenylcoumaran benzylic ether and isoflavonoid reductases are a new class of cross-reactive allergens in birch pollen, fruits and vegetables. J Biol Chem 268:5310-5320. doi: 10.1046/j.0014-2956.2001.02463.x

Kasahara H, Jiao Y, Bedgar DL, Kim SJ, Patten AM, Xia ZQ, Davin LB, Lewis NG (2006) *Pinus taeda* phenylpropenal double-bond reductase: Purification, cDNA cloning, heterologous expression in *Escherichia coli*, and subcellular localization in *P. taeda*. Phytochemistry 67: 1765-1780. doi: 10.1016/j.phytochem.2006.07.001

Kim WC, Kim JY, Ko JH, Kang H, Han KH (2014) Identification of direct targets of transcription factor MYB46 provides insights into the transcriptional regulation of secondary wall biosynthesis. Plant Mol Biol 85:589–599. doi: 10.1007/s11103-014-0205-x

Krizek DT, Britz SJ, Mirecki RM (1998) Inhibitory effects of ambient level of solar UV-A and UV-B on growth of New Red Fire lettuce. Plant Physiol 103:1-7. doi: 10.1034/j.1399-3054.1998.1030101.x

Kwon M, Davin LB, Lewis NG (2001) In situ hybridization and immunolocalization of lignan reductases in woody tissues: implications for heartwood formation and other forms of vascular tissue preservation. Phytochem

57:899–914. doi: 10.1016/S0031-9422(01)00108-X

Lee KH, Xiao Z (2003) Lignans in treatment of cancer and other diseases. Phytochem Rev 2, 341–362. Doi: 10.1023/B:PHYT.0000045495.59732.58

Lescot M, Déhais P, Thijs G, Marchal K, Moreau Y, Van de Peer Y, Rouzé P, Rombauts S (2002) PlantCARE, a database of plant cis-acting regulatory elements and a portal to tools for *in silico* analysis of promoter sequences. Nucleic Acids Res 30:325-327. doi: 10.1093/nar/30.1.325

Matsuda F, Hirai MY, Sasaki E, Akiyama K, Yonekura-Sakakibara K, Provart NJ, Sakurai T, Shimada Y, Saito K (2010) AtMetExpress Development: A Phytochemical Atlas of Arabidopsis Development. Plant Physiol 152:566-578. doi: 10.1104/pp.109.148031

Menges M, Hennig L, Gruissem W, Murray JAH (2002) Cell cycle-regulated gene expression in *Arabidopsis*. J Biol Chem 227: 41987-42002. doi: 10.1074/jbc.M207570200

Min TP, Kasahara H, Bedgar DL, Youn BY, Lawrence PK, Gang DR, Halls SC, Park HJ, Hilsenbeck JL, Davin LB, Lewis NG, Kang C (2003) Crystal structures of pinoresinol-lariciresinol and phenylcoumaran benzylic ether reductases and their relationship to isoflavone reductases. J Biol Chem 278: 50714-50723. doi: 10.1074/jbc.M308493200

Morreel K, Saeys Y, Dima O, Lu FC, Van de Peer,a Y, Vanholme R, Ralph J, Vanholme B, Boerjana W (2014) Systematic Structural Characterization of metabolites in *A. thaliana* via candidate substrate-product pair networks. Plant Cell 26: 929–945. doi: 10.1105/tpc.113.122242

Nakatsubo T, Mizutani M, Suzuki S, Hattori T, Umezawa T (2008) Characterization of *A. thaliana* pinoresinol reductase, a new type of enzyme involved in lignan biosynthesis J Biol Chem 283:15550-15557. doi: 10.1074/jbc.M801131200

Negi AS, Kumar JK, Luqman S, Shanker K, Gupta MM, Khanuja SP (2008) Recent advances in plant hepatoprotectives: a chemical and biological profile of some important leads. Med Res Rev 28:746-772. doi: 10.1002/med.20115

Niculaes C, Morreel K, Kim H, Lu FC, McKee LS, Ivens B, Haustraete J, Vanholme B, De Rycke R, Hertzberg M, Fromm J, Bulone V, Polle A, Ralph J, Boerjana W (2014) Phenylcoumaran benzylic ether reductase prevents accumulation of compounds formed under oxidative conditions in poplar xylem. Plant Cell 26: 3775–3791. doi: 10.1105/tpc.114.125260

Nose M, Bernards MA, Furlan M, Zajicek J, Eberhardt TL, Lewis NG (1995) Towards the specification of consecutive steps in macrolecular lignin assembly Phytochemistry 39: 71-79. doi: 10.1016/0031-9422(95)95268-Y

Okunishi T, Sakakibara N, Suzuki S, Umezawa T, Shimada M (2004)

Stereochemistry of matairesinol formation by Daphne secoisolariciresinol dehydrogenase. J Wood Sci 50:77–81. doi: 10.1007/s10086-003-0516-z.

Orr JD, Lynn DG (1991) Biosynthesis of dehydrodiconiferyl alcohol glucosides: Implications for the control of tobacco cell growth. Plant Physiol 98: 343-352. doi: 10.1104/pp.98.1.343

Paiva NL, Edwards R, Sun YJ, Hrazdina G, Dixon RA (1991) Stress responses in alfalfa (*Medicago sativa* L.) 11. Molecular cloning and expression of alfalfa isoflavone reductase, a key enzyme of isoflavonoid phytoalexin biosynthesis. Plant Mol Biol 17:653-667. doi: 10.1007/BF00037051

Paiva NL, Sun YJ, Dixon, RA, Vanetten HD, Hrazdina G (1994) Molecular-cloning of isoflavone reductase from Pea (*Pisum sativum* L.) - evidence for a 3-rdisoflavanone intermediate in (+)-pisatin biosynthesis. Arch Biochem Biophys 312:501-510. doi: 10.1006/abbi.1994.1338

Prasad K (1999) Reduction of serum cholesterol and hypercholesterolemic atherosclerosis in rabbits by secoisolariciresinol diglucoside isolated from flaxseed. Circulation 99: 1355-1362

Ralph S, Park JY, Bohlmann J, Mansfield SD (2006) Dirigent proteins in conifer defense: gene discovery, phylogeny, and differential wound- and insect-induced expression of a family of DIR and DIR-like genes in spruce (*Picea* spp.). Plant Mol Biol 60: 21–40. doi: 10.1007/s11103-005-2226-y

Ribeiro AB, Bolzani VD, Yoshida M, Santos LS, Eberlin MN, Silva DHS (2005) A new neolignan and antioxidant Phenols from *Nectandra grandiflora*. J Braz Chem Soc 16: 526-530. DOI: 10.1590/S0103-50532005000400005

Ruprecht C, Mutwil M, Saxe F, Eder M, Nikoloski Z, Persson S (2011) Large-scale co-expression approach to dissect secondary cell wall formation across plant species. Front Plant Sci 2:23. doi: 10.3389/fpls.2011.00023

Saguez J, Attoumbre J, Giordanengo P, Baltora-Rosset S (2013) Biological activities of lignans and neolignans on the aphid *Myzus persicae* (Sulzer). Arthropod Plant Interact 7:225-233. doi: 10.1007/s11829-012-9236-x

Sarry JE, Kuhn L, Ducruix C, Lafaye A, Junot C, Hugouvieux V, Jourdain A, Bastien O, Fievet JB, Vailhen D, Amekraz B, Moulin C, Ezan E, Garin J, Bourguignon J (2006) The early responses of *Arabidopsis thaliana* cells to cadmium exposure explored by protein and metabolite profiling analyses. Proteomics 6:2180-2198. doi: 10.1002/pmic.200500543

Shoji T, Winz R, Iwase T, Nakajima K, Yamada Y, Hashimoto T (2002) Expression patterns of two tobacco isoflavone reductase-like genes and their possible roles in secondary metabolism in tobacco. Plant Mol Biol 50:427–440. doi: 10.1023/A:1019867732278

Shu JC, Liang F, Liang J, Liang YH, Li FQ, Shao F, Liu RH, Huang HL (2015) Phenylpropanoids and neolignans from *Smilax trinervula*. FITOTERAPIA

104:64-68. doi: 10.1016/j.fitote.2015.05.010

Song LJ, Morrison JJ, Botting NP , Thornalley PJ (2005) Analysis of glucosinolates, isothiocyanates, and amine degradation products in vegetable extracts and blood plasma by LC–MS/MS. Anal Biochem 347:234-243. doi: 10.1016/j.ab.2005.09.040

Su WC, Fang JM, Cheng YS (1995) Flavonoids and lignans from leaves of *Cryptomeria japonica*. Phytochemistry 40: 563-566

Sumner LW, Amberg A, Barrett D, Beale MH, Beger R, Daykin CA, Fan TW-M, Fiehn O, Goodacre R, Griffin JL, Hankemeier T, Hardy N, Harnly J, Higashi R, Kopka J, Lane AN, Lindon JC, Marriott P, Nicholls AW, Reily D, Thaden JJ, Viant MR (2007) Proposed minimum reporting standards for chemical analysis. Metabolmics 3:211–221. doi:10.1007/s11306-007-0082-2

Suzuki S, Umezawa T, Shimada M (2001) Norlignan biosynthesis in *Asparagus officinalis* L.: the norlignan originates from two nonidentical phenylpropane units. J Chem Soc Perkin Trans 1: 3252–3257. doi: 10.1039/b107949b.

Suzuki S, Nakatsubo T, Umezawa T, Shimada M (2002) First *in vitro* norlignan formation with *Asparagus officinalis* enzyme preparation. Chem Commun 1088–1089. doi: 10.1039/b200217e

Suzuki S, Umezawa T (2007) Biosynthesis of lignans and norlignans. J Wood Sci 53:273–284. doi: 10.1007/s10086-007-0892-x

Takahashi K, Mori K (2006) Relationships between blackening phenomenon and norlignans of sugi (*Cryptomeria japonica*) heartwood. III: coloration of norlignans with alkaline treatment. J Wood Sci 52:134–139. doi:10.1007/s10086-005-0733-8

Tamura M, Tsuji Y, Kusunose T, Okazawa A, Kamimura N, Morid T, Nakabayashi R, Hishiyama S, Fukuhara Y, Hara H, Sato-Izawa K, Muranaka T, Saito K, Katayama Y, Fukuda M, Masai E and Kajita S (2014) Successful expression of a novel bacterial gene for pinoresinol reductase and its effect on lignan biosynthesis in transgenic *Arabidopsis thaliana* Appl Microbiol Biotechnol 98:8165–8177. doi: 10.1007/s00253-014-5934-x

Tiemann K, Inze D, von Montagu M, Barz W (1991) Pterocarpan phytoalexin biosynthesis in elicitor-challenged chickpea (*Cicer arietinum* L.) cell cultures purification, characterization and cDNA cloning of NADPH: isoflavone oxidoreductase. Eur J Biochem 200:751-757. doi: 10.1111/j.1432-1033.1991.tb16241.x

Tohge T, Nishiyama Y, Hirai MY, Yano M, Nakajima J, Awazuhara M, Inoue E, Takahashi H, Goodenowe DB, Kitayama M, Noji M, Yamazaki M, Saito K (2005) Functional genomics by integrated analysis of metabolome and transcriptome of *Arabidopsis* plants over-expressing an MYB transcription factor. Plant J 42:218–235. doi: 10.1111/j.1365-313X.2005.02371.x

Tohge T, Watanabe M, Hoefgen R, Fernie AR (2013) Shikimate and

phenylalanine biosynthesis in the green lineage. Front Plant Sci 4. doi: 10.3389/fpls.2013.00062

Umezawa T, Davin LB, Lewis NG (1991) Formation of lignans (-)-secoisolariciresinol and (-)-matairesinol with *Forsythia intermedia* cell-free extracts. J Biol Chem 266:10210–10217

Umezawa T (2003a) Diversity in lignan biosynthesis. Phytochem Rev 2:371–390. doi: 10.1023/B:PHYT.0000045487.02836.32

Umezawa T. 2003b. Phylogenetic distribution of lignan producing plants. Wood Res 90, 27–110.

Vander mijnsbrugge K, Beeckman H, De Rycke R, Van Montagu M, Engler G, Boerjan W (2000) Phenylcoumaran benzylic ether reductase, a prominent xylem protein, is strongly associated with phenylpropanoid biosynthesis in lignifying cells. Planta 211: 502-509. doi: 10.1007/s004250000326

Vassão DG, Kim SJ, Milhollan JK, Eichinger D, Davin LB, Lewis NG (2007) A pinoresinol-lariciresinol reductase homologue from the creosote bush (*Larrea tridentata*) catalyzes the efficient *in vitro* conversion of *p*-coumaryl/coniferyl alcohol esters into the allylphenols chavicol/eugenol, but not the propenylphenols *p*-anol/isoeugenol. Arch Biochem Biophys 465:209-218. doi: 10.1016/j.abb.2007.06.002

von Heimendahl CBI, Schäfer KM, Eklund P, Sjöholm R, Schmidt TJ, Fuss E (2005) Pinoresinol–lariciresinol reductases with different stereospecificity from *Linum album* and *Linum usitatissimum*. Phytochem 66:1254–1263. doi: 10.1016/j.phytochem.2005.04.026

Weng JK, Chapple C (2010) The origin and evolution of lignin biosynthesis. New Phytol 187: 273–285. doi: 10.1111/j.1469-8137.2010.03327.x

Whetten R, Sederoff R (1995) Lignin biosynthesis. Plant Cell 7: 1001–1013.

Wingate VPM, Lawton MA, Lamb CJ (1988) Glutathione causes a massive and selective induction of plant defense genes. Plant Physiol 86: 206-210

Xue W, Ruprecht C, Street N, Hematy K, Chang C (2012) Paramutation-Like Interaction of T-DNA Loci in *Arabidopsis*. PLOS ONE 7:e51651. doi:10.1371/journal.pone.0051651

Yonekura-Sakakibara K, Tohge T, Matsuda F, Nakabayashi R, Takayama H, Niida R, Watanabe-Takahashi A, Inoue E, Saito K (2008) Comprehensive flavonol profiling and transcriptome coexpression analysis leading to decoding gene–metabolite correlations in *Arabidopsis*. Plant Cell 20:2160–2176. doi: 10.1105/tpc.108.058040

Yousefzadi M, Sharifi M, Behmanesh M, Moyano E, Bonfill M, Cusido RM, Palazon J (2010) Podophyllotoxin: Current approaches to its biotechnological production and future challenges. ENG LIFE SCI 10: 281-292. doi:

10.1002/elsc.201000027

Zhao Q, Zeng YN, Yin YB, Pu YQ, Jackson LA, Engle NL, Martin MZ, Tschaplinski TJ, Ding SY, Ragauskas AJ, Dixon RA (2014) Pinoresinol reductase 1 impacts lignin distribution during secondary cell wall biosynthesis in *A. thaliana*. Phytochem 112:170-178. doi: 10.1016/j.phytochem.2014.07.008

Zhang YM, Tan NH, He M, Lu Y, Shang SQ, Zheng QT (2004) Sequosempervirin A, a novel spirocyclic compounds from Sequoia sempervirens. Tetrahedron Lett 45:4319–4321. doi: 10.1016/j.tetlet.2004.04.038

Zhang YM, Tan NH, Yang YB, Lu Y, Cao P, Wu YS (2005) Norlignans from Sequoia sempervirens. Chem Biodivers 2: 497-505. DOI: 10.1002/cbdv.200590030